ELECTRODE MATERIALS FOR ELECTROORGANIC SYNTHESIS

BY

Mohammed Rafique

A thesis submitted for the degree of

MASTER OF PHILOSOPHY

December 1986

Department of Chemistry
University of Southampton

ACKNOWLEDGEMENTS

I would like to express my sincere thanks to Dr. D. Pletcher for his invaluable help and constant encouragement during both the research and writing of this thesis.

My thanks also go to my wife Hamida and my children for their support and encouragement during the past three years.

I am also grateful to the Government of Pakistan for providing me with financial support.

Finally, I am grateful to Mrs K. Welfare for the incredibly quick and efficient way in which she typed this thesis.

UNIVERSITY OF SOUTHAMPTON

ABSTRACT

FACULTY OF SCIENCE
CHEMISTRY

Master of Philosophy

ELECTRODE MATERIALS FOR ELECTROORGANIC SYNTHESIS

by Mohammed Rafique

The aim of the investigation was to develop new electrode materials suitable for selective electroorganic reactions. Two types of material have been studied, various $Ni(OH)_2$ in basic media and cobalt spinels in acid solution.

The oxidation of alcohols to carboxylic acids at smooth nickel and electrodeposited $Ni(OH)_2$ have been shown to be selective reactions and the formation of a high surface area material leads to a substantial increase in current density. The mechanism of the reactions have been monitored using cyclic voltammetry and steady state methods. The high surface area electrodes have been used for the controlled current oxidation of 2,2'-dimethyl-1,3-propanediol to 2,2'-dimethyl malonic acid; at 8 mA cm^{-2} the selectivity is good but the current efficiency only 31 % (O_2 evolution also occurs).

A preliminary study of the behaviour of Co_3O_4 and $Zn_xCo_{3-x}O_4$ electrodes using cyclic voltammetry is also reported. The materials are stable in strong acid and it is to be expected that the oxidation state of cobalt species within the lattice may be cycled between two and three. The higher oxidation state could react with organic molecules to give a catalytic cycle.

CONTENTS

CHAPTER 1

INTRODUCTION

CHAPTER 1

1.1 Electroorganic Synthesis

Electrochemical reactions involving organic compounds are amongst the oldest known reactions[1], but they did not achieve any commercial significance in the early days. By the turn of the century a large number of organic compounds had been prepared by electrolytic methods in the laboratory[2-7], but only a few electroorganic reactions have been carried out on an industrial scale. Such reactions include the reduction of benzoic acid to benzyl alcohols[8];

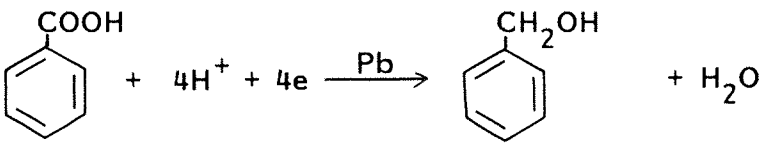

and the reduction of salicylic acid to salicylaldehyde[9]

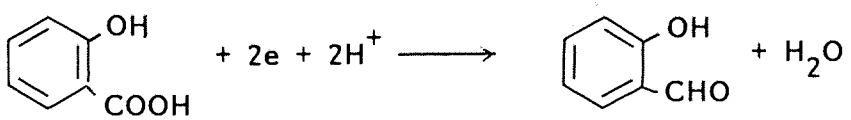

The production of lead tetramethyl and tetraethyl[10] by the oxidation of Grignard reagents has also been a successful large scale process. The appropriate Grignard reagent in a mixture of ethers is discharged at a lead anode; the resulting radicals react to form tetraalkyl lead

$$4RMgCl + Pb - 4e \longrightarrow R_4Pb + 4MgCl^+$$

The cations on discharge give elemental magnesium and magnesium chloride

$$4MgCl^+ + 4e \longrightarrow 2Mg + 2MgCl_2$$

The magnesium then reacts with excess alkyl halide to regenerate Grignard reagent. A further example is the production of periodic acid, used as an intermediate in the manufacture of dialdehyde starch[11]

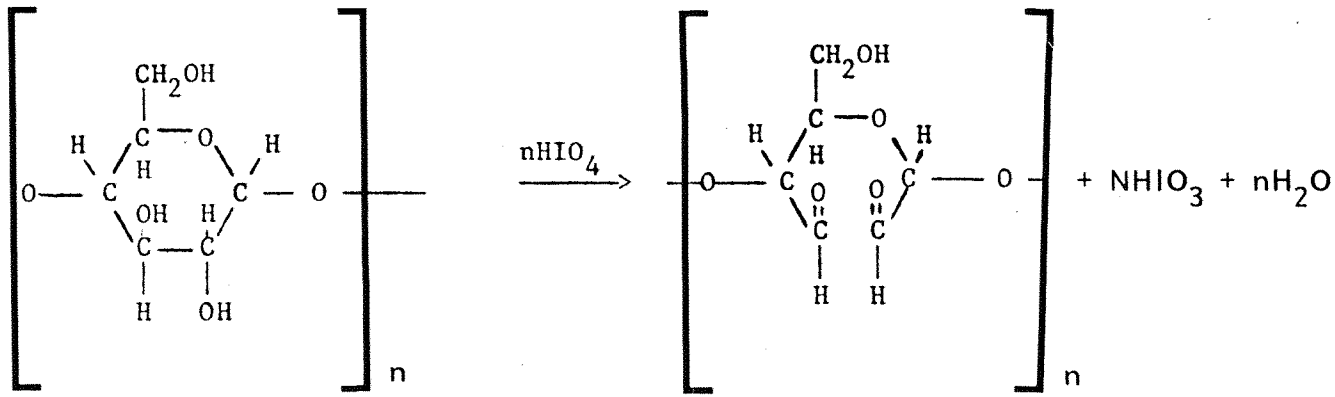

$$nH_2O + nHIO_3 \xrightarrow{-2ne} nHIO_4 + 2n\ H^+$$

1.2 Advantages of Electroorganic Processes

(i) Electroorganic synthesis can require cheaper and more readily available feedstock than alternative chemical routes.

(ii) Electroorganic synthesis usually utilises mild process conditions and low temperatures and this should lead to better selectivity and lower process costs.

(iii) Electroorganic processes can have high chemical yields so that downstream recovery and purification is simplified.

(iv) Electrosynthesis can be made more competitive and economic, when chemical products are made at both the electrodes (paired synthesis). There are several examples where the anode and the cathode reactions have been coupled to synthesise organic compounds. Wille and coworker[12] have reported a continuous process for the electrosynthesis of sulphones by cathodic reduction of sulphur dioxide in the presence of organic halides; the organic halides consumed in the cathodic process is re-generated at the anode. The cathode reaction is the reduction of sulphur dioxide to its anion radical which is followed by a comparatively slow nucleophilic substitution reaction with organic halide.

$$SO_2 + e \longrightarrow SO_2^{-\cdot}$$

$$2SO_2^{-\cdot} + 2RX \longrightarrow R\text{-}SO_2\text{-}R + 2X^- + SO_2$$

The halide ions are oxidised at the anode to elemental halogen, which is then reduced by sulphur dioxide to form hydrobromic acid which further reacts with the alcohol to regenerate organic halide. The overall anode reaction is

$$2Br^- - 2e \longrightarrow Br_2$$

$$Br_2 + SO_2 + 2H_2O \longrightarrow 2HBr + H_2SO_4$$

$$2HBr + 2ROH \longrightarrow 2RBr + 2H_2O$$

The current efficiency for the formation of sulphones is nearly 80%. Another example of such coupled processes is the production of propylene oxide from propylene and sodium bromide[13]. Bromine is the main product at the anode but it equilibrates with water to form hypobromite and bromide ions.

$$2Br^- - 2e \rightleftharpoons Br_2$$
$$Br_2 + H_2O \longrightarrow HOBr + H^+ + Br^-$$

The hypobromite reacts with dissolved propylene to produce the bromohydrin

$$CH_3 - CH = CH_2 + HOBr \longrightarrow CH_3—CHOHCH_2Br.$$

The main reaction at the cathode is the evolution of hydrogen and formation of hydroxide

$$2H_2O + 2e \longrightarrow H_2 + 2OH^-.$$

The bromohydrin reacts with the cathodically generated base to form propylene oxide regenerating the bromide ion

$$CH_3CHOH - CH_2Br + OH^- \longrightarrow CH_3—\underset{\diagdown\,O\,\diagup}{CH}—CH_2 + H_2O + Br^-$$

1.3 Problems Encountered in Electroorganic Synthesis

Despite the fact that many organic conversions have been carried out electrochemically, there remain problems which prevent the widespread commercial exploitation of organic electrosynthesis. Firstly, it must be recognised that organic electrosynthetic processes are complex. Usually, the overall electrode reaction is not a simple electron transfer process, but a sequence of electron transfer and coupled chemical processes either on the electrode surface or in the homogeneous solution close to the electrode surface. In other words, the electron transfer process simply produces organic intermediates (e.g. carbanions, carbonium ions, radicals, ion radicals), which all too frequently have a

range of reactions available to them. Hence it can be difficult to achieve the selectivity in organic products by only controlling the electrode potential. The parameters which have a significant effect on electroorganic synthesis are:

a. electrode potential

b. electrode materials

c. pH, electrolyte

d. concentration of electroactive species + other reactants

e. temperature

f. cell design including mass transport conditions.

The electrode potential plays a significant role in electroorganic synthesis, since the products, current efficiency, and space time yields, all depend on it. Electrode materials also influence reactions in a number of ways and will be discussed here in detail. The mechanism, rate, and the products can all depend strongly on the electrode material. The most commonly used anode materials are Pt, C and PbO_2, and these may be used for the oxidation of such diverse organic substrates as olefins, aromatic and saturated hydrocarbons[5,14]. Fe and Ni are the most useful materials in alkaline media where they are relatively stable to corrosion. Nickel and monel are excellent for electrofluorination reactions in liquid HF[15,16]. Other useful alloys for aromatic reactions include ferrosilicon for the nitration of aromatic hydrocarbons[17]. The most widely used cathode materials are mercury, lead, tin, copper, iron, aluminium, platinum, nickel and carbon.

Some examples (see figure 1 and 2) illustrating the influence of electrode materials are discussed here to demonstrate the complexities involved in electroorganic reactions.

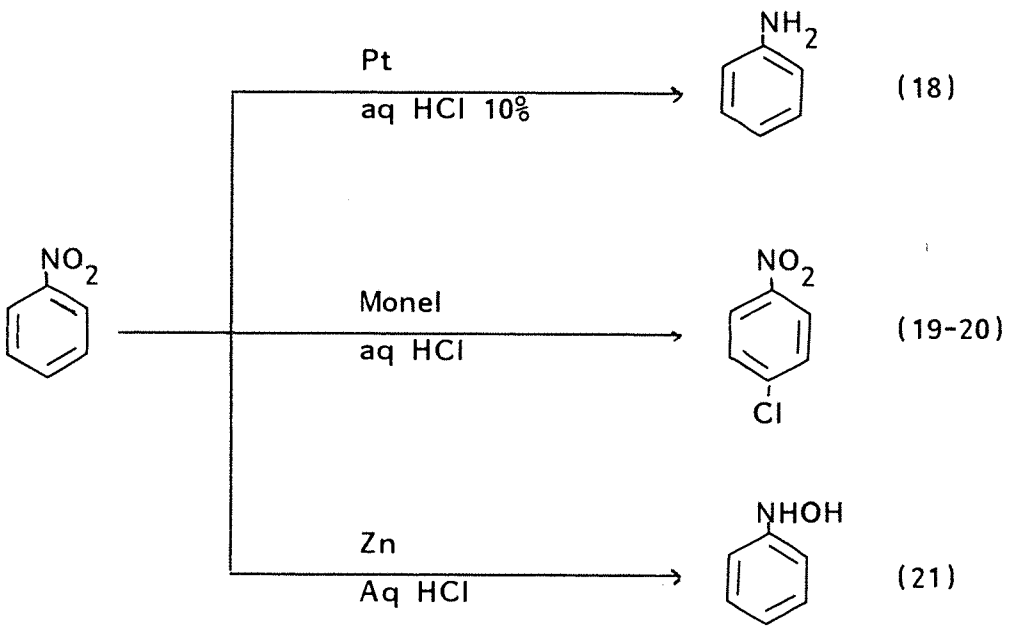

Figure 1

The diversity of products generated during electroreduction of nitrobenzene depends on the electrode material, as well as on the solvent and supporting electrolyte, and other factors such as temperature and reactant concentration.

Acetone can be converted to propane, isopropyl alcohol, pinacol or di-isopropyl mercury as shown in figure 2. Other variables, such as pH, concentration of reactant and temperature also cause the changes in the products.

Another significant parameter in the electroorganic synthesis is the cell design. The presence or absence of a separator, the mass transport regime, the arrangement of the anode-cathode gap and the potential distribution at both electrodes all play important roles in the overall performance of the cell. In the past, progress in the development of cell components and the technology essential for successful operation has been slow. In the last few years, however, major advances have been made in developing electrolytic cells of large electrode area per unit volume of reactors e.g. monopolar and bipolar bed

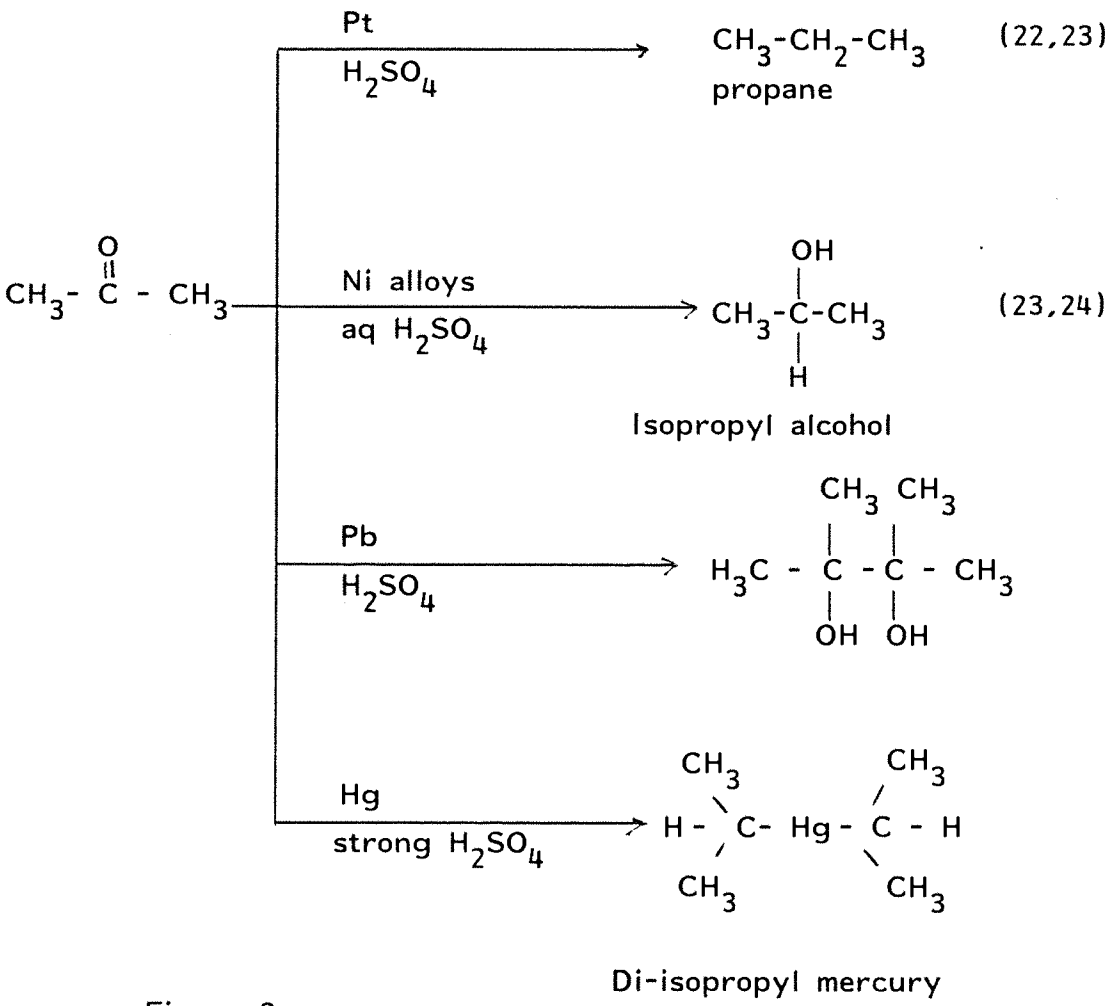

Figure 2

cells[25-26], filter press type cells[27-30], fluidized bed cells[31.34], trickle tower cells[35-36] etc. and it is believed that these may permit more electrochemical processes to be used in the chemical industry.

1.4 Electrochemical Oxidation

The oxidation of organic compounds can be carried out either (i) by a direct electrochemical route or (ii) by an indirect route.

1.4.1 Direct Electroorganic Synthesis

This type of process is based on the direct electron transfer from the organic substrate to the anode. The electron transfer

process simply produces an organic intermediate (e.g. radical, carbonium ion, etc.), which then reacts according to its environment. For example, the product from the oxidation of anthracene is initially the radical cation, but in the presence of pyridine, the electrolysis leads to the pyridinium salt[37]

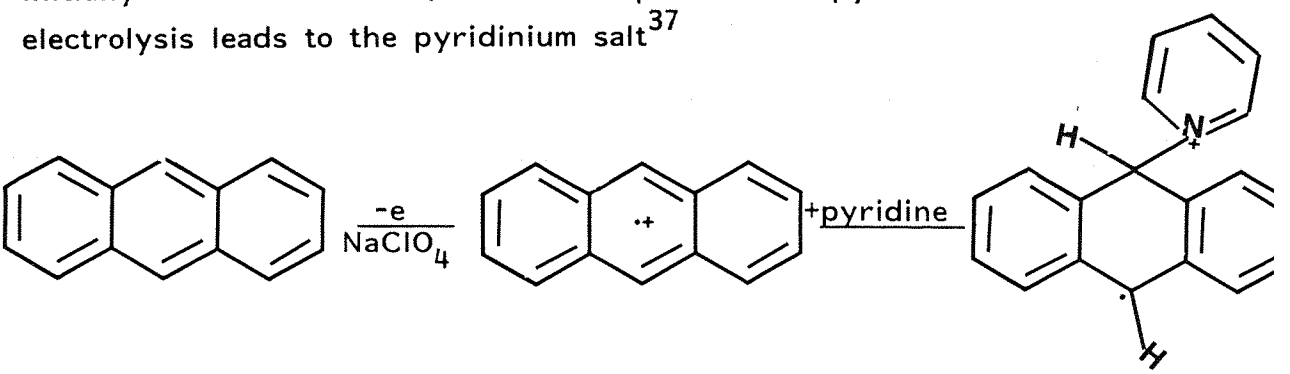

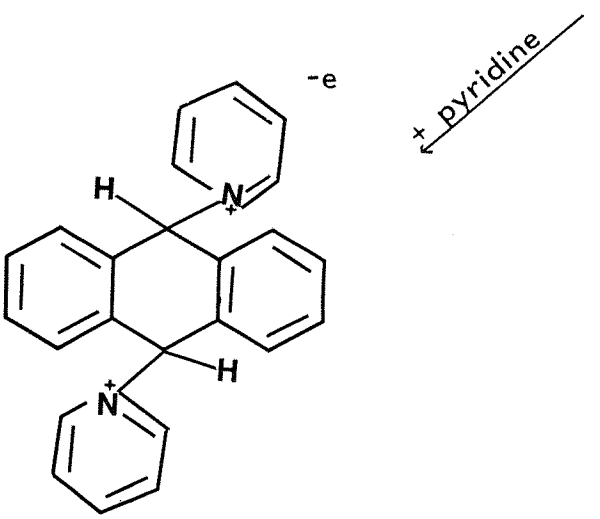

Pyridinium salt

but oxidation in acetonitrile in the presence of ethanol gave bianthrone[37].

Electrolysis has been used to generate cation radicals from many molecules e.g. phenothiazine[38], dithiohydroquinone dimethyl ether[39], 1,2,4,5-tetramethylbenzene[40], azoacridine[41], and triethylene diamine[42].

A major development in the last 25 years was the recognition that the Kolbe reaction could lead to carbonium ions[43]. The forma-

tion of such ionic species became more important at higher voltage and seems to be especially favoured with structures that give rise to relatively stable carbonium ions. For example, when exo- or endo-norbornane-2-carboxylic acid was electrolysed in the presence of tri-ethylamine in methanol, exo-norbornyl-methyl ether was the product.

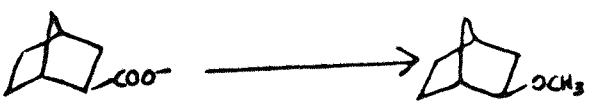

exo-norbornyl-methyl ether

Under similar conditions exo- or endo-5-norbornene-2-carboxylic acid gave 3-methoxynortricyclene.

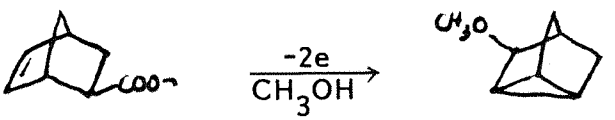

Further evidence of the formation of the carbonium ion intermediate is the formation of N-tert-butylacetamide during electrolysis of pivalic acid in acetonitrile containing a small amount of water[44].

$$(CH_3)_3CCOO^- \xrightarrow[CH_3CN]{-2e} (CH_3)_3\ CNHCOCH_3$$

N-tert-butyl acetamide.

Carbonium ion intermediates are apparently formed even from a simple aliphatic acid if a carbon anode is employed.

1.4.2 Indirect Electrosynthesis

In an indirect electrosynthesis, an oxidising or reducing agent is generated at the working electrode. This is then responsible for oxidation (or reduction) of the organic substrate e.g.

$$X - ne \longrightarrow Y$$

$$Y + R \longrightarrow X + O$$

There are many examples where the redox couple is free in solution. Couples commonly considered for use in indirect oxidation include Ce^{3+}/Ce^{4+}, Co^{2+}/Co^{3+}, Mn^{2+}/Mn^{3+}, $Cr^{3+}/Cr_2O_7^{--}$, Br_2/Br^- etc.

Oxidation occurs by homogeneous reaction with the organic compound present in dissolved form, or as a "second phase" and the regeneration of the redox species. The reaction with the organic compound is carried out either in-situ or in a two stage process. Indirect reaction involving homogeneous species are well studied by several authors[45-51]. Kramer and coworkers[49] have reported a high current efficiency for the indirect electrochemical oxidation of toluene and chlorotoluene to the corresponding aldehydes using the Ce^{3+}/Ce^{4+} redox system.

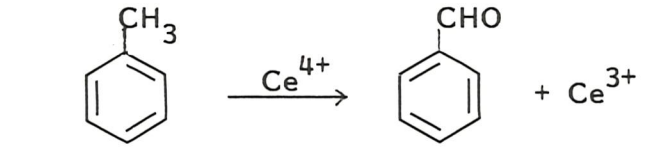

$$Ce^{3+} - e \xrightarrow{\text{anode}} Ce^{4+}$$

The conversion of anthracene to anthraquinone[52] is another example of such a process. A concentrated solution of chromium(III) in aqueous sulphuric acid is oxidised at a Pb (or Pb covered in-situ by PbO_2) anode

$$2Cr^{3+} + 7H_2O - 6e \longrightarrow Cr_2O_7^{2-} + 14\ H^+$$

and the dichromate is then reacted with anthracene

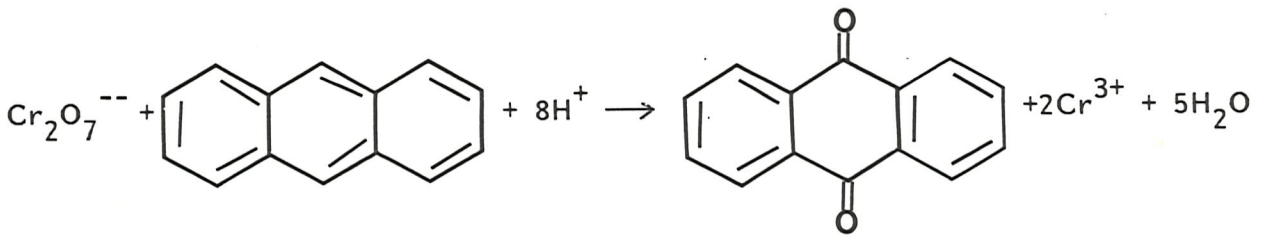

Other examples are the higher oxidation states of molybdenum[53], ruthenium[54] and osmium[55], adsorbed on platinum or platinum black which oxidise alcohols, formaldehyde and formic acid.

$$Mo^{(VI)}_{ads} + HCHO \xrightarrow[H_2SO_4]{\text{Pt black}} Mo^{(V)}_{ads} + CO_2 + H_2O.$$

The indirect method has a number of advantages:

1. Since the chemical reaction can take place in the boundary between two phases (e.g. in an emulsion), it is possible to use a sparingly soluble or completely immiscible feedstock and still have a high concentration of the species reacting at the electrode.

2. When the chemical reaction between the catalyst and the organic substrate is fast, the indirect electroorganic synthesis can be carried out with a high current density.

3. If the chemical reaction is slow the catalyst, after the generation, together with the organic substance can be transferred to another reactor and perhaps refluxed. After completion of the reaction the spent reagent can be recycled into the working electrode compartment.

1.5 Objective of this investigation

This thesis is about electrode materials. Two types of new anode material have been investigated. One is the electrodeposited nickel hydroxide electrode which is known to behave well in alkaline media, and indeed, has been used for electroorganic synthesis. Particularly of interest was the electrochemical oxidation of 2,2-dimethyl-1,3-propanediol to 2,2-dimethyl propanedioc acid at this material.

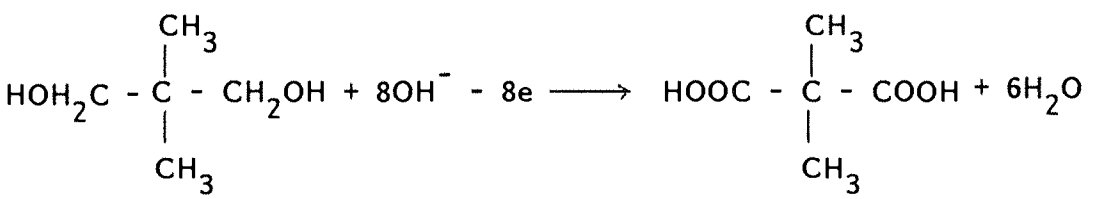

The other is a series of spinels of general formula $M_xCo_{3-x}O_4$ where M = Cu, Mg, Zn and where $x < 0 \leq 1,0$, which it was thought might be useful in acid media.

1.6 Nickel Hydroxide

Nickel when placed in an alkaline medium, immediately forms a surface layer of nickel hydroxide[56-59]. At low positive potentials,

below that required for bulk oxygen evolution, the surface undergoes oxidation[60-64]. This has been represented as

$$Ni(OH)_2 - e \rightleftharpoons NiOOH + H^+$$

There is a rapid conversion of the surface layer of the hydroxide resulting in the formation of a few monolayers of a higher nickel oxide. This reaction is, however, much more complex than appears from the above equation since both reduced and oxidised forms of the oxide can exist as α, β, and γ phases and in the species NiOOH, the nickel can have any oxidation state between 2 and 4.

For a wide range of alcohols and amines, oxidation was found to take place at the same potential as that for the oxidation of the nickel surface[57,65-66].

The rate of reaction of the alcohols was found to be primary > secondary > tertiary. This is the opposite trend to that expected for a process involving direct electron transfer to the electrode from the organic substrate. Oxidation of aliphatic amines in basic media at a carbon electrode involves direct electron transfer with tertiary amines being oxidised at less anodic potentials than secondary, which are oxidised at less anodic potentials than primary amines[58]. At potentials at which the nickel hydroxide layer is not oxidised a 'normal' direct electron transfer process through the nickel hydroxide layer can be observed. Hence the oxidation of p-aminophenol, which occurs at +0.300V vs SCE, in a basic media at the nickel hydroxide electrodes, gives a diffusion controlled limiting current[58]. Some examples of the application of a nickel electrode in organic chemistry are as follows:

Primary alcohols, diol, secondary alcohols, and sugars are oxidised to carboxylic acids, dicarboxylic acids, ketones, and sugar acids respectively[58,65-66].

a. Primary straight chain alcohols.

$$R-CH_2-CH_2OH \xrightarrow[H_2O-4H^+]{-4e} R-CH_2COOH$$

b. Diol

$$HOCH_2—R—CH_2OH \xrightarrow[-4H^+]{-8e} HOOC—R—COOH$$

c. Secondary alcohols

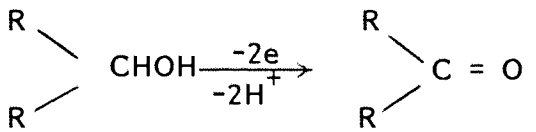

d. Oxidation of protected carbohydrate[67]

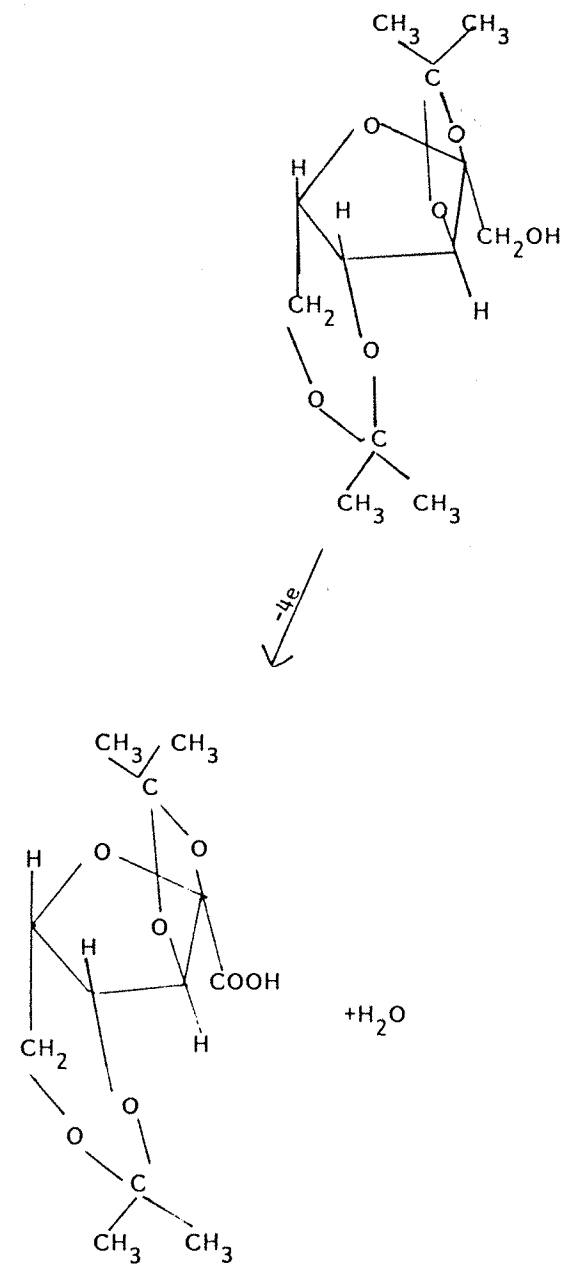

Primary amines, α,α'-substituted primary amines and secondary amines, are oxidised into nitriles, ketones, ketones and acids respectively[58].

e. Straight chain primary amines

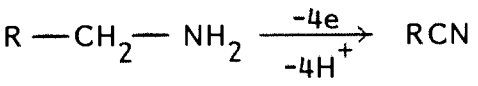

f. α,α'-substituted primary amines

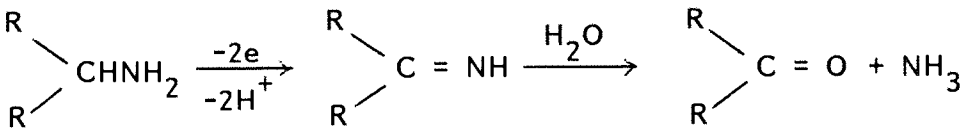

g. Secondary amines

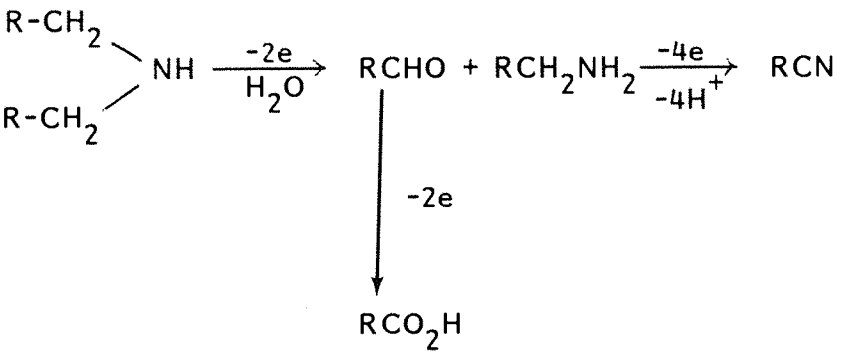

Primary amines are oxidised more rapidly than alcohols. The rate of oxidation decreases with the increase of carbon chain length in the alcohol or amine.

The value of the limiting current obtained for the process occurring at the higher nickel oxide was much less than expected for a diffusion controlled process.

An oxidation scheme for this process has been proposed[59], scheme 1.

$$Ni \xrightarrow{aq\ KOH} Ni(OH)_2 \overset{-e}{\rightleftharpoons} NiO(OH) + H^+$$

$$NiO(OH) + RCH_2OH \xrightarrow{r.d.s.} Ni(OH)_2 + R\dot{C}HOH$$

$$R\dot{C}HOH \xrightarrow{further\ steps} Products$$

Scheme 1

The rate determining step in this scheme was said to be the reaction of the organic compound and the higher nickel oxide, and hence from the limiting current, the rate constant for this process was obtained. Other authors using different experiments have come to the same conclusion concerning the rate determining step[68].

The nickel hydroxide electrode can be compared as an oxidising agent to the chemical oxidant 'nickel peroxide'[69-74], which is prepared by the precipitation of nickel hydroxide with base in the presence of hypochlorite. The rate determining step for this oxidant has been shown to be the abstraction of a hydrogen atom from the carbon α to the functional group[58,69]. A primary isotope effect for the hydrogen on the carbon α to the functional group was shown for the anodic oxidation of methanol and deuterated methanol $k_{CH_3OH}/k_{CD_3OH} = 7.0$[58] so a similar hydrogen atom abstraction reaction is assumed to be the rate determining step for both the electrochemical and chemical processes. Adsorption onto the electrode was also seen to be part of the rate determining step as the stereochemistry of the molecule was found to strongly influence the observed rate constants. The order of tertiary < secondary < primary has already been noted. Other indications are the effect of branching at the carbon α to the function group, and the increased rate of oxidation of cyclic compounds compared to the similar acyclic structures[58].

Preparatively, the nickel hydroxide electrode has been shown to

give carboxylic acid yields which compare favourably with or exceed those for conventional techniques for the oxidation of alcohols. This is particularly true for long chain alcohols and 4-alkenol[66]. Long chain and branched alcohols were oxidised at higher temperatures to increase the rate[65]. For example 2,4-octene-1,8-diol was oxidised to the corresponding dicarboxylic acid in an 80% yield[65]. Secondary alcohols and hydroxy steroids were also oxidised by the same authors in good yields[65]. The nickel hydroxide electrode has been used for the oxidation of protected carbohydrates 2,3:4,6-di-o-isopopylidene-L-sorbose to di-o-isoipropylidene-L-xylo-hexulosonic acid in a 90% yield[68]. Recently, much work has been undertaken on this reaction as it is an important stage in the synthesis of vitamin C. The problem with such electrodes is that they give high current efficiency only when the current densities are low. Therefore, it is desirable to have a high surface nickel hydroxide electrode for electroorganic synthesis. Such nickel hydroxide electrodes can be made under a variety of conditions. The two most common methods are:

a. Cathodic deposition of nickel hydroxide[67,75-77] from a nickel salt (0.1M $Ni(NO_3)_2$) solution.

b. Alternating anodic and cathodic polarisation in a solution of 0.1M $NiSO_4$ + 0.1M CH_3COONa + 0.005M NaOH[68,78-79].

The main purpose of these methods is to build up a thick layer of nickel hydroxide which should be porous and offer a large active area for oxidation. Much higher current density may then be obtained.

1.7 Spinel Oxide Electrode $M_xCo_{3-x}O_4$

(where M = Cu, Mg, Zn, $0 < x < 1$)

The family of mixed metal oxides are classified under the general term 'spinels' and include a number of technologically important materials which are isomorphous with mineral spinel (magnesium aluminate $MgAl_2O_4$). The spinel structure is a cubic close packed array of oxygen ions with metal cations distributed with some degree of coordina-

tion. A few spinels contain only one type of cation e.g. γ-Al_2O_3, but most contain cations in two or more valence states. The most common examples are illustrated as follows:

Mixed metal oxides of type $A^{II}B^{III}_2O_4$ (e.g. $FeCr_2O_4$, $ZnAl_2O_4$ and $Co^{II}Co^{III}O_4$), of type $A^{IV}B^{II}_2O_4$ (e.g. $TiZn_2O_4$ and $SnCo_2O_4$), and also of type $A^{I}_2B^{VI}O_4$ (e.g. Na_2MoO_4 and Ag_2MoO_4). The spinel of $A^{II}B^{III}_2O_4$ is called normal spinel while $A^{IV}B^{II}_2O_4$ is the inverse spinel.

The most commonly used spinel oxide electrode[80-83] is cobalt oxide Co_3O_4 which has been used commercially as a chlorine anode in sodium chloride solution. Caldwell et al[84-93] have studied chlorine evolution on surfaces prepared by coating a titanium substrate with a cobalt oxide spinel structure of the general formula $M_xCo_{3-x}O_4$ (M = Cu, Mg and Zn), where $0 < x < 1$. Preparation is relatively simple; the desired mixture of metal nitrates are applied as an aqueous solution to an acid etched (1M HF : 5M HNO_3) or sandblasted titanium substrate and then thermally oxidised between 275° to 450° for one hour to form oxides. The coating step is repeated 6 to 12 times until the desired coating thickness is reached. These coatings give low over-potentials for chlorine evolution in sodium chloride and cobalt spinel oxide coatings are in use in several Dow Chemical chlorine plants[94]. Titanium coated with a cobalt oxide spinel layer of the formula $M_xCo_{3-x}O_4$ (where M is Cu, Mg or Zn) was studied with the intention that these electrodes may be suitable for the electroorganic reactions and/or oxygen evolution in sulphuric acid.

CHAPTER 2

EXPERIMENTAL

CHAPTER 2

EXPERIMENTAL

2.1 The cells

Kinetic experiments were carried out using two different cells, although both were two compartment, three electrode cells. Investigation of the nickel hydroxide system took place using a cell holding 25 cm^3 and it is shown in figure 2.1. The nickel working electrode was a disc (0.2 cm^2), encased in a Teflon sheath which could be positioned directly above a fixed Luggin capillary leading to the reference compartment. The secondary electrode was a platinum gauze fixed below the Luggin capillary. The experiments using a titanium coated cobalt oxide electrode spinel structure and electodeposited nickel hydroxide on a nickel wire were carried in a cell of the type shown in figure 2.2. The working electrode was inserted into the cell from the top and was surrounded by a platinum spiral secondary electrode sealed into the working compartment from the bottom of the cell. The reference electrode compartment was separated from the working compartment through an adjustable Luggin capillary.

Constant current electrolyses were carried out using cells shown in figure 2.3 and figure 2.4. Electrolyses with smooth nickel were carried out using the cell shown in figure 2.3. It is a one compartment two electrode cell with a capacity of about 120 cm^3. The electrodes consisted of a nickel sheet and a copper sheet of size 20 x 5.5 cm (110 x 2 = 220 cm^2), separated from each other by two polymer grids and arranged in a way to give a "Swiss Roll". This arrangement of working and secondary electrodes gave a large surface area of active electrode (220 cm^2) within the cell. This is important when working with processes involving low current densities. The solution was stirred by a stream of nitrogen and also by the hydrogen produced at the secondary electrode. This ensured a high rate of mass transport

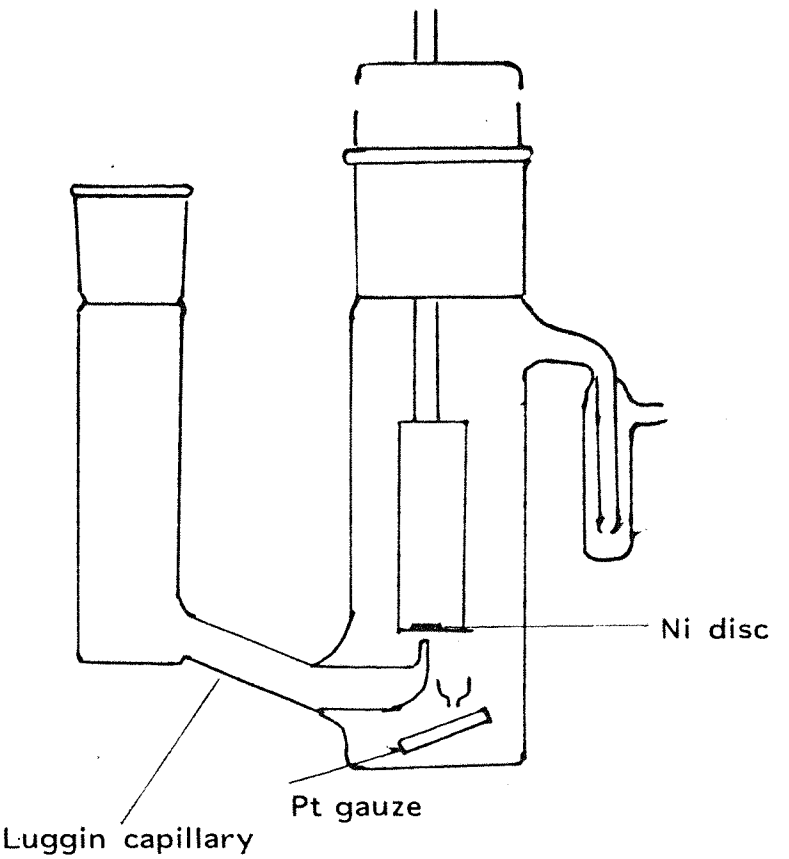

Fig. 2.1 Cell used for the kinetic investigation of a nickel hydroxide system.

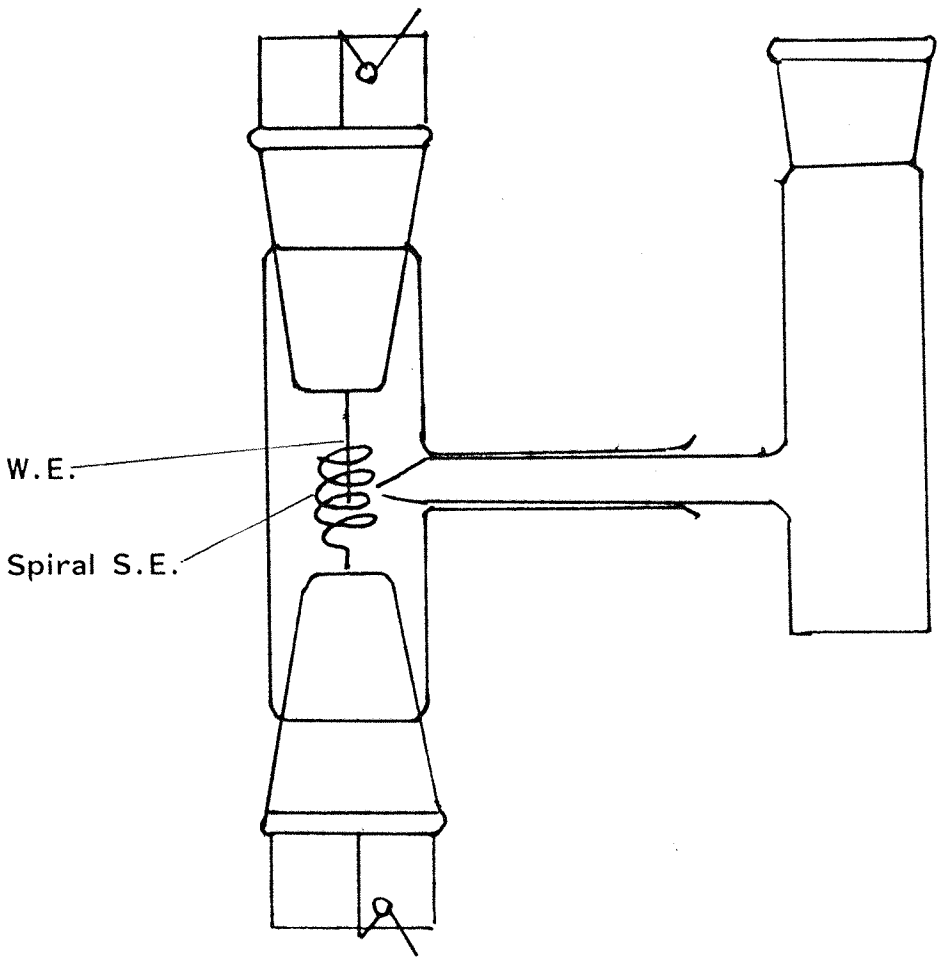

Fig. 2.2 Cell used for experiments with Ti supported cobalt oxide spinel structure electrode of the general formula $M_xCo_{3-x}O_4$ where M is Cu, Mg or Zn.

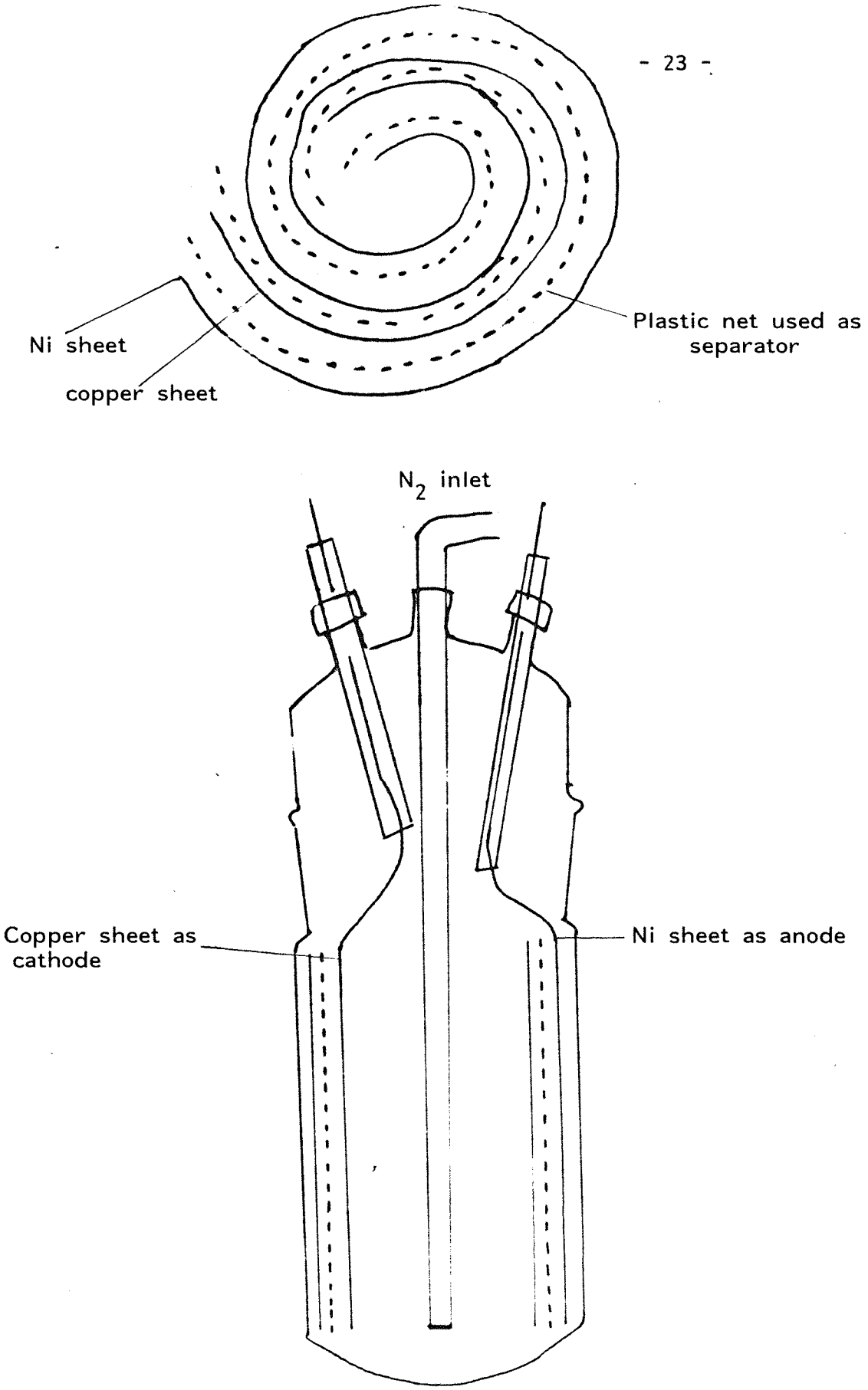

Fig. 2.3 Swiss Roll cell used for a constant current electrolysis.

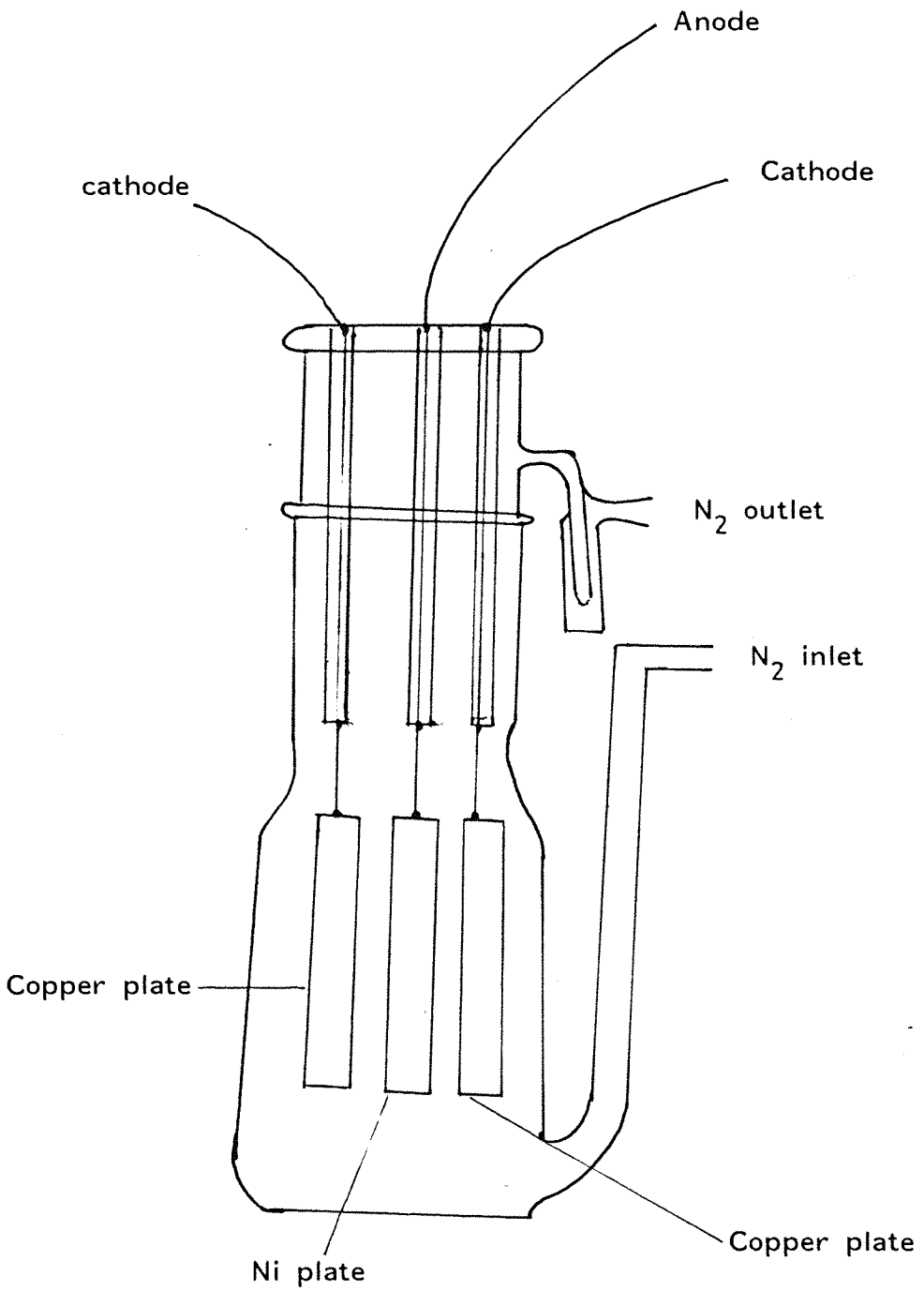

Fig. 2.4 Cell used for constant current electrolysis at an electrodeposited nickel hydroxide electrode.

to the electrode surface. All the cells used were constructed of glass and had inlets and outlets which allowed nitrogen to be passed through the solution. This removed oxygen which is reduced electrochemically and can interfere with the process under observation. Electrolyses with the electrodeposited $Ni(OH)_2$ electrode were carried out in a beaker type cell shown in figure 2.4. The working electrodeposited nickel hydroxide electrode was placed in between two copper plate cathodes. The electrodeposited nickel hydroxide electrode was prepared by a cathodic deposition from a 0.1M nickel nitrate at a constant current of 17 mA until a charge of 31C had been passed.

2.2. Electrodes

(a) Reference electrode

In all experiments a saturated potassium chloride calomel electrode (S.C.E.) was used as the reference electrode (a Radiometer type K401).

(b) Working electrodes

The nickel disc electrode was prepared from 99.99% Ni rod. A slice was cut from the rod. The disc was soldered to a steel rod, about 20 cm long and covered with a PTFE sheath, diameter about 3 cm, so that only the face of the disc was exposed. The electrode is sketched in figure 2.5. The nickel hydroxide electrode was prepared by cathodic deposition from 0.1M $Ni(NO_3)_2$ at 2 mA cm^2 into a nickel disc (area 0.2 cm^{-2}). Before deposition the disc (0.2 cm^2) was cleaned with filter paper and immersed in 20% HCl for about five minutes. The deposition charge was 0.6 C cm^{-2}. Spinel cobalt oxide electrodes of the general formula $Zn_xCo_{3-x}O_4$, where $0 \leqslant x \leqslant 1$ were prepared by first degreasing titanium wire (0.31 cm^2) with 1M HF:5MHNO_3. Solutions of $Zn(NO_3)_2$ and $Co(NO_3)_2$, each 1M were mixed in the ratio x:3-x and sprayed over the titanium wire. After each

coating, the solution was dried at a moderate temperature below 100°C in a drying oven for about 10 minutes. The coating step was repeated up to six to twelve times. After the final coating step, the nitrate coating was oxidised in a furnace at 275° - 450°C for an hour. The electrode is sketched in figure 2.6.

2.3 Pretreatment of the electrode

The Ni disc was first polished with emery paper and then on moist Metron polishing cloth, together with Banner Scientific alumina of decreasing size, 0.1 micron and 0.05 micron, until the surface looked smooth and bright. The electrodes were then washed with distilled water. The electrodeposited nickel hydroxide and the spinel oxide electrodes were washed with distilled water.

2.4. Instrumentation

Most of the electrochemical experiments were carried out using a Hi-Tek Instruments potentiostat, Model DT 2101 and a waveform generator, model PPR1. Cyclic voltammograms were recorded on an x-y recorder, model 60000. Steady state current vs potential plots were obtained, either with the above apparatus or simply the Hi-Tek potentiostat and using a point by point technique. Analysis of the products by gas-liquid chromatography was carried out using a Pye Unicam GCD chromatograph with a flame ionization detector. The carrier gas was nitrogen. Peaks were recorded using a Tekman y-t recorder, and concentrations were determined by comparison of peak areas with those obtained for standard solutions.

2.5 Solvent and electrolyte preparation

Aqueous solutions were prepared using triple distilled water. AnalaR potassium hydroxide and also AnalaR sulphuric acid were used as electrolytes.

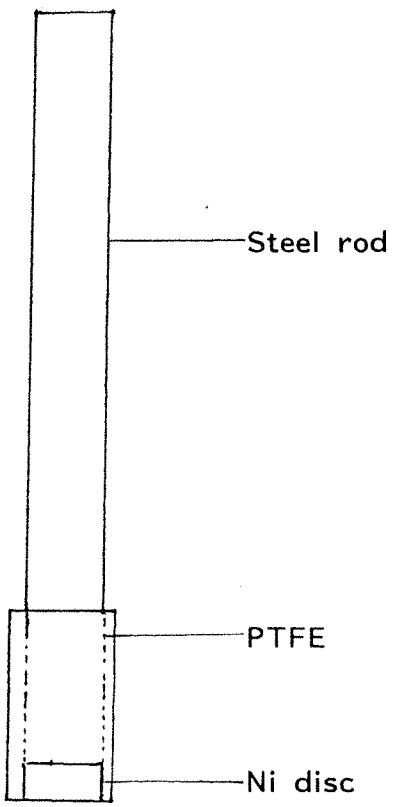

Fig. 2.5 Nickel disc electrode

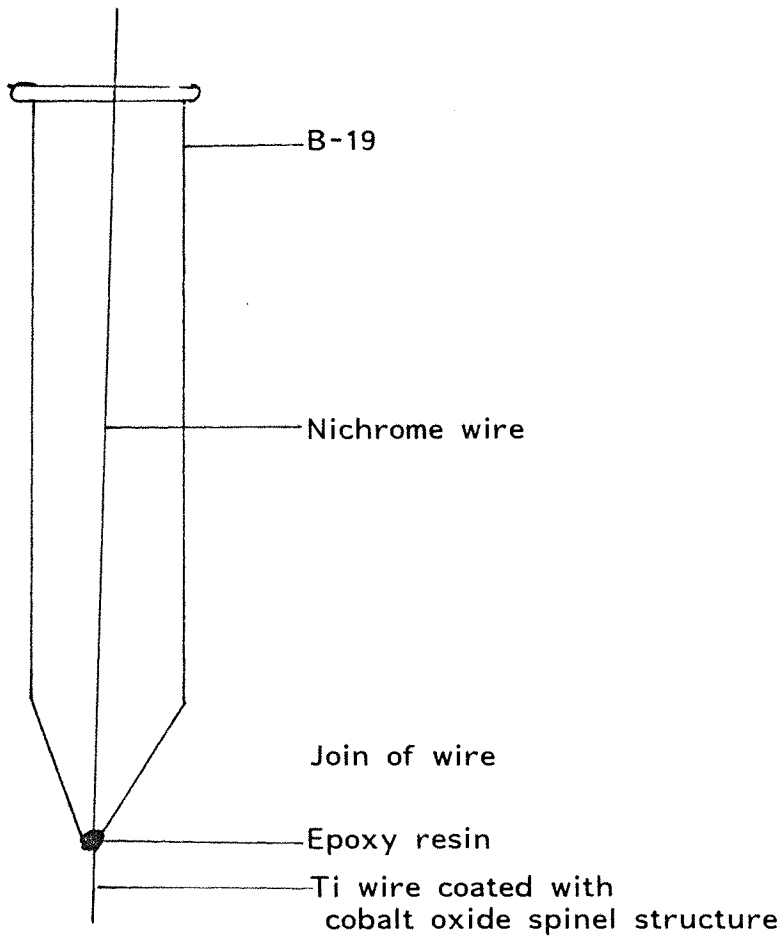

Fig. 2.6 Titanium wire coated with Cobalt oxide spinel structure.

2.6 General procedure

(a) Cyclic voltammetry

Cyclic voltammograms were run between preset limits with the indicated sweep rates. The solution was deoxygenated by bubbling oxygen-free nitrogen gas for between 10 to 15 minutes prior to any electrochemical experiment. Prior to the electrochemical measurements the nickel electrode was cleaned by polishing with 0.05 micron alumina powder, washed with distilled water and was then cycled in the electrolysis medium between preset limits until the charge associated with Ni^{II}/Ni^{III} transition became constant. The other electrodes were not deliberately cycled before use.

(b) Steady state currents vs potential plots

These were obtained by one of two methods. In the first, the current obtained from a slow linear sweep ($0.001V\ s^{-1}$) between two predetermined potentials was recorded directly using an x-y recorder. In the second case a potential was applied to the system and one minute allowed for the system to come to a steady state before a current reading was taken. In this way a table of data of potential and currents was obtained which allowed a steady state current potential plot to be constructed.

(c) Controlled current electrolysis

In this type of electrolysis, the current applied to the system is kept constant at a value below the limiting current estimated from the steady state current vs potential plot for the concentration of substrate involved. The electrolysis is continued until the charge calculated from Faraday's law [Q = nxFx number of moles of the substrate] has been passed to complete the desired transformation. At the end of the electrolysis the solutions were neutralized using Amberlite IR-120(H), a strong acid exchange resin, in a batchwise process, until the pH of the

solution, as recorded by a WPACD 30 pH meter, reached a constant value, indicating that ion exchange had ceased. The resin was then filtered off to leave a neutralized aqueous solution of electrolysed material, free from large quantities of inorganic ions and ready for analysis. Water was removed from the electrolysed material by gentle heat and a water pump.

(d) Product analysis

In all cases, the products from the oxidations at Ni anodes were organic acids. After extraction from the alkaline electrolyte by the technique described above, the following procedure was used for quantitative analysis. The method is actually described for the experiment where the substrate was 2,2-dimethyl-1,3-propanediol.

0.1 gram malonic acid (as internal standard) was added to the neutralised extract from the electrolysis of 2,2-dimethyl-1,3-propanediol and the mixture was esterified with BF_3/CH_3OH solution under reflux conditions for 1-5 hours. The mixture was then transferred to a 100 ml separating funnel with 30 ml dimethyl ether, and 20 ml of saturated sodium hydrogen carbonate. The funnel was shaken vigorously, and the layers then allowed to separate. The aqueous layer was discarded. The organic layer was dried with anhydrous sodium sulphate in a 50 ml beaker. The organic mixture was decanted into another 50 ml beaker and the sodium sulphate washed with 10 ml of diethylether. The ether solutions were combined and the solvent evaporated. 2 ml diethylether was added to the residue and 2 µl was injected into the glc. A 5% OV101 column at a temperature 110°C was used; carrier gas was nitrogen, flow rate 20 cm^3 min^{-1}. Two major peaks were observed. The retention time of the first peak was the same as that of 2,2-dimethyldimethylmalonate as shown in figure 2.7. Similar time of the second peak (electrolysed product) was the same as that of 2,2-dimethylmalonate as shown in figure 2.7. Similar work up and analysis was used for the oxidation of 2-cyanoethanol and the glc traces are shown in figure 2.8.

Fig. 2.7 A glc trace for the identification of product from a preparative electrolysis of 2,2-dimethyl-1,3-propanediol at an electrodeposited $Ni(OH)_2$ electrode. 5% OV 101 column, T = 110°C, nitrogen flowrate 20 cm^3 min^{-1}. (a) Electrolysis carried out at 17 mA cm^{-2}. (b) Electrolysis carried out at 8 mA cm^{-2}. (c) standard.

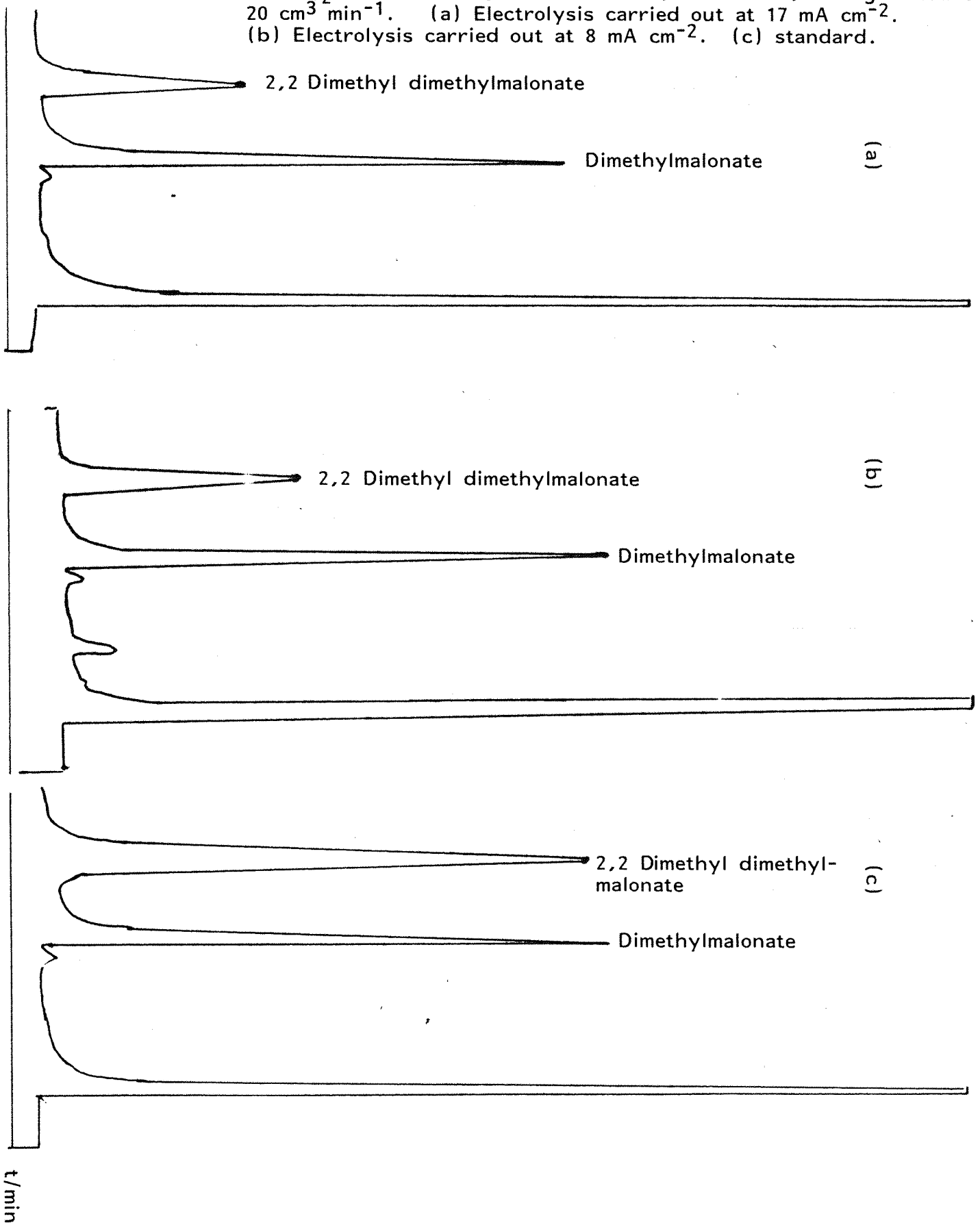

Fig. 2.8 A glc trace for the identification of products from a preparative electrolysis of 2-cyanoethanol in 1M KOH at an electrode $Ni(OH)_2$ electrode. 5% OV 101 column, T = 110°C, nitrogen flow rate 20 cm^3 min^{-1}. (a) electrolysis carried out at 7 mA cm^{-2}, (b) at 10 mA cm^{-2}, (c) standard (methyloxalate), (d) standard (methylcyanoacetate).

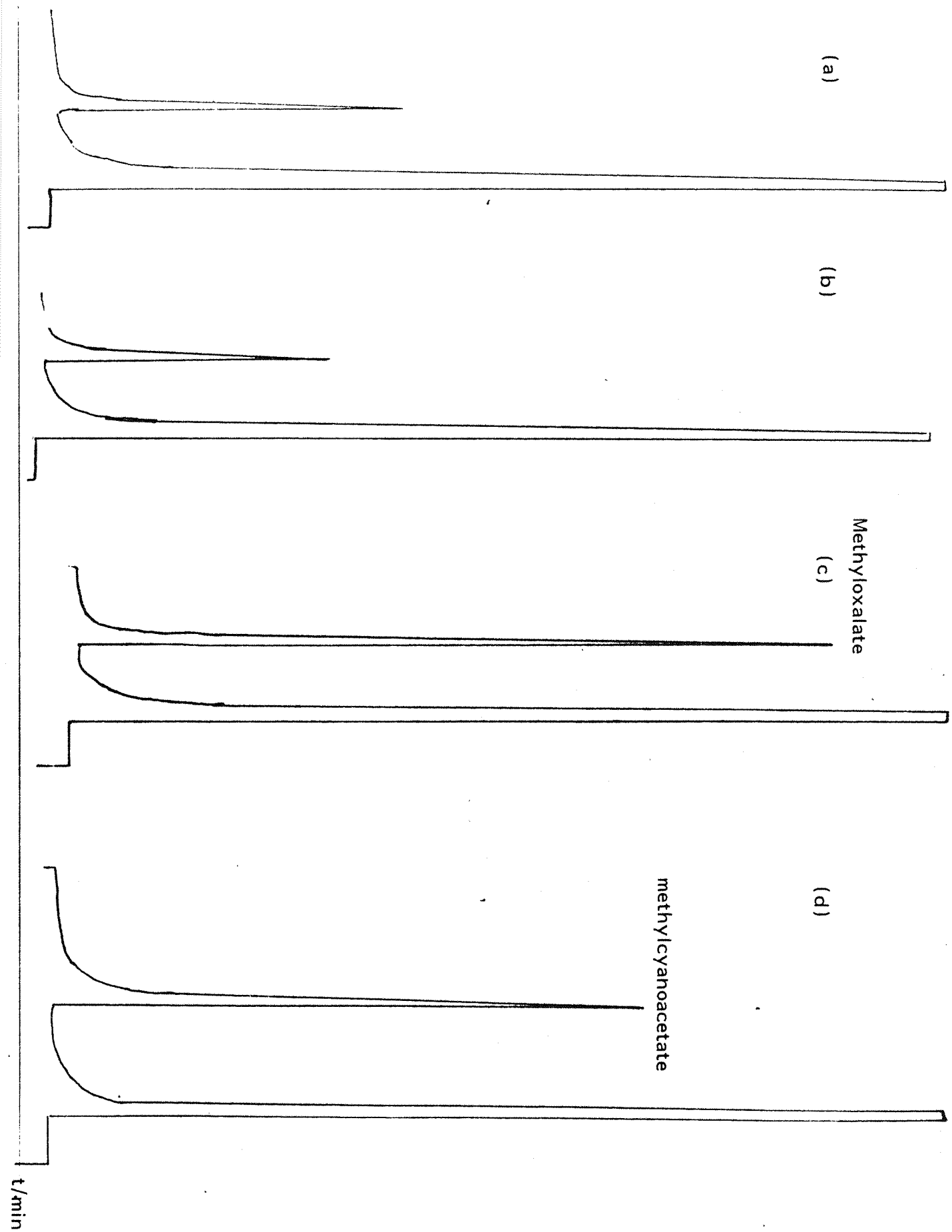

2.7 Chemicals used are as follows

1.	Acetic acid AnalaR	May and Baker
2.	Amerlite IR-120(H) AnalaR	BHD Chemicals
3.	Borontrifluoride in methanol (mixture 14%)	BDH Chemicals
4.	Cobalt nitrate	BDH Chemicals
5.	Chloroform	Koch-Light
6.	Copper nitrate	BDH Chemicals
7.	2-Cyanoethanol	Sigma
8.	Cyanoacetic acid	Aldrich
9.	Diethylether	May and Baker
10.	2,2-dimethyl-1,3-propanediol	Koch-Light
11.	2,2-dimethylmalonic acid	Aldrich
12.	Ethanol	James Burrough
13.	Hydrofluoric acid	Hopkin and Williams
14.	Malonic acid	BDH Chemicals
15.	Nickel nitrate	BDH Chemicals
16.	Nitric acid	May and Baker
17.	Oxalic acid	BDH Chemicals
18.	Petroleum ether (40-60%)	BDH Chemicals
19.	Potassium hydroxide	BDH Chemicals
20.	Sodium hydrogen carbonate	BDH Chemicals
21.	Sodium chloride	BDH Chemicals
22.	Sodium sulphate anhydrous	BDH Chemicals
23.	Sulphuric acid (AnalaR)	May and Baker
24.	Zinc nitrate	BDH Chemicals

CHAPTER 3

RESULTS AND DISCUSSION

CHAPTER 3

3. Results and Discussion

3.1 Nickel in Basic Media

3.1.1 Cyclic Voltammetric studies at a Nickel Disc Electrode in 0.1M Potassium Hydroxide

The cyclic voltammograms for a nickel disc electrode (area 0.2 cm^2) in 0.1M potassium hydroxide, run between O mV and 700 mV are shown in figure 3.1. At 0 mV the nickel immediately oxidises to give a surface layer of $Ni(OH)_2$, and well formed peaks are observed for the oxidation of the nickel hydroxide layer to a higher valency oxide at $E_p \simeq 480$ mV vs SCE and for the reverse process at Ep $\simeq$ 410 mV. Oxygen evolution occurs at a slightly more positive potential than the anodic peak, approximately 600 mV. The peak currents are proportional to the sweep rate i.e. the charge associated with the oxidation and reduction are independent of scan rate (the charges are measured as the shaded areas under the peaks in the figure). The ratio of charges Q_C/Q_A is approximately one. The data are summarised in table 3.1.

The curves obtained were identical to those reported by previous workers[57,59]; the general view of the literature is that the peaks can be reported by the equation

$$Ni(OH)_2 - e \rightleftharpoons NiOOH + H^+$$

3.1.2 Cyclic Voltammetric studies at a Nickel Disc Electrode in 1M Potassium Hydroxide

The cyclic voltammograms in 1M potassium hydroxide, run between 0 mV and 510 mV are shown in figure 3.2. Again at 0 mV the nickel immediately oxidises to give a surface of $Ni(OH)_2$, and well formed peaks are observed for the oxidation of nickel hydroxide to a higher valency oxide at $E_p \simeq 360$ mV vs SCE and for the reverse reduction at $E_p \simeq 285$ mV. The values are similar to those reported

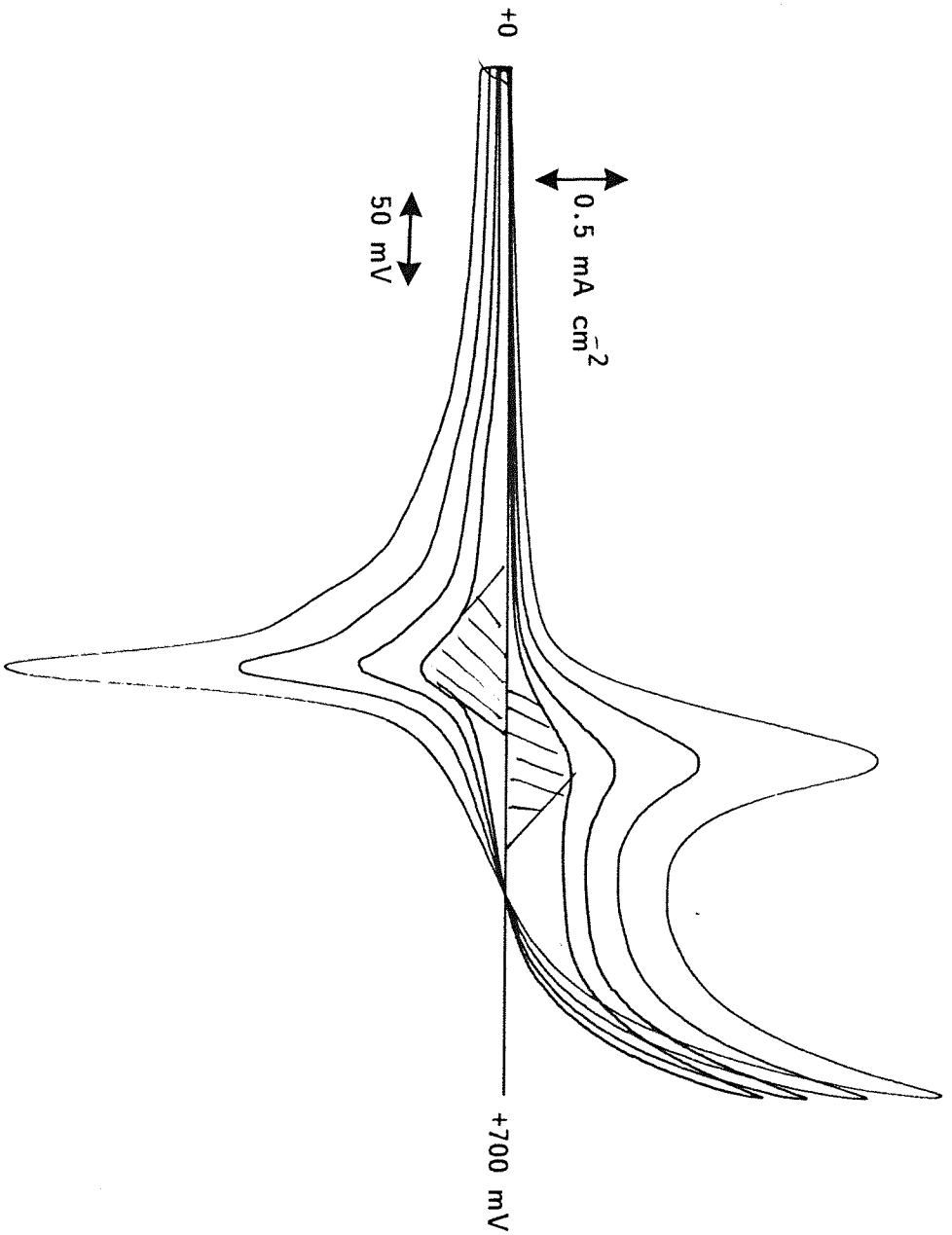

Figure 3.1 Voltammograms for a Ni electrode in 0.1M KOH run between 0 mV and 700 mV vs. SCE at potentials sweep rates of 25, 50, 100 and 200 mV s^{-1}.

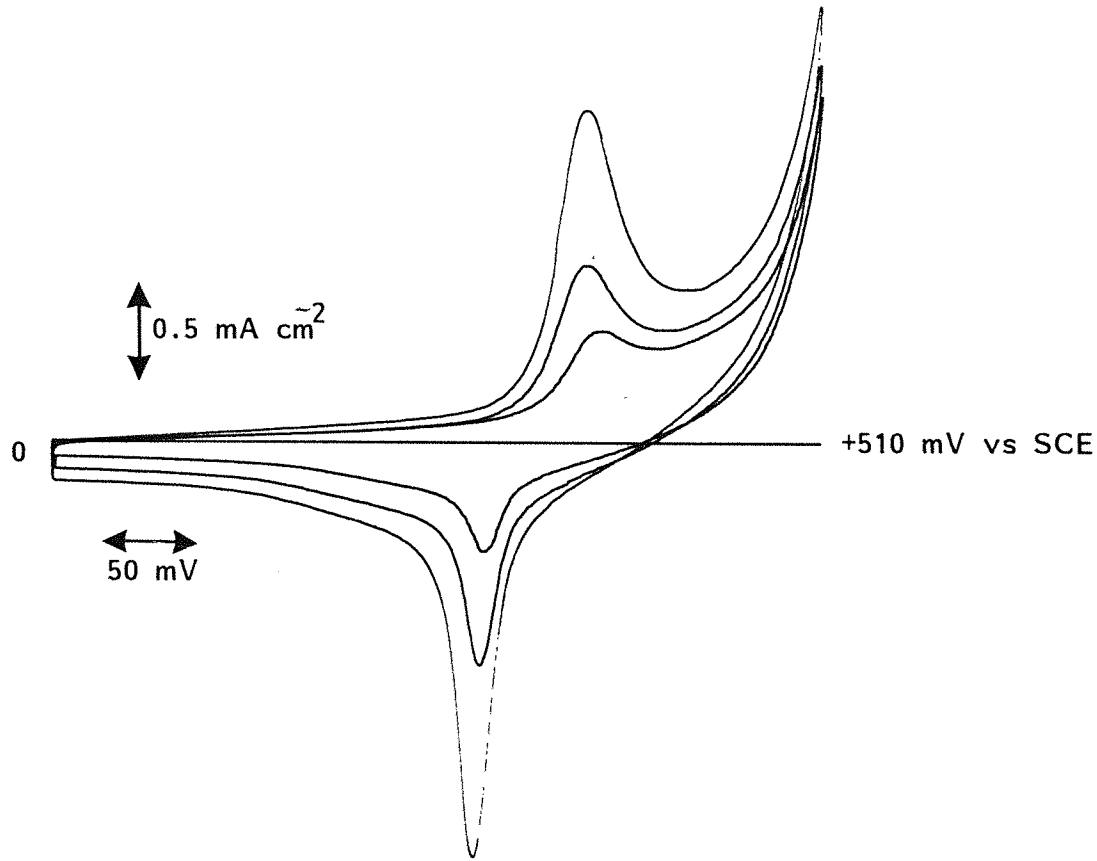

Figure 3.2 Voltammograms for a Ni electrode in 1M KOH run between 0 mV and 510 mV vs SCE at potential sweep rates of 25, 50 and 100 mV s^{-1}.

by previous workers[57,68]. Oxygen evolution commences at about +510 mV so it can be seen that in the stronger base the whole cyclic voltammogram is shifted to less positive potentials, i.e. the Ni(II) → Ni(III) oxidation and O_2 evolution both occur more easily. The peak currents are proportional to sweep rate. The ratio of charges Q_C/Q_A is equal to one.

3.1.3 Cyclic Voltammetric studies at an Electrodeposited Nickel Hydroxide Electrode in 1M Potassium Hydroxide

The electrode was prepared by cathodic deposition of nickel-hydroxide[67,75-77] onto a nickel disc (area 0.2 cm^2) from a 0.1M $Ni(NO_3)_2$ solution with a constant current density of 2 mA cm^{-2}; the charge passed was 0.6C cm^{-2}. The cyclic voltammograms in 1M potassium hydroxide, run between 0 mV and 530 mV, are shown in figure 3.3. Well formed peaks are observed for the oxidation of nickel hydroxide layer to a higher valence oxide at $E_p \simeq 300$ mV vs SCE and for the reverse process at $E_p \simeq 235$ mV; oxygen evolution commences at +530 mV. The peak currents are proportional to the square root of the potential scan rate, see figure 3.4. Hence the results are quite different to a polished nickel disc electrode when the peak currents are proportional to the potential scan rate as shown in table 3.1. Also the currents and charges associated with the oxidation of the thick, electrodeposited $Ni(OH)_2$ layers are much higher. This confirms that with the thick layers, the rate determining step is diffusion of a species through the layer. With the thin layers on the polished Ni all the layer is oxidised and reduced. Again with the thick layers, the charge in the forward scan (measured as the shaded area under the oxidation peaks) are higher than the charge in the reverse scan (measured as the shaded area under the reduction peaks) and these thick layers are not completely reduced at faster scan rates. The data are summarised in table 3.1.

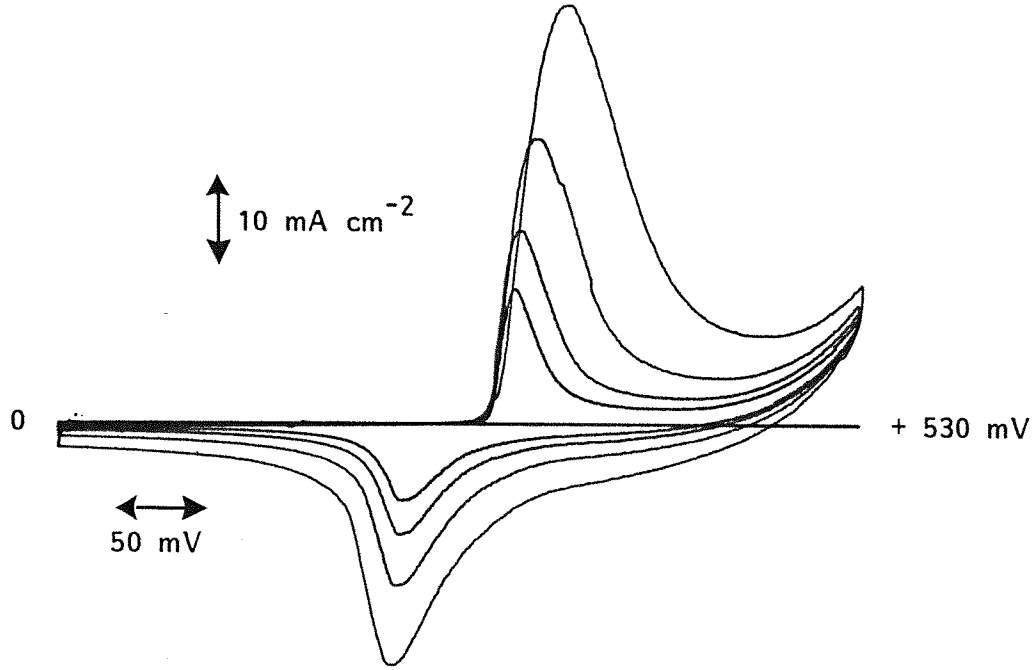

Figure 3.3 Voltammograms for an electrodeposited $Ni(OH)_2$ electrode in 1M KOH run between 0mV and +530 mV vs SCE. Potential sweep rates 5, 10, 20 and 40 mV s^{-1}. $Ni(OH)_2$ deposited onto Ni (0.2 cm^2) at 2 mA cm^{-2} from a 0.1M $Ni(NO_3)_2$. Deposition charge 0.6C cm^{-2}.

Type of electrode	C_{OH^-}	Sweep rate	I_p^a	I_p^c	Q_A	Q_C	Q_C/Q_A
		$mV\ s^{-1}$	$mA\ cm^{-2}$	$mA\ cm^{-2}$	$mC\ cm^{-2}$	$mC\ cm^{-2}$	
Ni disc electrode ($0.2\ cm^2$)	0.1M	25	0.4	0.6	2.5	2.6	1.0
	0.1M	50	0.8	1.05	3.0	3.0	1.0
	0.1M	100	1.45	1.75	3.2	3.0	1.0
	0.1M	200	2.6	2.85	3.2	3.0	1.0
	1M	25	0.65	0.75	3.5	3.5	1.0
	1M	50	1.15	1.4	3.5	3.6	1.0
	1M	100	2.15	2.55	3.5	3.6	1.0
Electrodeposited $Ni(OH)_2$ onto a Ni disc ($0.2\ cm^2$)	1M	5	21	9	183	153	0.8
	1M	10	34	15	221	150	0.7
	1M	20	49	23	233	155	0.7
	1M	40	72	33	243	128	0.5

Table 3.1

Data from cyclic voltammograms in potassium hydroxide taken over a range of sweep rates at a nickel smooth and electrodeposited nickel hydroxide electrode.

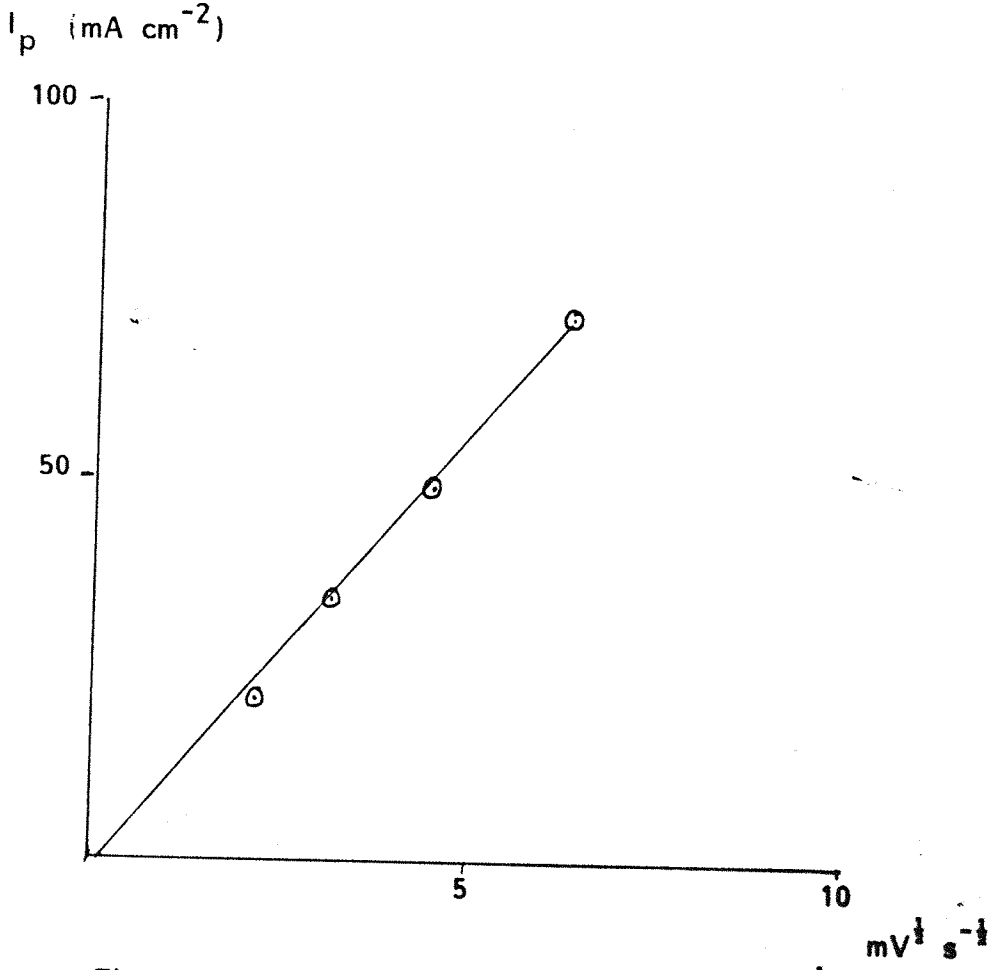

Figure 3.4 Plot of peak current (I_p) vs $\nu^{\frac{1}{2}}$ for voltammograms obtained for an electrodeposited $Ni(OH)_2$ electrode in 1M KOH.

3.2 Oxidation of Organic Compounds on Nickel in Basic Media

3.2.1 Oxidation of Ethanol

3.2.1.1 Cyclic Voltammetry for 0.1M Ethanol at a Polished Nickel Electrode in 1M Potassium Hydroxide.

Figure 3.5 shows a cyclic voltammogram run at a nickel disc electrode for a 0.1M ethanol in 1M potassium hydroxide at a sweep rate 100 mV s^{-1}. On the forward sweep an oxidation peak at $E_p \simeq 440$ mV vs SCE was obtained. On the reverse sweep an anodic peak is again seen at the same potential but at a slightly lower current density. The observation of this anodic peak on the reverse sweep may suggest that the activity of the surface for ethanol oxidation passes through a maximum and decreases again at more positive potentials, perhaps because the nickel layer becomes over-oxidised. For example, blockage of the surface by a species such as NiO_2 has recently been proposed[95] for the deactivation of the nickel oxide electrode during oxygen evolution. Also there is a small reduction peak at $E_p \simeq 205$ mV, but with ethanol present Q_c/Q_A is obviously much less than one. On the other hand the anodic peak current is small compared to that expected for a diffusion controlled oxidation of the ethanol (< 5%) and hence the oxidation of ethanol is slow. This conclusion is consistent with the observation of the small cathodic peak. By comparison with figure 3.2, it can be seen that the addition of ethanol leads to an increase in the peak current density by an order of two, and also shifted to more positive potential (80 mV). The curve obtained was identical to that reported by Robertson[96].

3.2.1.2 Cyclic Voltammetry for a 0.1M Ethanol at an Electrodeposited Nickel Hydroxide Electrode in 1M Potassium Hydroxide

The electrode was prepared by cathodic deposition of nickel hydroxide from a 0.1M nickel nitrate solution at a constant current density of 2 mA cm^{-2} onto a nickel disc (area 0.2 cm^2); the charge passed was 0.6C cm^{-2}. Figure 3.6 shows a cyclic voltammogram run

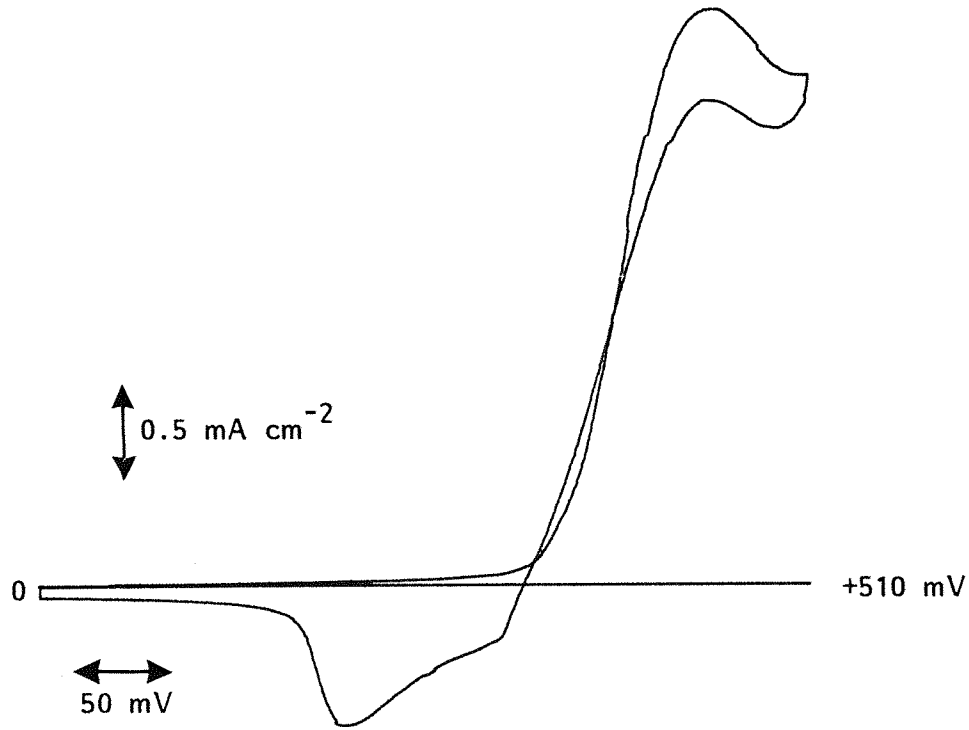

Figure 3.5 Voltammogram for a Ni electrode in 1M KOH + 0.1M ethanol run between 0 and 510 mV vs SCE at a sweep rate of 100 mV s^{-1}.

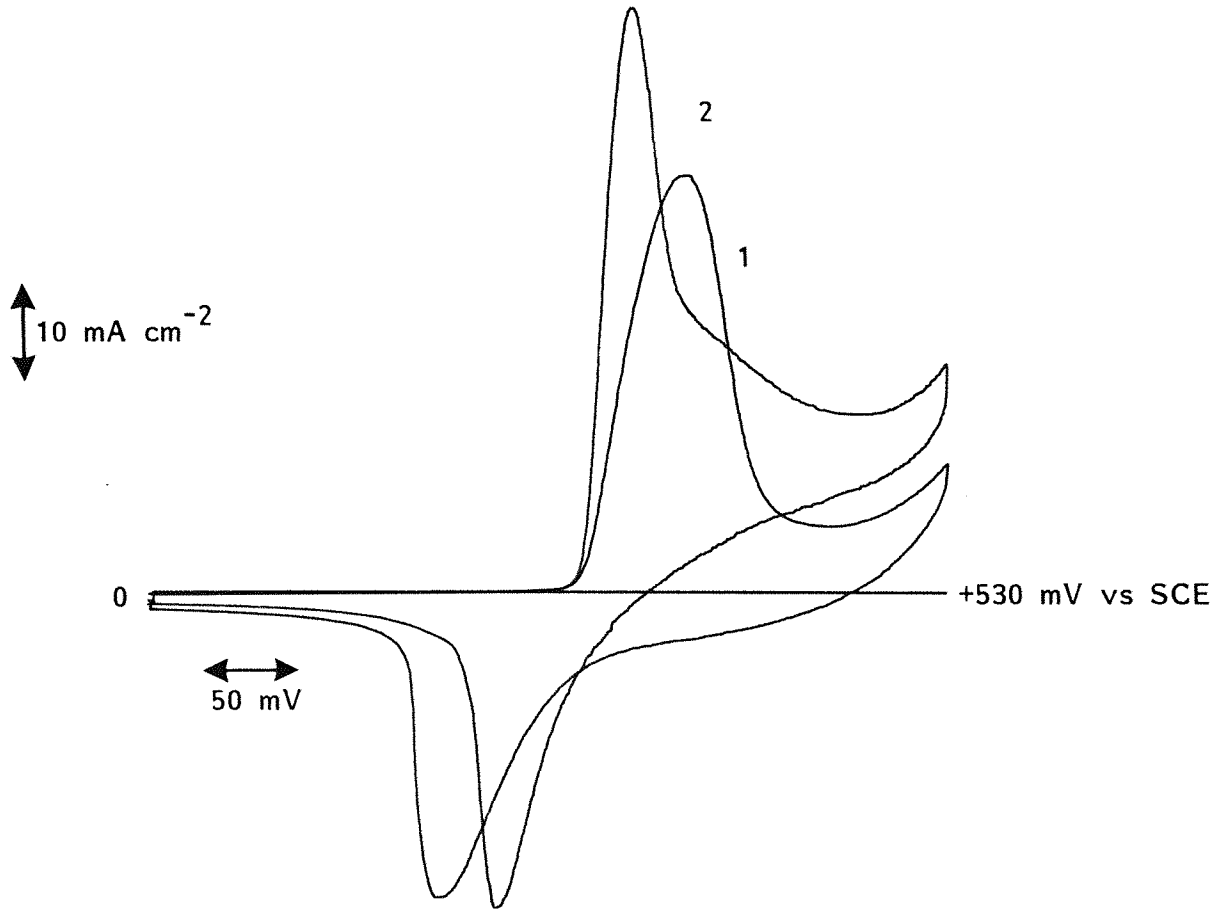

Figure 3.6 Voltammograms for an electrodeposited $Ni(OH)_2$ (1) without organic substrate (2) with organic substrate (0.1M ethanol) in 1M KOH run between 0 mV and 530 mV at a sweep rate of 20 mV s^{-1}. The electrode was prepared by cathodic deposition of $Ni(OH)_2$ from a 0.1M $Ni(NO_3)_2$ at a constant current density 2 mA cm^{-2} onto a Ni disc (0.2). Charge passed 0.6 C cm^2.

at an electrodeposited $Ni(OH)_2$ electrode for 0.1M ethanol in 1M potassium hydroxide at a sweep rate of 20 mV s^{-1}. A well formed oxidation peak at $E_p \simeq 320$ mV vs SCE was obtained, and a reduction peak at $E_p \simeq 195$ mV, which is comparable in height to the peak obtained in the absence of organic substrate. Hence the oxidation of ethanol is slow and may not occur within the bulk oxide at least on the timescale of cyclic voltammetry. Even so, oxidation of ethanol is clearly occurring and the current density at this thick oxide is much larger than that at the polished Ni surface. Oxygen evolution appears to be inhibited by the addition of ethanol.

3.2.1.3 Steady state I-E curves

Steady state I-E data were obtained by manual stepping of the potential. An increment of 10-15 mV was used and the current was noted after one minute at each potential. Figure 3.7 shows a steady state current vs potential plot over the range 0 mV and 650 mV for a 0.1M ethanol in 0.1M potassium hydroxide at polished nickel (in the absence of ethanol, no steady state current is observed below 0.5V. It can be seen that there is a well formed oxidation wave $E_{\frac{1}{2}}$ = 445 mV, but the current in the plateau region (0.6 mA cm^{-2}) is much less than that expected from a diffusion controlled oxidation of ethanol (maybe 40 mA cm^{-2}). The half wave potential $E_{\frac{1}{2}}$ = 445 mV coincided with the potential where the higher nickel oxide is produced in 0.1M potassium hydroxide. Similarly steady state current vs potential plots for the oxidation of ethanol on polished nickel and an electrodeposited nickel hydroxide electrode in 1M potassium hydroxide were obtained and are shown in figure 3.8 and figure 3.9. Figure 3.8 shows the behaviour for a 0.1M ethanol in 1M potassium hydroxide at polished nickel; there is a well formed oxidation wave, $E_{\frac{1}{2}}$ = 345 mV, but the current in the plateau region (1.7 mA cm^{-2}) is again much less than that expected from a diffusion controlled oxidation of ethanol. The value of the limiting current density obtained, however, is higher than in 0.1M KOH and also high in comparison to that reported earlier[59,68]. The half wave potential $E_{\frac{1}{2}}$ = 345 mV coincided with that where the higher nickel oxide is produced in 1M potassium hydroxide. Figure

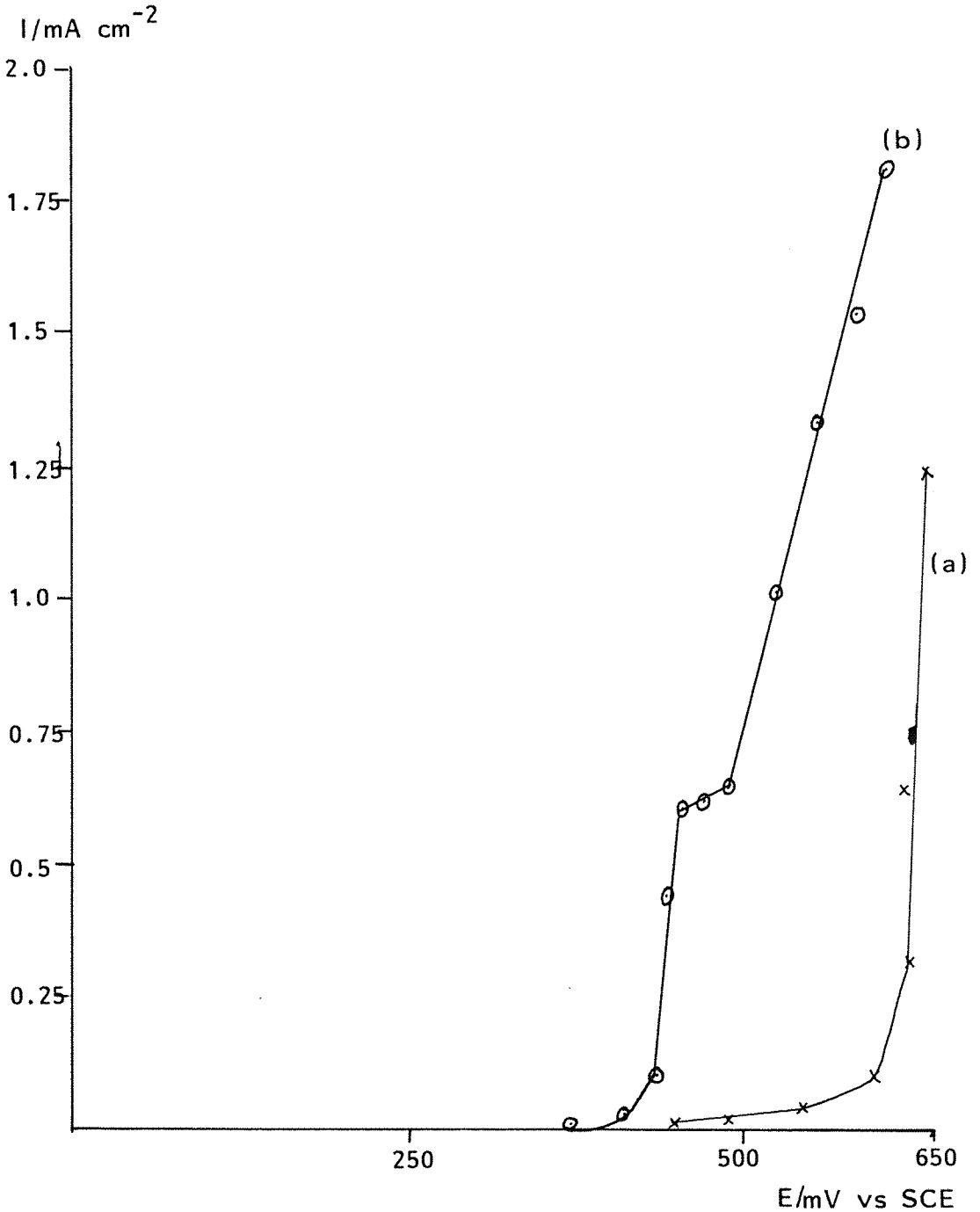

Figure 3.7 Steady state I-E curves for
(a) 0.1M KOH
(b) 0.1M EtOH in 0.1M KOH
at a Ni electrode.

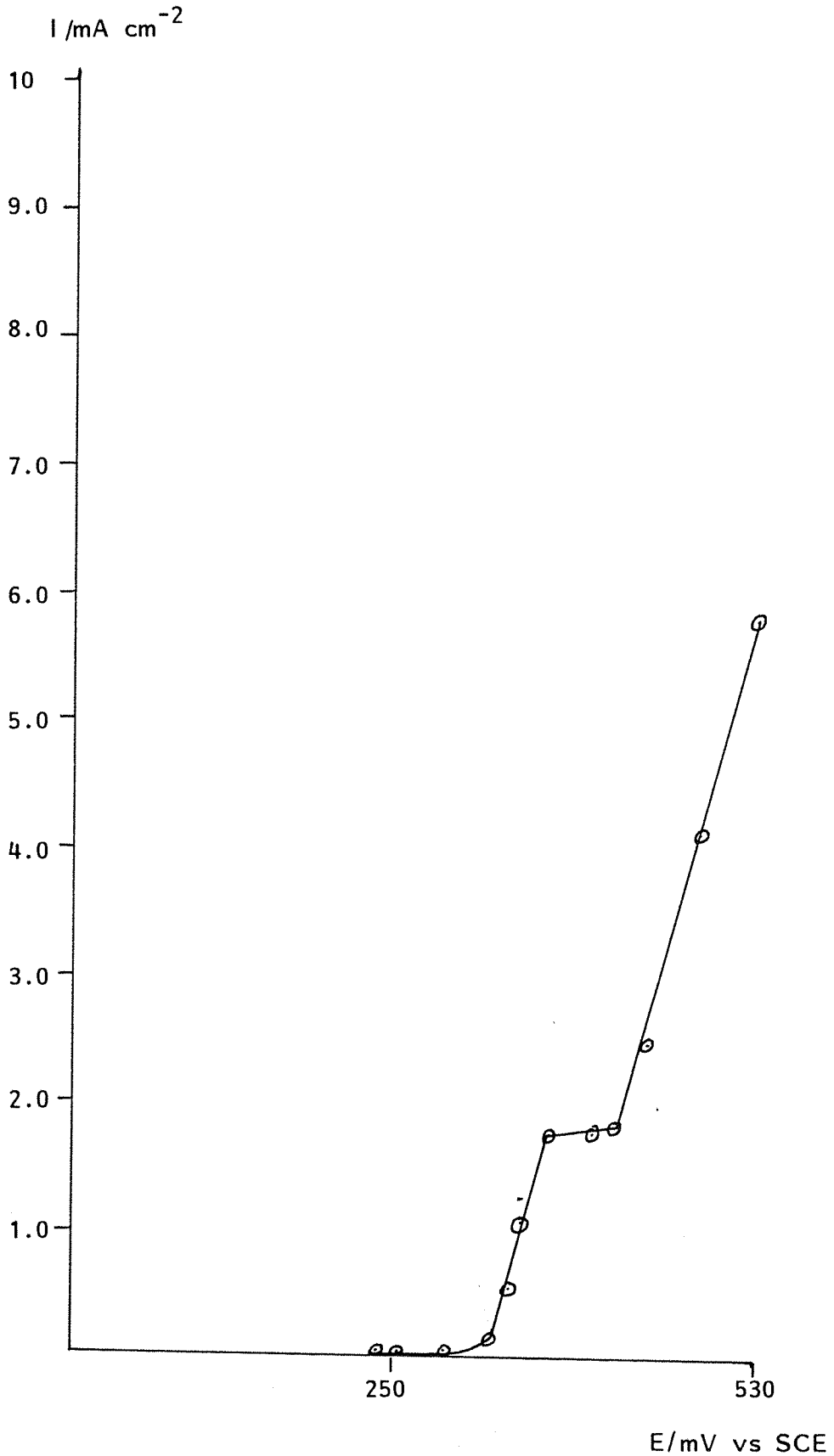

Figure 3.8 Steady state I-E curve for ethanol (0.1M) in 1M KOH at a Ni disc electrode (0.2 cm^2).

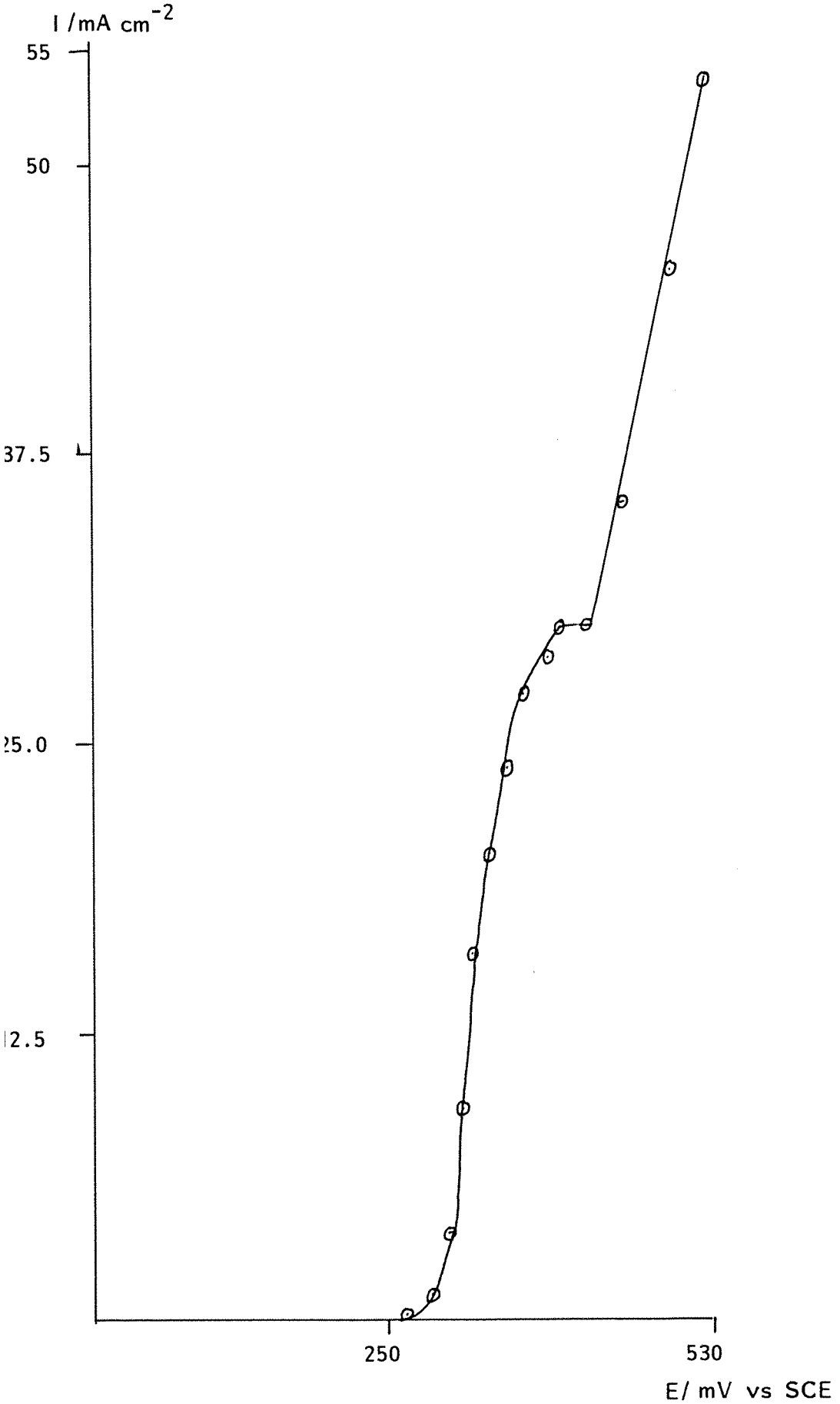

Figure 3.9 Steady state I-E curve for ethanol (1M) in 1M KOH at $Ni(OH)_2$ deposited onto a Ni wire (0.6 cm^2) from a 0.1M $Ni(NO_3)_2$ at a constant current density 2 mA cm^{-2}.
Deposition charge 0.72C cm^{-2}.

3.9 shows a steady state current vs potential plot for the oxidation of ethanol at an electrodeposited nickel hydroxide electrode (prepared in a similar way to that in Section 3.2.1.2) in 1M potassium hydroxide. A well formed oxidation wave $E_{\frac{1}{2}}$ = 325 mV is seen and the current in the plateau region (30 mA cm^{-2}) is much higher than at the polished disc and is approaching that expected for a diffusion controlled oxidation of ethanol. Certainly the electrodeposited nickel hydroxide appears to be much more active than polished nickel. The extent to which this is simply a surface area effect is uncertain.

3.2.1.4 Electrolysis of ethanol at a nickel smooth electrode in 1M potassium hydroxide

The objective of these electrolyses were to check the behaviour of the "Swiss Roll" cell and the work up procedure and analysis. Electrolysis was performed at several constant current densities (1.2 to 4 mA cm^{-2}) in the Swiss Roll Cell, see figure 2.3. These values were chosen on the basis of the steady state current vs potential plot where the limiting current was 1.75 mA cm^{-2}. Sufficient charge for a four electron/molecule oxidation was passed since the expected reaction was

$$CH_3CH_2OH + 4OH^- - 4e \longrightarrow CH_3COOH + 3H_2O$$

At the end of the electrolysis, the solution was neutralised by stepwise addition of an ion exchange resin, type IR-120(H), until the pH of the solution reached a constant value (pH = 2.8). The resin was then filtered off to leave an aqueous solution of electrolysis product free of inorganic salts. This was analysed by gas-liquid chromatography using a one metre 5% Porpak Q column. Results from the analysis are shown in table 3.2. Calculation showed that at the lowest current density (1.2 mA cm^{-2}) the cell converted the ethanol to acetic acid with 85% current efficiency. This is probably an underestimate since ethanol is likely to be lost during the electrolysis as a result of evaporation in the nitrogen stream used for mixing the solution. This yield compares with a 98% current yield reported earlier[57-58] using unstirred solution and controlled potential electrolysis

Table 3.2 Glc analysis of the electrolysis of 0.1M ethanol in 1M potassium hydroxide at a smooth nickel electrode (using a Swiss Roll Cell) at a constant current density.

Porapak Q column T = 165°C					
Current density mA cm^{-2}	Ethanol peak area before electrolysis	Peak areas after electrolysis		% EtOH left	Current efficiency/%
		EtOH	HOAc		
1.2	8.04	0.49	3.41	6	85
2.4	6.25	0.73	1.92	12	48
4	6.75	2.94	0.24	44	6
Standard 0.1M CH_3COOH	-	-	4.0	-	-

in quite a different cell design but is similar to that reported by Court[98] in another Swiss Roll cell. The current efficiency from the constant current electrolysis is often lower than for the comparable constant potential electrolysis due to the potential increase which occurs as the concentration of substrate diminishes; this leads to increase to secondary reactions such as oxygen evolution. Also it can be seen from table 3.2 that the current efficiency drops sharply as the current density is increased.

3.2.2 Oxidation of 2,2-dimethyl-1,3-propanediol

3.2.2.1 Cyclic voltammogram for a 0.1M 2,2-dimethyl-1,3-propanediol at a nickel disc electrode (0.2 cm^2) in a 1M potassium hydroxide

Figure 3.10 shows a voltammogram run at polished nickel for a solution of 0.1M 2,2-dimethyl-1,3-propanediol in 0.1M potassium hydroxide at a sweep rate 100 mV s^{-1}. On the forward sweep, a well formed oxidation peak ($E_p \simeq 550$ mV vs SCE) was observed, and the reverse sweep again shows an anodic peak at the same potential but it is slightly smaller. Formation of this peak was discussed in the previous section 3.2.1.1 (for review see ref. 95). The anodic peaks are larger than in the absence of organic substrate and there is only a small reduction peak at $E_p \simeq 385$ mV. Hence the oxidation of 2,2-dimethyl-1,3-propanediol occurs on the nickel hydroxide surface but is slow. In fact the oxidation peak is only about 1% of that expected for a diffusion controlled oxidation. Oxygen evolution commences before the positive limit, but appeared to occur only at a potential more positive than in the absence of organic substrate.

3.2.2.2 Cyclic voltammetry for 0.1M 2,2-dimethyl-1,3-propanediol at a nickel disc electrode in 1M potassium hydroxide

Figure 3.11 shows a voltammogram run at a nickel electrode (0.2 cm^2) for a solution of 0.1M 2,2-dimethyl-1,3-propanediol in 1M potassium hydroxide. Figure 3.11 shows the similar behaviour

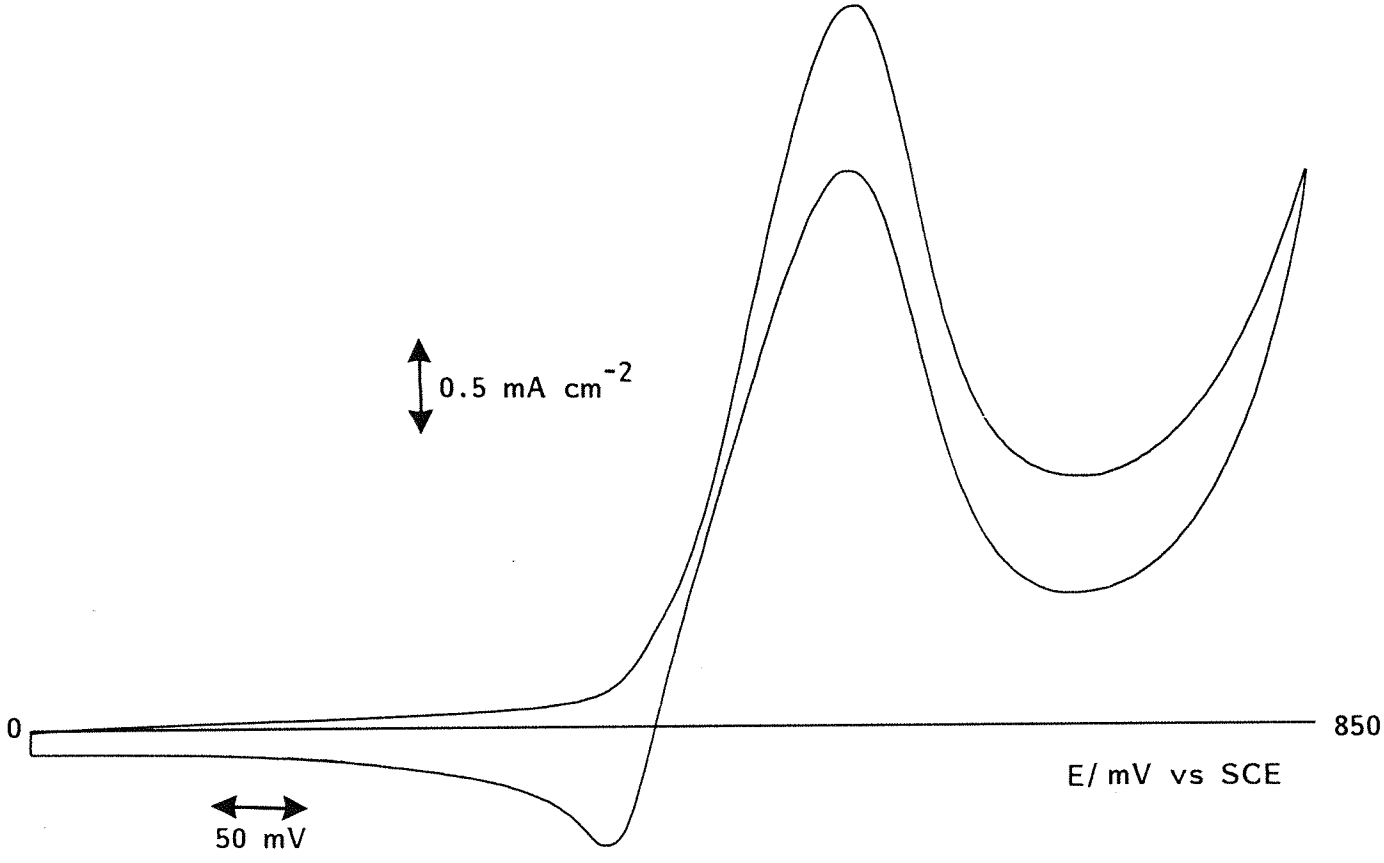

Figure 3.10 Cyclic voltamogram for a Ni smooth disc electrode in 0.1M KOH + 0.1M 2,2-dimethyl-1,3-propanediol run between 0 mV and 850 mV vs SCE. Potential sweep rate 100 mV s^{-1}.

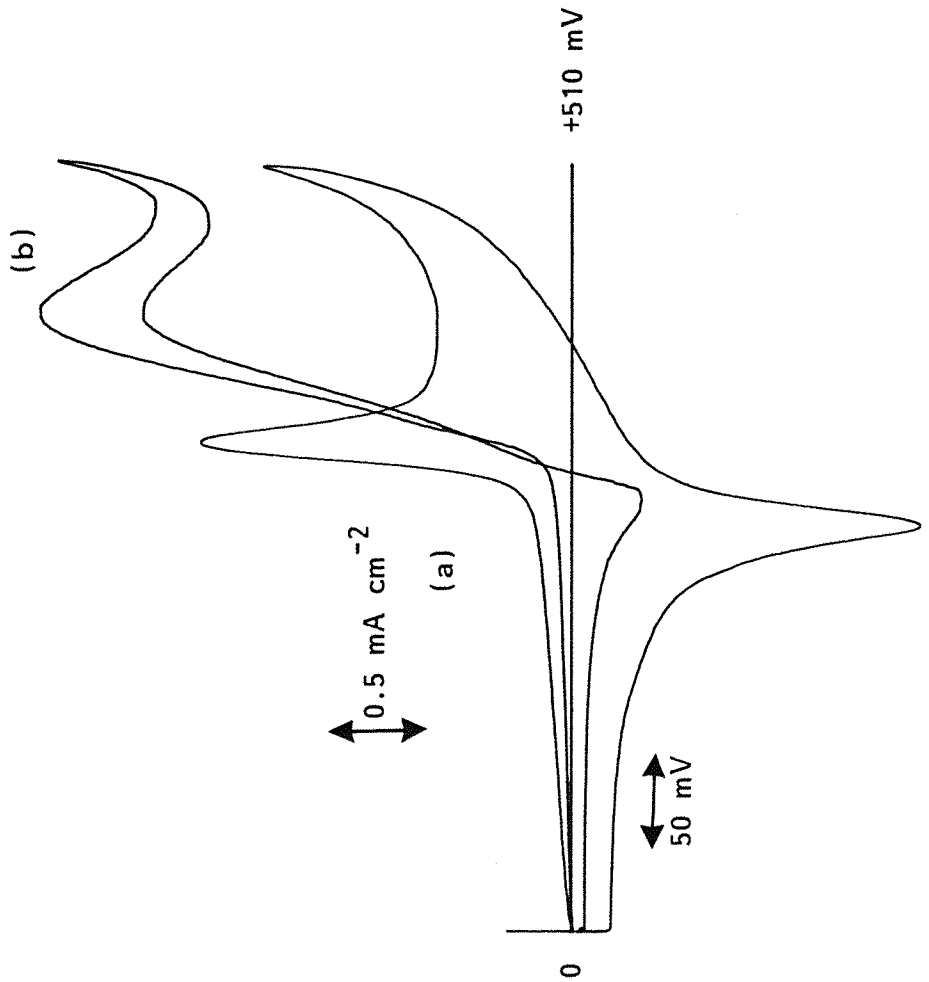

Figure 3.11 Voltammogram for a nickel disc electrode (0.2 cm^2) (a) 1M KOH and (b) 1M KOH + 0.1M 2,2-dimethyl-1,3-propanediol run between 0 mV and 510 mV vs SCE at a sweep rate 100 mV s^{-1}.

to that described in Section 3.2.1.1. Again the forward sweep shows a well formed oxidation peak ($E_p \simeq 405$ mV), and the reverse sweep shows that an anodic peak occurred at the same potential but is slightly smaller. Also there is a reduction peak at $E_p \simeq 285$ mV, which is smaller in comparison to the peak obtained in the absence of organic substrate and hence 2,2-dimethyl-1,3-propanediol oxidation is slow. Oxygen evolution commences at +510 mV.

3.2.2.3 Cyclic voltammetry for 0.1M 2,2-dimethyl-1,3-propanediol at an electrodeposited nickel hydroxide electrode in 1M potassium hydroxide

The electrode was prepared by the method described in section 3.2.1.2. Figure 3.12 shows a cyclic voltammogram run at an electrodeposited nickel hydroxide for a solution of 0.1M 2,2-dimethyl-1,3-propanediol in 1M potassium hydroxide at a relatively slow sweep rate (20 mV s^{-1}). A well formed oxidation peak ($E_p \simeq 355$ mV vs SCE) was observed and a reduction peak at $E_p \simeq 220$ mV, which is slightly smaller in comparison to the peak obtained in the absence of organic substrate. While the oxidation of 2,2-dimethyl-1,3-propanediol is slow, it can be seen that the current density for its oxidation is substantial at this electrodeposited nickel hydroxide electrode. It was observed that oxidation of 2,2-dimethyl-1,3-propanediol occurred at a slightly higher potential (55 mV) than that where the higher nickel oxide is produced in 1M potassium hydroxide. The shape of the I-E curve is very similar to that reported for ethylamine by Robertson[97].

3.2.2.4 Steady state I-E curves for 2,2-dimethyl-1,3-propanediol

The steady state I-E curves were obtained in a similar way to those in Section 3.2.1.3. Figure 3.13 shows a steady state current vs potential plot over the range 0 mV and 650 mV for a 0.1M 2,2-dimethyl-1,3-propanediol in 0.1M potassium hydroxide at polished nickel. It was observed that there was no plateau but a well formed oxidation peak ($E_p \simeq 460$ mV vs SCE) was obtained, indicating the onset of a passivation process (for review see ref. 95).

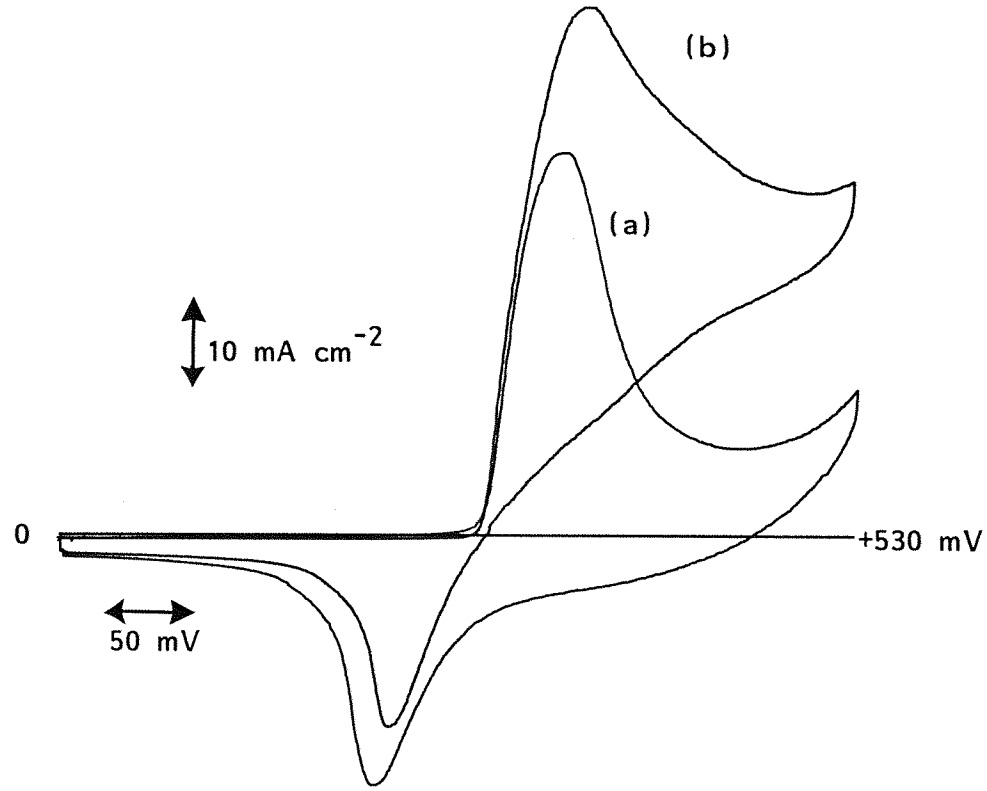

Figure 3.12 Voltammogram for electrodeposited $Ni(OH)_2$ on a nickel disc (10.2 cm^2) in 1M KOH (a) without organic substrate, (b) with organic substrate in 1M KOH, run between 0 mV and 530 mV vs SCE at a sweep rate of 20 mV s^{-1}.

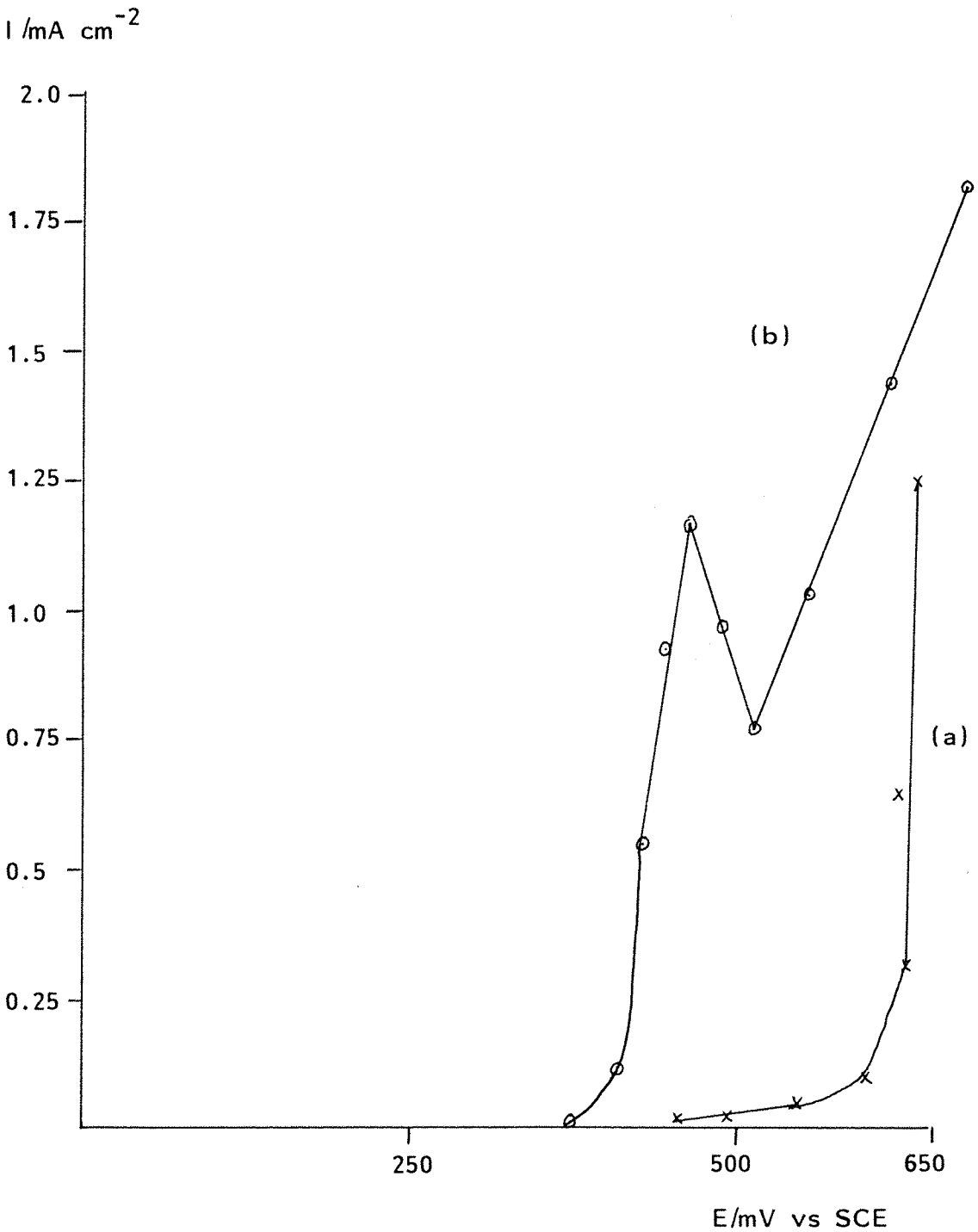

Figure 3.13 Steady state I-E curves for
(a) 0.1M KOH
(b) 0.1M 2,2-dimethyl-1-3-propanediol in 0.1M KOH
at a Ni electrode.

Oxygen evolution does not occur at the peak potential and, indeed, there is no steady state current in the absence of organic compound. Again the oxidation peak ($E_p \simeq 460$ mV vs SCE) coincides with the potential where the higher nickel oxide is produced in 0.1M potassium hydroxide.

Similarly a steady state current vs potential plots for the oxidation of 0.1M 2,2-dimethyl-1,3-propanediol in 1M potassium hydroxide at polished nickel and an electrodeposited nickel hydroxide electrode are shown in figure 3.14 and figure 3.15. Figure 3.14 shows a similar behaviour to that in figure 3.13. Again a well formed oxidation peak ($E_p \simeq 400$ mV vs SCE) was obtained, which is less positive than that where oxygen is evolved, showing the oxidation of 2,2-dimethyl-1,3-propanediol. Figure 3.15 shows a steady state current vs potential plot over the range 0 mV and 530 mV for a 0.1M 2,2-dimethyl-1,3-propanediol in 1M potassium hydroxide at an electrodeposited nickel hydroxide (prepared in a similar way to that described above). A well formed oxidation wave $E_{\frac{1}{2}} = 330$ mV vs SCE is observed and the current densities are very high compared to the polished nickel. Even so, the current in the plateau region (35 mA cm^{-2})is still less than that expected from a diffusion controlled oxidation of 2,2-dimethyl-1,3-propanediol. The increase in the limiting current density is probably due to an increase of roughness of the electrode. The half wave potential ($E_{\frac{1}{2}} \simeq 330$) coincided with that where the higher nickel oxide is produced in 1M potassium hydroxide. Data are summarised in table 3.3. The value of the limiting current density obtained from the steady state current vs potential plots varied from individual compounds as can be seen in table 3.3. All these values are, however, well below the value to be expected for a diffusion limited current which can be found by substituting estimated values into the equation

$$i_L^D = \frac{nFDc^{\infty}}{\delta}$$

where n = number of electrons transferred. For the conversion of one primary hydroxyl group to carboxylate group, n = 4. For

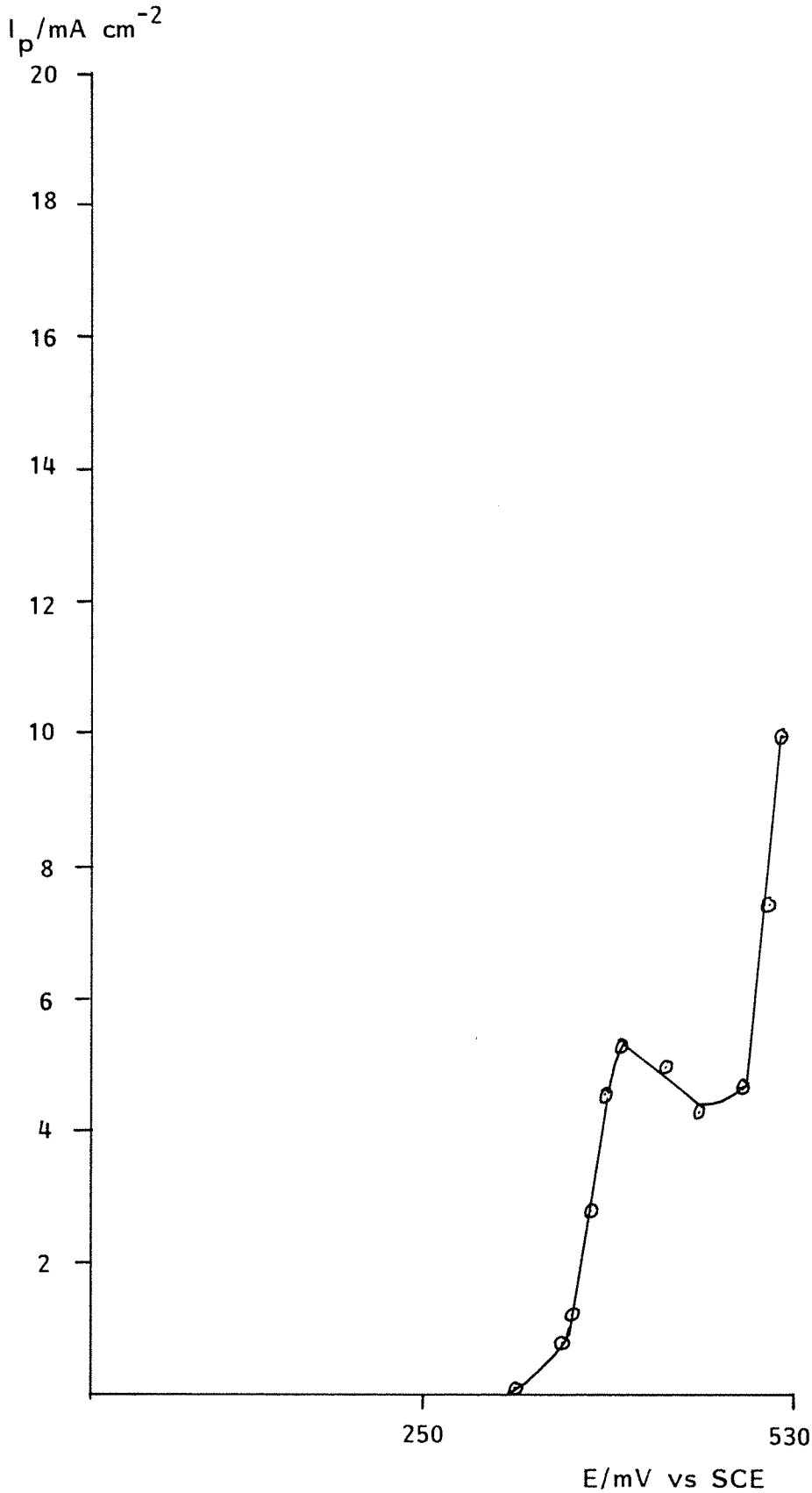

Figure 3.14 Steady state I-E curve for 0.1M 2,2-dimethyl-1,3-propanediol in 1M KOH at Ni disc electrode (0.2 cm^2)/

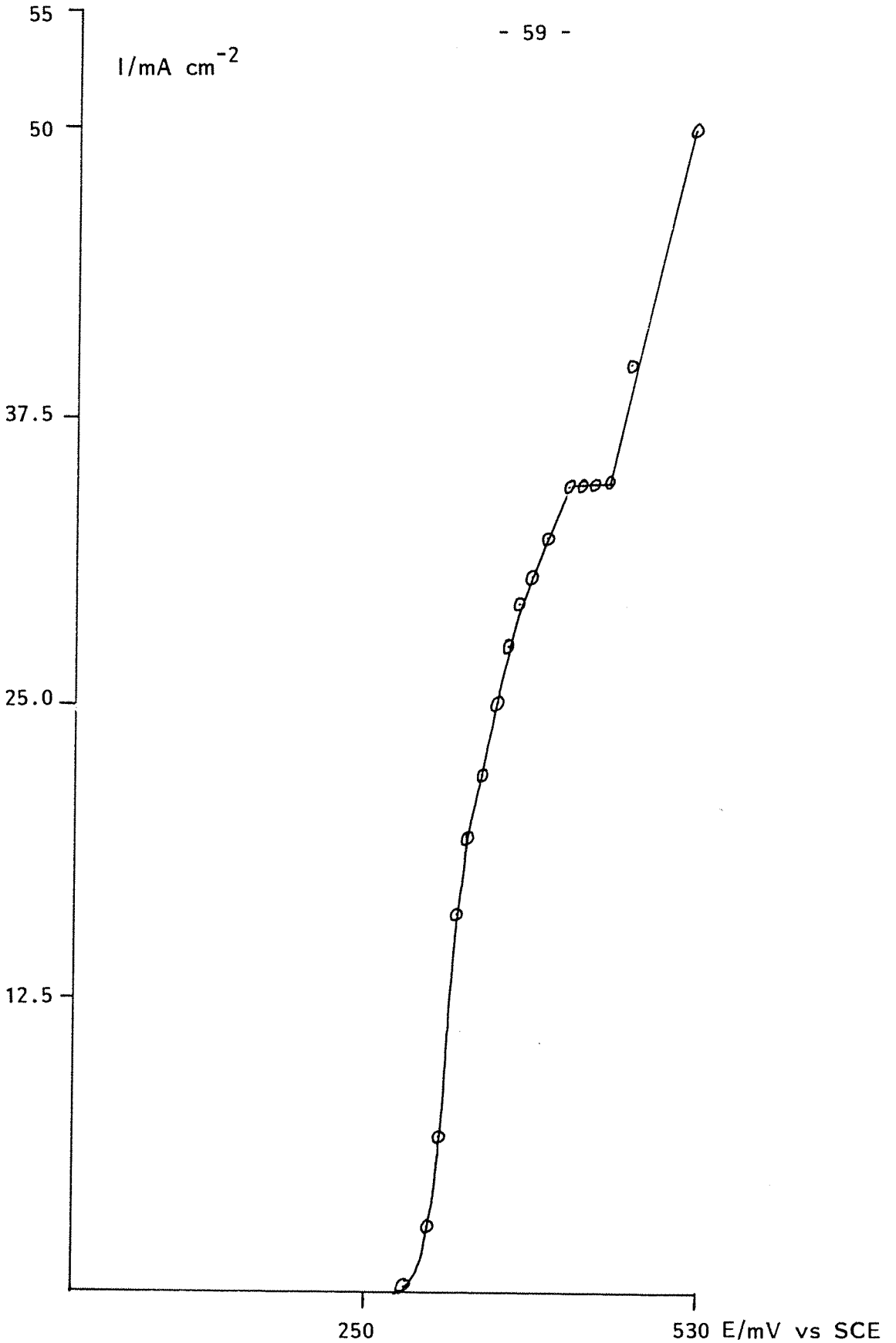

Figure 3.15 Steady state I-E curve for 0.1M 2,2-dimethyl-1,3-propanediol in 1M KOH at an electrodeposited nickel hydroxide electrode (0.6 cm^2), prepared at constant current density of 2 mA cm^{-2} with total charge 0.72C cm^{-2}.

example, for ethanol n = 4 electrons per molecule, whereas for 2,2-dimethyl-1, 3-propanediol n = 8 electrons per molecule

F = Faraday constant (10^5C mol^{-1})

D = Diffusion coefficient, typically 10^{-5} cm^2 s^{-1}

c^{∞} = Bulk concentration of organic species = 10^{-4} mole cm^{-3} (for a 0.1M solution)

δ = Nernst diffusion layer thickness, typically 10^{-2} cm.

Therefore the value of the limiting currents for n = 4 electrons per molecule and for n = 8 electrons per molecule processes should be about 40 mA cm^{-2} and 80 mA cm^{-2} respectively. As reported for the simple alcohols[57], the steady state limiting currents are much smaller and therefore appear to be kinetically controlled. The variation in the value of the limiting current for different compounds as reported in table 3.3 is dependent upon the following factors.

1. The number of electrons involved in the oxidation of the organic molecule.

2. The roughness of the electrode surface.

3. The rate of reaction between the organic compound and the oxidised nickel surface[67,69].

4. Temperature

5. Concentration

The current depends on the number of electrons involved in the oxidation. This will depend on the number of primary hydroxyl groups available for oxidation and also on how far they are oxidised. For example, oxidation of ethanol to acetic acid, cyanoethanol to cyano-

acetic acid would both be four electron processes, whereas oxidation of 2,2-dimethyl-1,3-propanediol to 2,2-dimethylpropanedioc acid would be an eight electron process. The real area of nickel oxide surface available as an oxidising agent is very much affected by the roughness of the nickel surface which may be enhanced by depositing a thick layer of nickel hydroxide. By cathodic deposition of a nickel hydroxide[67,75-77] before electrolysis a much thicker oxidising layer is obtained. The porosity of this layer offers a much higher active area, enabling the current density and the limiting current of a reaction to be increased by an order of magnitude, as seen in table 3.3.

It has been claimed[67,69] that it is the ease of the hydrogen atom abstraction from the carbon α to the hydroxyl group which will determine the rate of reaction and hence the current. The stereochemistry of the molecule will also affect the extent of adsorption onto an electrode; this was also seen to be part of the rate determining step. The order of primary alcohol > secondary alcohol > tertiary alcohol has been noted. The value of limiting current is also affected by the variation of concentration and temperature.

3.2.2.5 Electrolysis of 2,2-dimethyl-1,3-propane diol at a smooth nickel electrode in 1M potassium hydroxide (using the Swiss Roll Cell).

Electrolyses of 100 cm^3 of 0.1M 2,2-dimethyl-1,3-propanediol in 1M potassium hydroxide were performed at constant current densities of 0.5 mA cm^{-2} and 2.5 mA cm^{-2} in the Swiss Roll Cell, see figure 2.3. These values were selected from the steady state current vs potential plots, i.e. figure 3.14. Oxidation to 2,2-dimethylpropanedioc acid would be an eight electron/molecule process

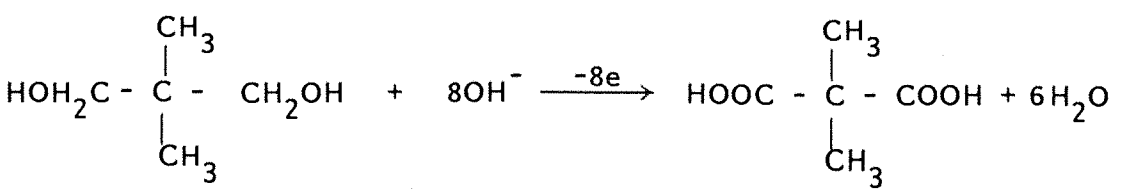

Table 3.3 Value of the limiting current for the oxidation of 0.1M organic substrate in potassium hydroxide at a nickel disc and an electrodeposited nickel hydroxide electrode

Substrate	Limiting currents mA cm^{-2}		
	X	XX	XXX
0.1M ethanol	0.6	1.75	30
0.1M 2-cyanoethanol	-	0.95	29
0.1M 2,2-dimethyl-1,3-propanediol	-	-	35

Footnotes:

X = 0.1M KOH at Ni disc (0.2 cm^2)

XX = 1M KOH at Ni disc (0.2 cm^2)

XXX = 1M KOH at an electrodeposited $Ni(OH)_2$ electrode at a constant current (2 mA cm^{-2}) on a Ni wire (0.6 cm^2).

Therefore, sufficient charge for an eight electron process, as calculated using Faraday's law of electrolysis (i.e. Q = nxFx number of moles of the substrate, where n = 8 and F is the Faraday constant 10^5C mol^{-1}) was passed. At the end of the electrolyses the solution was neutralised using IR-120 (H) resin and isolated from the solution by removing water on a rotary evaporator. The residue was esterified after addition of an internal standard (the procedure is described in the experimental section). The sample was then injected into a 5% OV-101 glc column. Results from the analysis are shown in table 3.4. Calculations showed that at the lowest current density (0.5 mA cm^{-2}) the cell converted the 2,2-dimethyl-1,3-propanediol to 2,2-dimethylpropanediocacid with 22% current efficiency. This is an unexpected low value.

3.2.2.6 Electrolysis of 2,2-dimethyl-1-3-propanediol at an electrodeposited nickel hydroxide electrode in 1M potassium hydroxide

The electrode was prepared in a similar way to those in section 3.1.3. Electrolysis of 0.1M 2,2-dimethyl-1,3-propanediol in 1M potassium hydroxide at an electrodeposited nickel hydroxide electrode was carried out in a beaker cell where the plate working electrode had a counter electrode plate on either side, see figure 2.4, at a constant current density (typically 8 mA cm^{-2} and 17 mA cm^{-2}). These values were chosen from the steady state current vs potential plot where the limiting current was 35 mA cm^{-2}. At the end of the electrolysis, the solution was worked up and analysed as described earlier. The results from the analyses are shown in table 3.5. Calculations showed that at the lowest current density (8 mA cm^{-2}) the cell converted 2,2-dimethyl-1,3-propanediol to 2,2-dimethyl propanediocacid with a 31% current efficiency. This current efficiency is 40% higher than compared with a smooth nickel anode (Swiss Roll Cell) even though the current density is higher. This is probably due to an increase in the surface roughness on forming the electrodeposited nickel hydroxide layer. More charge leads to an increase in the product yield (see table 3.5) but the current

Table 3.4 Glc analysis of esterified product from the electrolysis of 2,2-dimethyl-1,3-propane diol in 1M potassium hydroxide at a nickel electrode at constant current density

5% OV 101 column T = 110°C							
Sample (2 μL)	I mA cm^{-2}	A1 cm^2	A2 cm^2	A3 cm^2	A4 cm^2	Product yield/%	Current efficiency
1. Electrolysed product after esterification	0.5	-	-	1.2	0.54	22	22
2. " "	2.5	-	-	1.22	0.42	17	17
3. Standard 0.1g malonic acid + 0.1g dimethyl malonic acid esterified	-	1.2	1.83	-	-	-	-

Footnote: A1 = Dimethylmalonate
A2 = Dimethyldimethylmalonate } standard solution
A3 = Dimethylmalonate
A4 = Electrolysed product.

$$\text{Yield} = \frac{A_4 \times A_1}{A_2 \times A_3 \times \text{expected acid}}$$

Current efficiency = % product yield based on product yield expected by Faraday's law.

Table 3.5 Glc analysis of esterified product from the electrolysis of 2,2-dimethyl-1,3-propanediol (0.1 M) in 1M potassium hydroxide at an electrodeposited nickel hydroxide electrode.

5% OV 101 Column T = 110°C									
Sample 0.5 µL	No. of mmoles of substrate	I mA cm^{-2}	Charge passed C	Area cm^2 A1	A2	A3	A4	Product yield %	Current efficiency %
1. Electrolysed product	5	8	4000	-	-	4.2	1.575	31	31
2. " "	7.5	17	6000	-	-	4.6	0.95	17	17
3. " "	4.5	17	7344	-	-	4.12	1.26	25	12
4. " "	4.5	17	17626	-	-	4.88	1.93	32	7
5. Standard 0.1g malonic acid + 0.1g dimethyl malonic acid	-	-	-	4.4	4.08	-	-	-	-

Footnote: A1 = Dimethylmalonate
A2 = Dimethyldimethylmalonate } Standard solution
A3 = Dimethylmalonate
A4 = Dimethyldimethylmalonate (electrolysis product)

efficiency drops off as a side reaction; probably O_2 evolution becomes more important.

3.2.3 Oxidation of 2-cyanoethanol

3.2.3.1 Steady state I-E curve for 0.1M 2-cyanoethanol in 1M potassium hydroxide at a nickel disc electrode (0.2 cm^2)

The steady state I-E curves were obtained in a similar way to those described in previous sections. Figure 3.16 shows a steady state current vs potential plot for a 0.1M 2-cyanoethanol in 1M potassium hydroxide at a nickel disc electrode (0.2 cm^2). An oxidation wave $E_{\frac{1}{2}}$ = 400 mV vs SCE was observed, but the current in the plateau region (0.95 mA cm^2) is very low. The half wave potential $E_{\frac{1}{2}}$ = 400 mV coincided with that where the higher nickel oxide is produced in 1M potassium hydroxide.

A steady state I-E plot for the oxidation of 2-cyanoethanol in 1M potassium hydroxide at an electrodeposited nickel hydroxide electrode is shown in figure 3.17. A well formed oxidation wave $E_{\frac{1}{2}}$ = 370 mV was observed, and the current in the plateau region (29 mA cm^{-2}) is again, as expected, much enhanced. The half wave potential ($E_{\frac{1}{2}}$ = 370 mV) occurred at a slightly higher potential (70 mV) than that where a higher nickel oxide is produced in 1M potassium hydroxide using an electrodeposited nickel hydroxide electrode.

3.2.3.2 Electrolysis of 2-cyanoethanol at an electrodeposited nickel hydroxide electrode

The electrode and cell were as described in the previous section. Electrolyses of 0.1M 2-cyanoethanol in 1M potassium hydroxide was carried out at a constant current density (typically 7 mA cm^{-2} or 10 mA cm^{-2}). These values were chosen from the steady state current vs potential plots, i.e. figure 3.17. At the end of the electrolysis, the solution was neutralised using IR-120 (H) resin (the detailed procedure is described above). The electrolysis product was esterified with a BF_3/CH_3OH mixture. A sample was

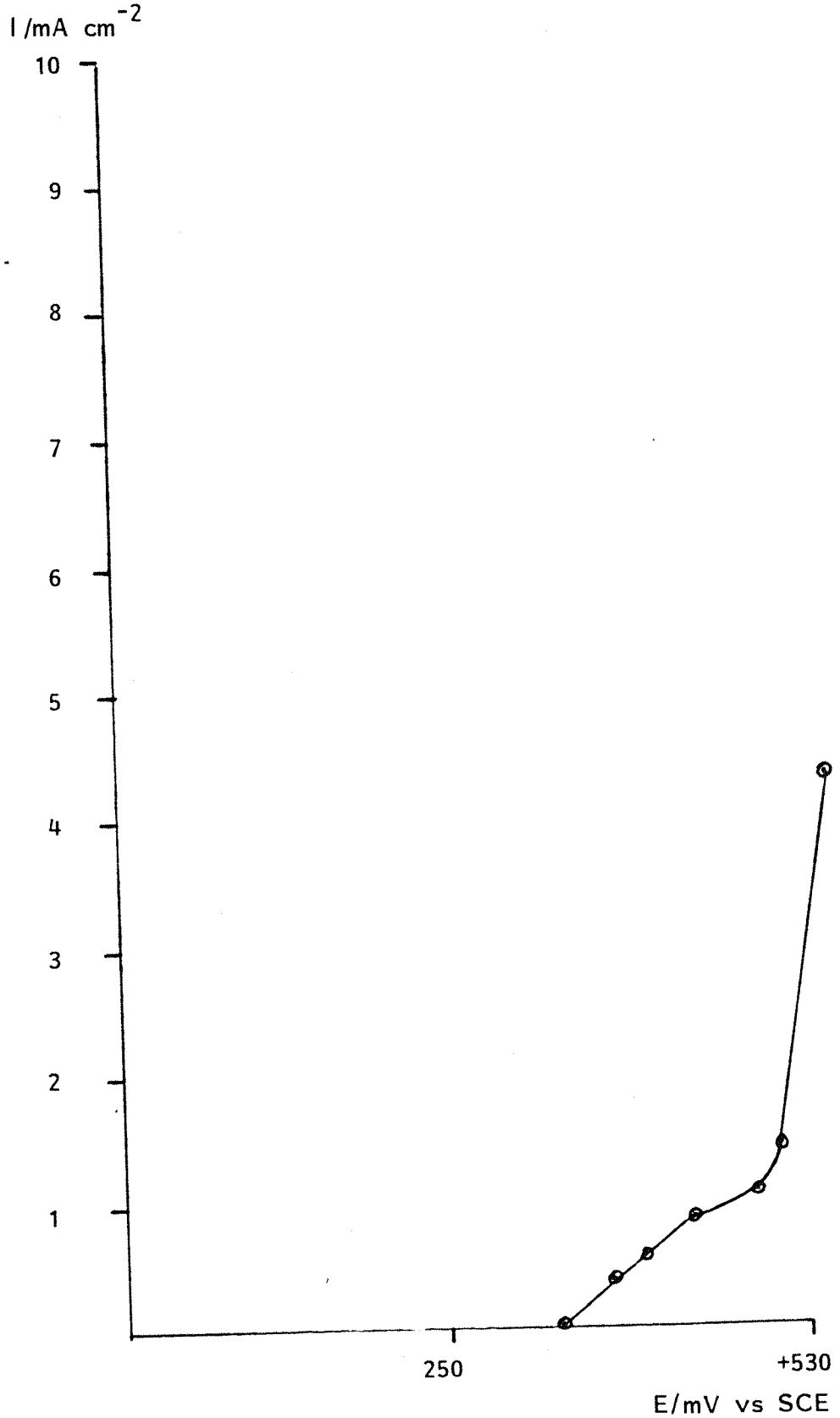

Figure 3.16 Steady state I-E curve for 0.1M cyanoethanol in 1M KOH at Ni disc electrode (0.2 cm^2).

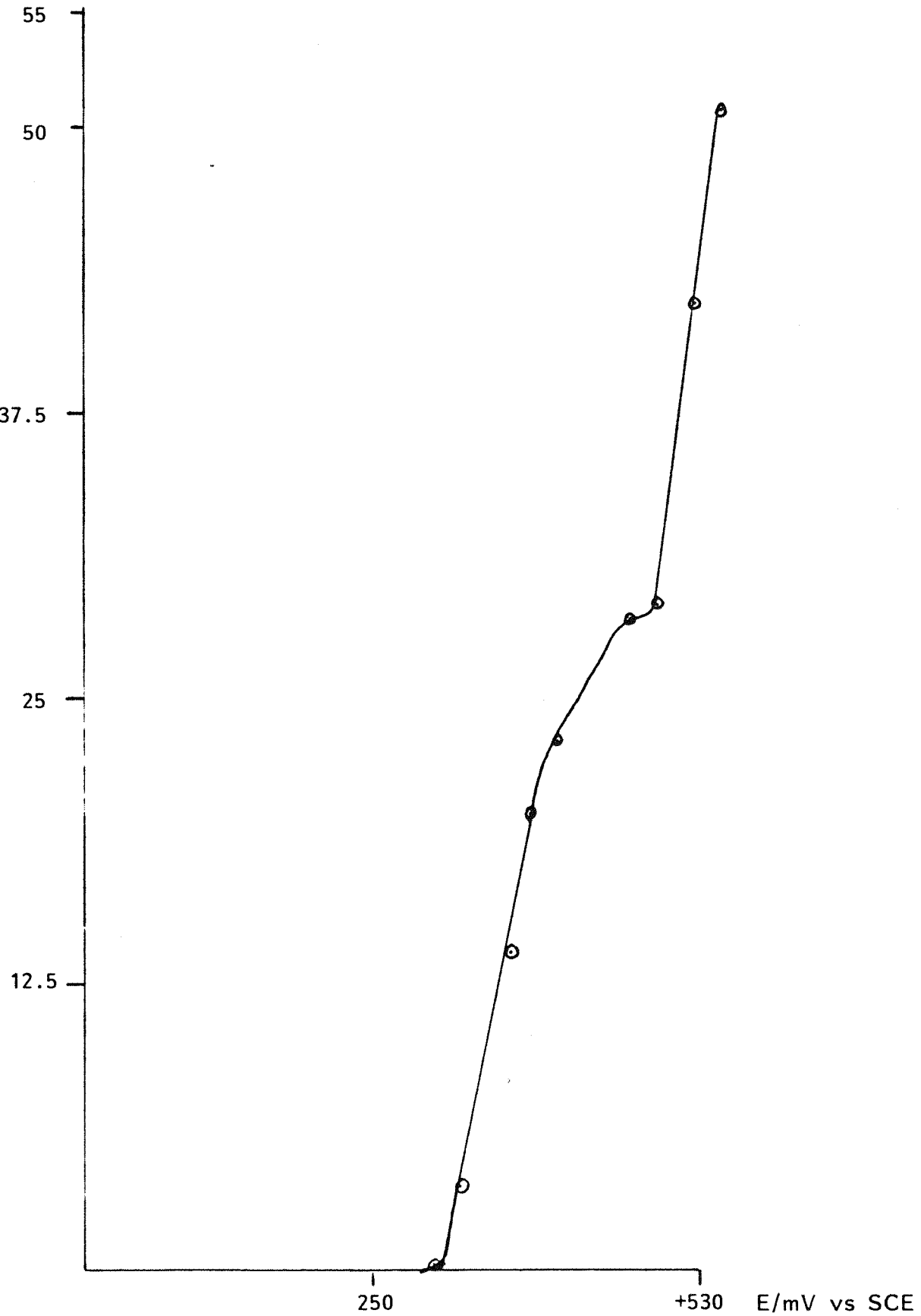

Figure 3.17 Steady state I-E curve for 0.1M cyanoethanol in 1M KOH at an electrodeposited nickel hydroxide electrode (0.6 cm^2) prepared at constant current density of 2 mA cm^{-2} with total charge 0.43C cm^{-2}.

analysed by using a 5% OV 101 glc column. Results from the analysis are shown in table 3.6. It was found that the retention time of the product differed from that of the expected product (methyl cyanoacetate) by about 31% but was identical to that for dimethyl oxalate. This confirmed that the product of the electrolysis is oxalic acid, not cyanoacetic acid. The mechanism for the formation of this unexpected product was probed further in the following experiments.

1. 0.1M cyanoethanol dissolved in water was left for 12 hours, then the water was removed by gentle heating under reduced pressure. Infrared spectra showed a band in the region 2060 cm^{-1} which is due to N ≡ C group (cf IR for pure $NCCH_2$-CH_2OH). Hence cyanoethanol is stable in a neutral aqueous solution.

2. 0.1M cyanoethanol dissolved in 1M potassium hydroxide was left for about 6 hours and then treated with the same work up procedure. Infrared spectra showed a band in the region 1720 cm^{-1}, which is due to -COOH group, but no peak at 2060 cm^{-1}. This showed that cyanoethanol undergoes hydrolysis upon prolonged treatment with potassium hydroxide even at room temperature. Hence the interpretation of the preparative electrolysis must take into account this hydrolysis reaction, and it is likely that the oxalic acid arises by the route on the next page. If this reaction pathway is correct the formation of oxalic acid is a 10 electron process and this is the assumption made in estimating the yield, see table 3.6.

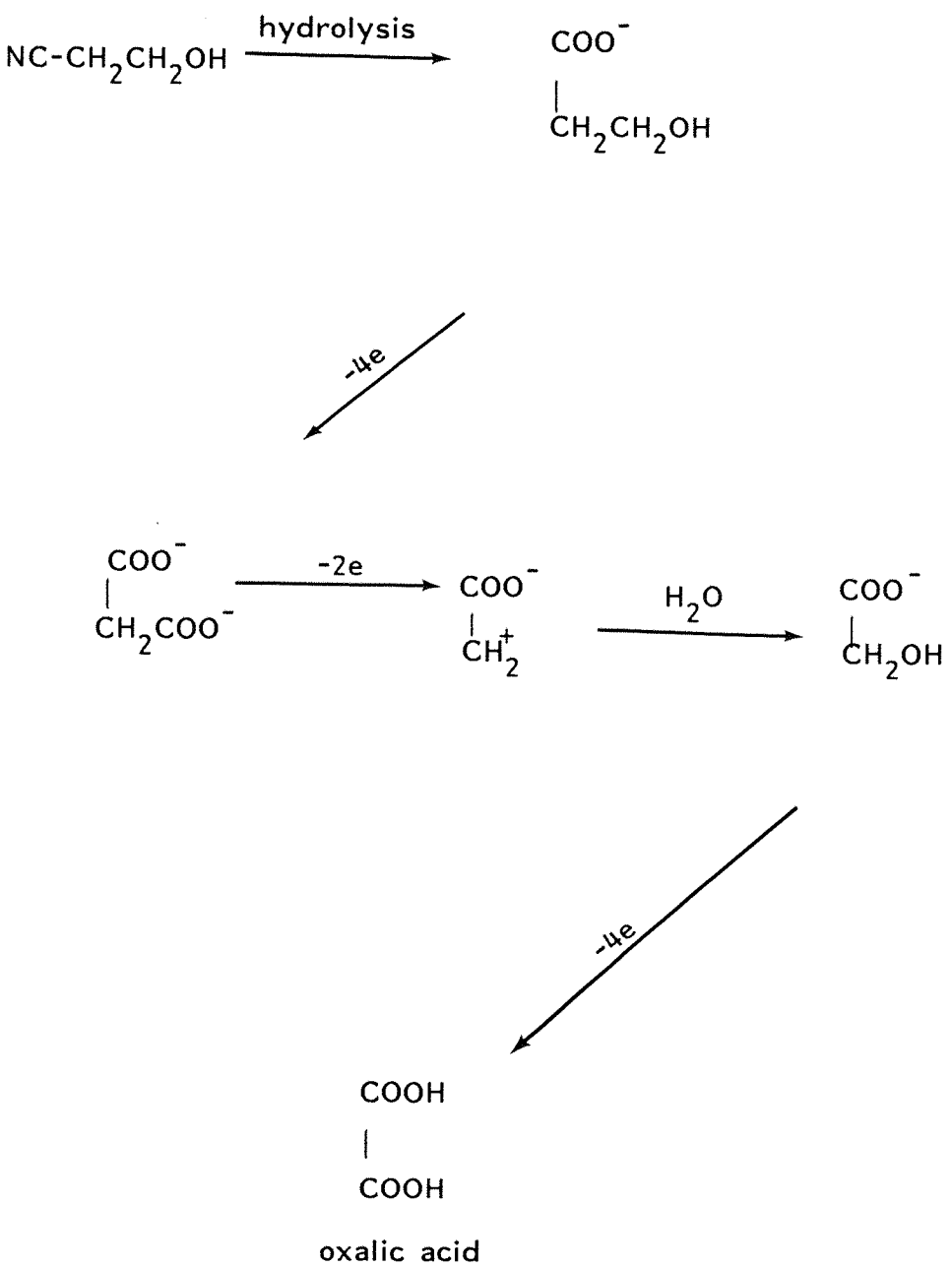
NC-CH2CH2OH
hydrolysis
COO-
CH2CH2OH
-4e
COO-
CH2COO-
-2e
COO-
CH2+
H2O
COO-
CH2OH
-4e
COOH
COOH

oxalic acid

Table 3.6 Glc analysis of the electrolysis of 0.1M 2-cyanoethanol in 1M potassium hydroxide at an electrodeposited nickel hydroxide electrode at a constant current density

5% OV 101 Column T = 110°C				
Sample 2 µL	I mA cm^{-2}	Retention time minutes	Peak area cm^2	Current yield of oxalic acid %
1. 2-cyano ethanol electrolysed and esterified	7	2.4	0.865	46
2. 2-cyanoethanol electrolysed and esterified	10	2.4	0.7	37.5
3. Standards				
(a) 0.1g cyanoacetic acid esterified	-	3.1	4.1	-
(b) 0.1g oxalic acid esterified	-	2.4	3.7	-

CHAPTER 4

Cobaltoxide spinel structure of the formula $Zn_xCo_{3-x}O_4$ in sulphuric acid.

CHAPTER 4

4.1 Study of Cobalt Oxide (Co_3O_4) Spinel Structure in Acidic Media.

4.1.1 Cyclic voltammetric behaviour in sulphuric acid

The electrodes were prepared by coating onto a titanium electrode substrate a layer with a cobalt oxide spinel structure (Co_3O_4) in a similar way to that described in the previous literature[97,99]. The preparation is relatively simple. A solution of 1M cobalt nitrate was sprayed onto an acid etched ($HF:HNO_3$) titanium wire area (0.31 cm^2) and the water was evaporated in a laboratory oven to leave a layer of cobalt nitrate. These coating steps were repeated 6 to 12 times before the nitrate on the surface was thermally oxidised at 275°C for an hour to form oxide.

The cyclic voltammograms in 5M sulphuric acid, run between 0 mV and 1900 mV are shown in fig. 4.1. Well formed oxidation peaks are observed at all sweep rates; at 50 mV s^{-1} $E_p \simeq$ 1340 mV vs S.C.E. On the reverse scan only very small reverse peaks occurred at +560 mV and the oxidation is clearly irreversible. The ratio of Q_C/Q_A is less than 0.1. Oxygen evolution commences at approximately 1840 mV. The peak potential (E_p) shifted to more positive potential with increasing the sweep rate, see table 4.1. A plot of oxidation peak current density against the square root of sweep rate, figure 4.2, is linear. This suggests that the anode reaction is diffusion controlled beyond the peak and this is confirmed by the shape of the peak. On the other hand, the peak current densities are very low for diffusion control with respect to any species in solution. Figure 4.3 shows the I-E response to repetitive cycling of the potential between 0 mV and 1700 mV. It can be seen that during the early cycles, a slight decrease in peak current density is observed but

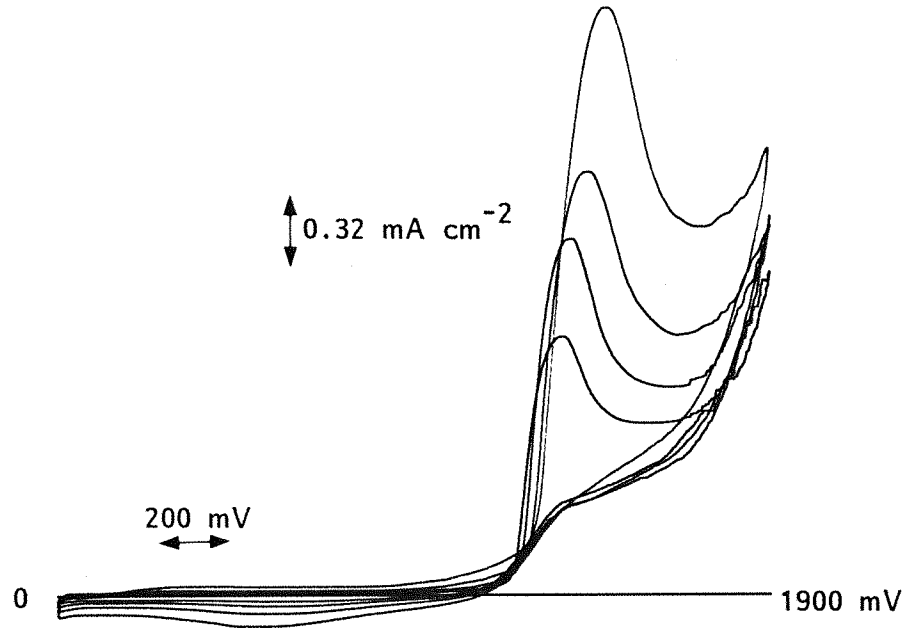

Fig. 4.1 Cyclic voltammogram in 5M sulphuric acid at a sweep rate, (i) 50 mV s^{-1}, (ii) 100 mV s^{-1}, (iii) 200 mV s^{-1} and (iv) 400 mV mV s^{-1} at a cobalt oxide spinel structure Co_3O_4.

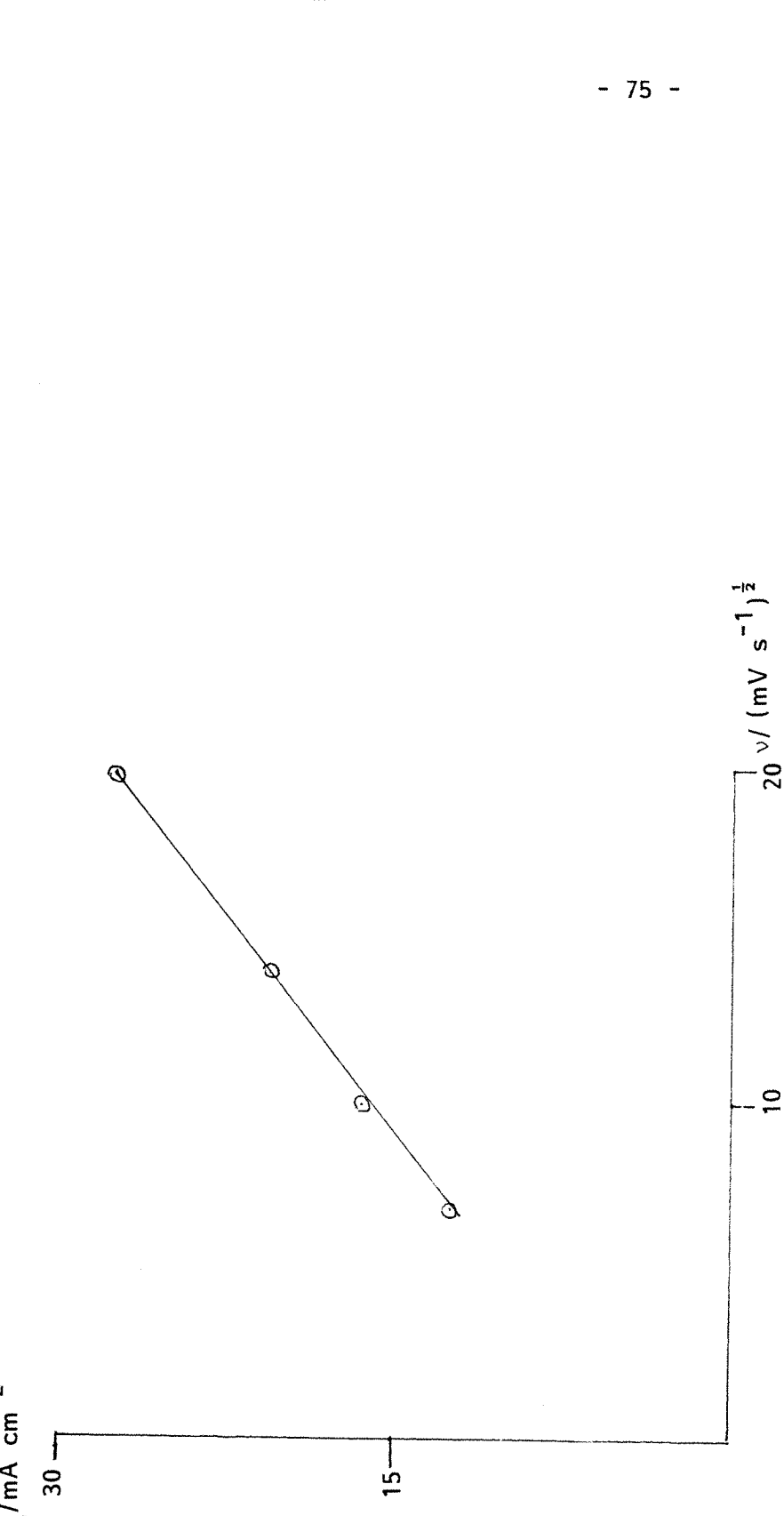

Fig. 4.2 Plot of I_p vs $\nu^{\frac{1}{2}}$ for cobalt oxide (Co_3O_4) spinel structure electrode in 5M sulphuric acid.

TABLE 4.1

Sweep rate $mV\ s^{-1}$	E_p mV	I_p $mA\ cm^{-2}$	Total charge under the oxidation peak $mC\ cm^{-2}$	Charge under the reduction peak $mC\ cm^{-2}$
50	1340	1.3	18	0.22
100	1380	1.8	13	0.22
200	1440	2.0	7	0.16
400	1500	2.6	5	0.14

Data obtained for a voltammogram in 5M sulphuric acid for a cobalt oxide spinel structure electrode (Co_3O_4)

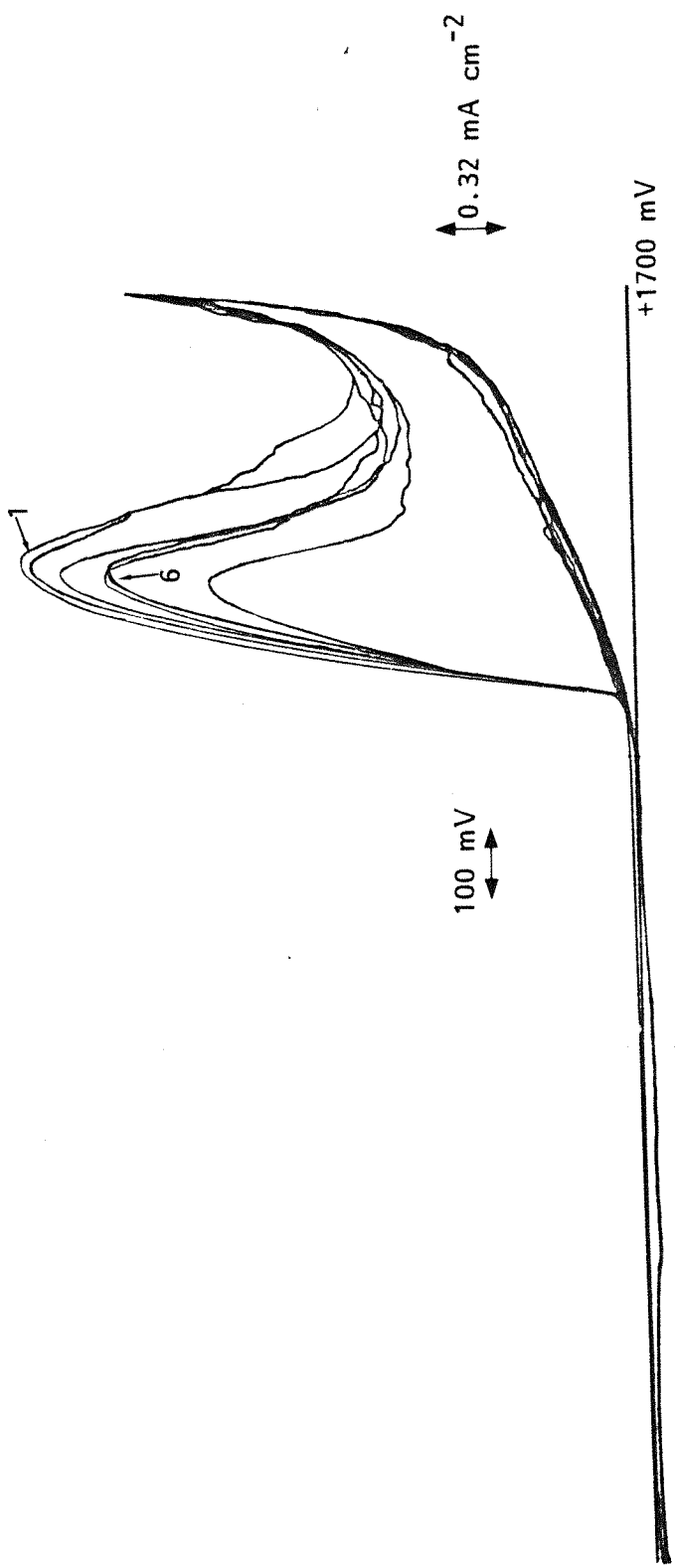

Fig. 4.3 Cyclic voltammogram in 5M sulphuric acid at a repetitively cycled i.e. 400 mV s^{-1}, at a cobalt oxide spinel structure Co_3O_4.

by about the sixth a steady state situation seems to have been reached and peak occurs at the same potential as the first cycle; the peak current is only 10-15% lower. During such extended experiments the colour of the oxide surface changes from brown to blue, the colour expected for a Co(III) species. The cyclic voltammetric response was also investigated in other H_2SO_4 concentrations; the curves for 1M and 9.3M are shown in figures 4.4 and 4.5. In the more concentrated acid, the anodic peak occurs at 1450 mV and has a similar shape to that in 5M H_2SO_4. Moreover the peak current density is similar. On the other hand, no cathodic peak can be observed and there is a small nucleation loop close to the foot of the peak. In 1M H_2SO_4 the anodic peak is absent even when the current sensitivity is increased by a factor of a thousand. Figure 4.6 shows the steady state I-E response in 5M H_2SO_4 in the form of a Tafel plot. Although the currents are low, it is clear that a steady state process is occurring in the potential region above 1100 mV.

Several electrode reactions could lead to the observed anodic currents in the region +1100 mV to +1700 mV. In principle the anodic process could be direct oxidation of a species in solution. It is perhaps more likely that the current arises from a mechanism such as

$$(Co^{2+})_s \xrightarrow{-e} (Co^{3+})_s$$

where s denotes the surface of electrode

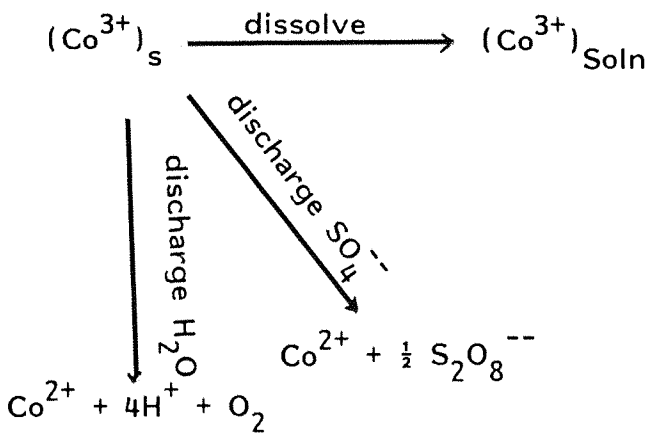

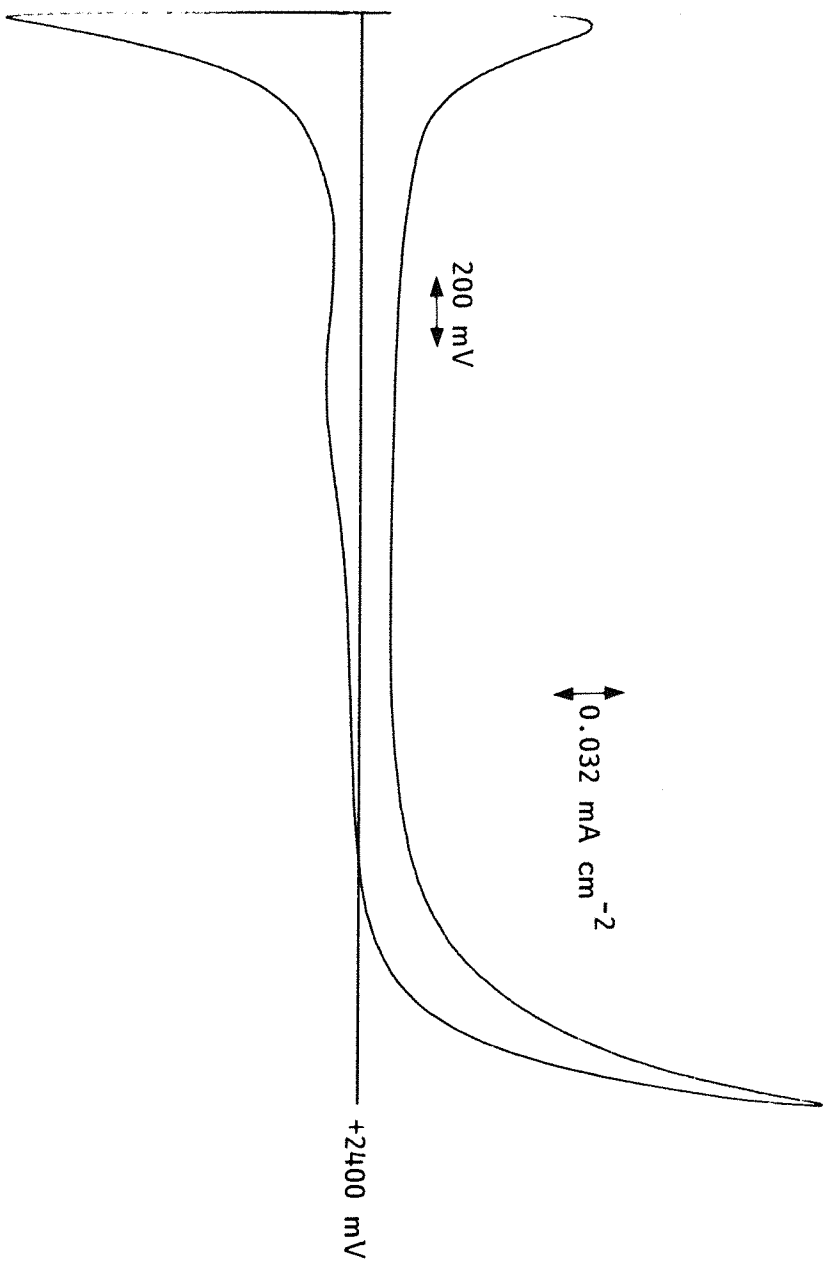

Fig. 4.4 Cyclic voltammogram in 1M sulphuric acid at a sweep rate of 500 mV s^{-1} at a cobalt spinel structure Co_3O_4/

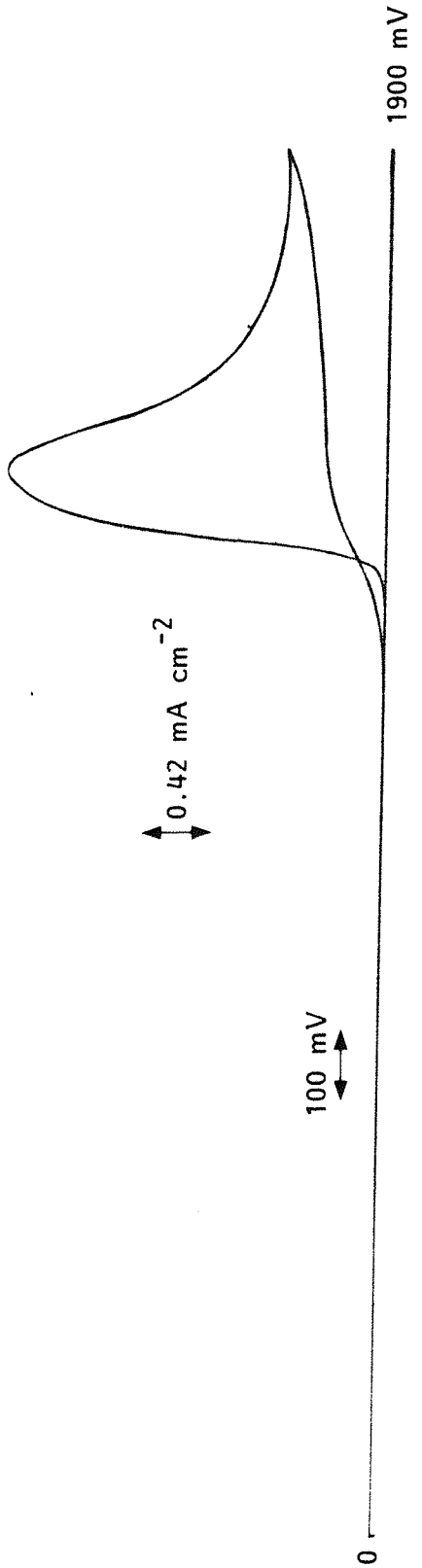

Fig 4.5 Cyclic voltammogram in 9.3M sulphuric acid at a sweep rate 200 mV s^{-1} at a cobalt oxide spinel structure electrode (Co_3O_4).

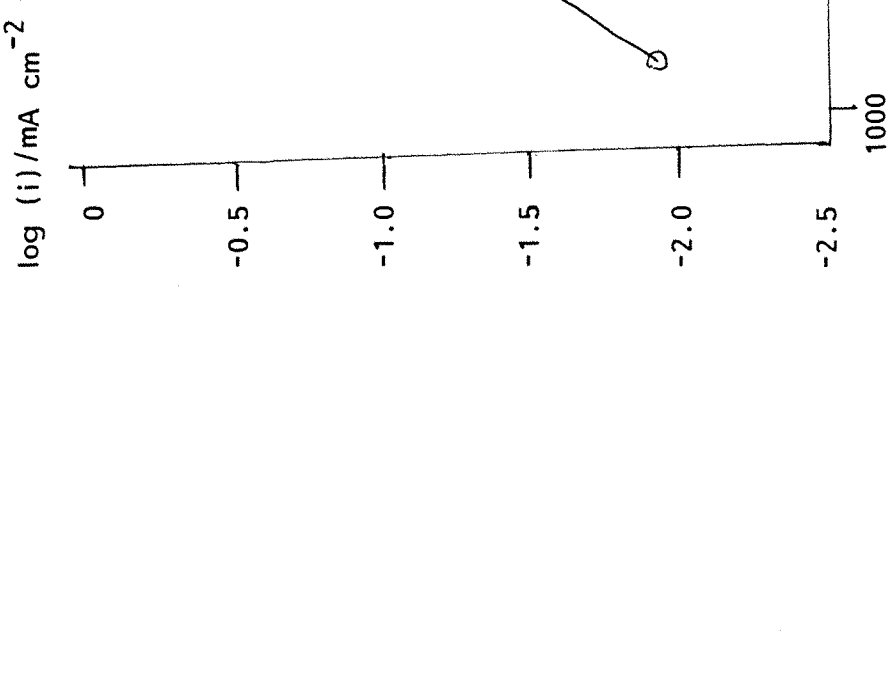

Fig. 4.6 Log i-E curve for cobalt oxide spinel structure in 5M sulphuric acid.

In all such mechanisms, however, there must be a strong limitation in the rate, as the peak current density is very low. This slow step could, as in the case of Ni in base, be the chemical reaction between the Co(III) species and H_2O or SO_4^{--}. In view of the shape of the voltammetric peak and the dependence of the peak current on scan rate ($I_p \propto \nu^{\frac{1}{2}}$), it is more likely that the slow step is a transport process within the relatively thick oxide coating. If this is the case, however, it is not clear why the cyclic voltammogram depends so strongly on H_2SO_4 concentration. Maybe protonation of an oxide species is essential to the conversion of Co_3O_4 to a higher cobalt oxide. Oxygen evolution in sulphuric acid occurred at a higher potential compared to that reported by Shub et al[100] for the oxygen evolution in 1M $HClO_4$. This could be due to the blockage of electrode surface by SO_4^{--} ions.

Since Co_3O_4 has been reported to be a good catalyst for the Cl^-/Cl_2 couple[80-83], a few curves were run for Cl^- oxidation in 5M H_2SO_4. Figure 4.7 shows the I-E response for 5M H_2SO_4 + 5M NaCl run at 300 mV s^{-1}. In order to observe any oxidation current in the potential range expected, it was necessary to increase the current sensitivity substantially. Figure 4.7 shows only an anodic wave at $E_p \sim 1420$ mV with a current density of 14 μA cm^{-2}. This is, of course, very low compared to the peak current (2.6 mA cm^{-2}) observed in the absence of Cl^-. Similar experiments were run with lower Cl^- concentration and in the lowest $[Cl^-]$, the anodic wave is barely visible even at the high current sensitivity. Figure 4.8 shows a plot of anodic wave height vs $[Cl^-]$ and this confirms that the curves get bigger with increasing $[Cl^-]$.

These results clearly indicate that in concentrated H_2SO_4 the Co_3O_4 is a very poor catalyst for Cl_2 evolution. Since this is in sharp contrast to the known behaviour at pH = 4, it suggests that either acid or sulphate species inhibit Cl_2 evolution. If the former, it could be taken as further evidence that protonation of the cobalt oxide is important in determining its behaviour.

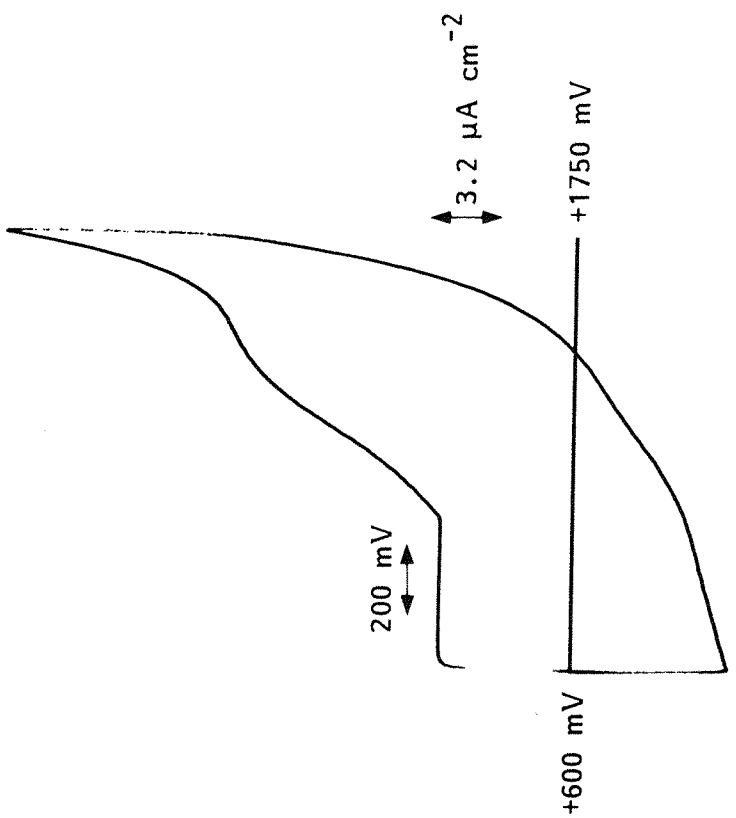

Fig. 4.7 Cyclic voltammogram in 5M sulphuric acid + 5M sodium chloride at a sweep rate 300 mV s^{-1} for a cobalt oxide spinel structure electrode.

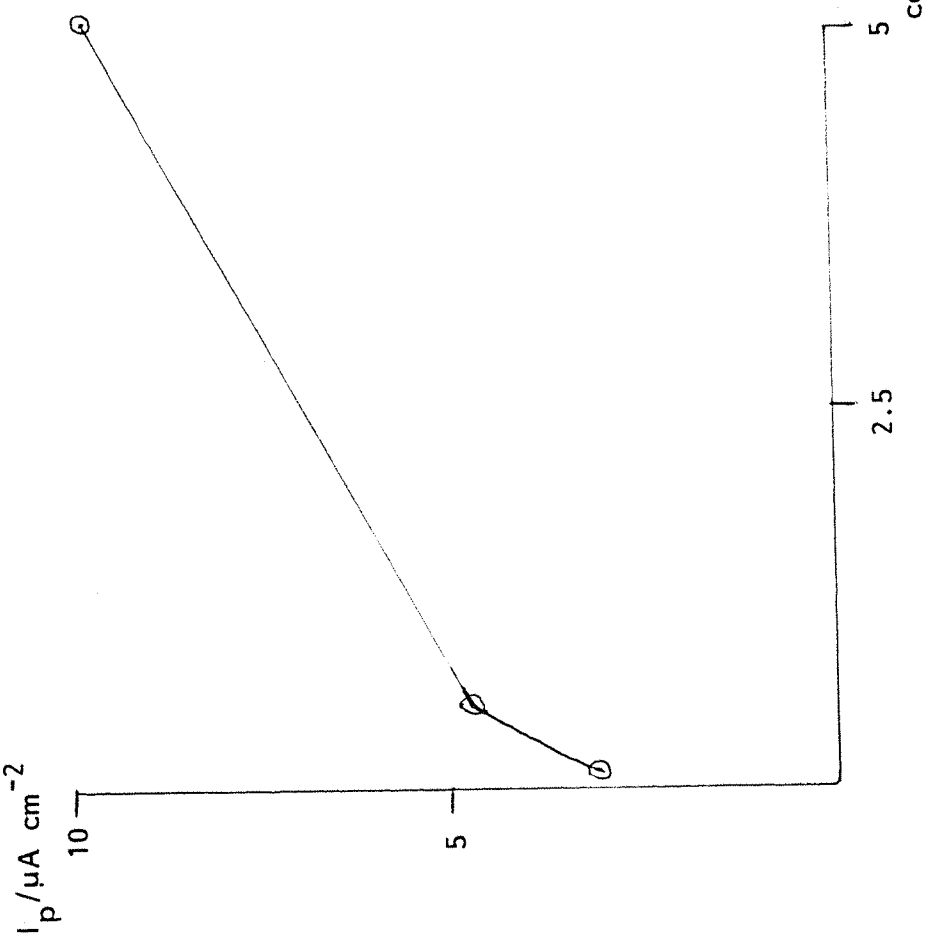

Fig. 4.8 Plot of peak height ($\mu A\ cm^{-2}$) vs the concentration of chloride in 5M sulphuric acid for a cobalt oxide spinel electrode.

Reduction Process

A voltammogram was recorded between +500 mV to -550 mV vs S.C.E. in a 5M H_2SO_4 at a sweep rate of 200 mV s^{-1}. A cathodic current at -510 mV on the forward sweep was observed in the reverse sweep anodic current at -210 mV. The typical voltammogram is shown in figure 4.9. The anodic current is significantly smaller than the cathodic current. A similar experiment in 1M H_2SO_4 also carried out shows significantly smaller current than in 5M H_2SO_4. The voltammogram is shown in figure 4.10.

4.1.2 Cyclic voltammetric behaviour in 5M sulphuric acid at a $M_xCo_{3-x}O_4$ electrode

The electrodes were prepared by mixing the desired proportion of the two metal nitrate solutions and otherwise using the procedure described above. Cyclic voltammograms for $Zn_xCo_{3-x}O_4$ (where x = 0.1 and 0.4) in 5M sulphuric acid are shown in figures 4.11 and 4.12. An anodic peak for Co_3O_4 was observed at 1520 mV. With the mixed spinels, this peak is much reduced in size and, indeed, within $Zn_{0.4}O_4$ it is barely visible. This behaviour is to be expected if the anodic process involves oxidation of Co(II) to Co(III). In $Zn_{0.4}Co_{2.6}O_4$ many of the Co(II) atoms in the lattice are replaced by Zn(II) which will not be oxidable.

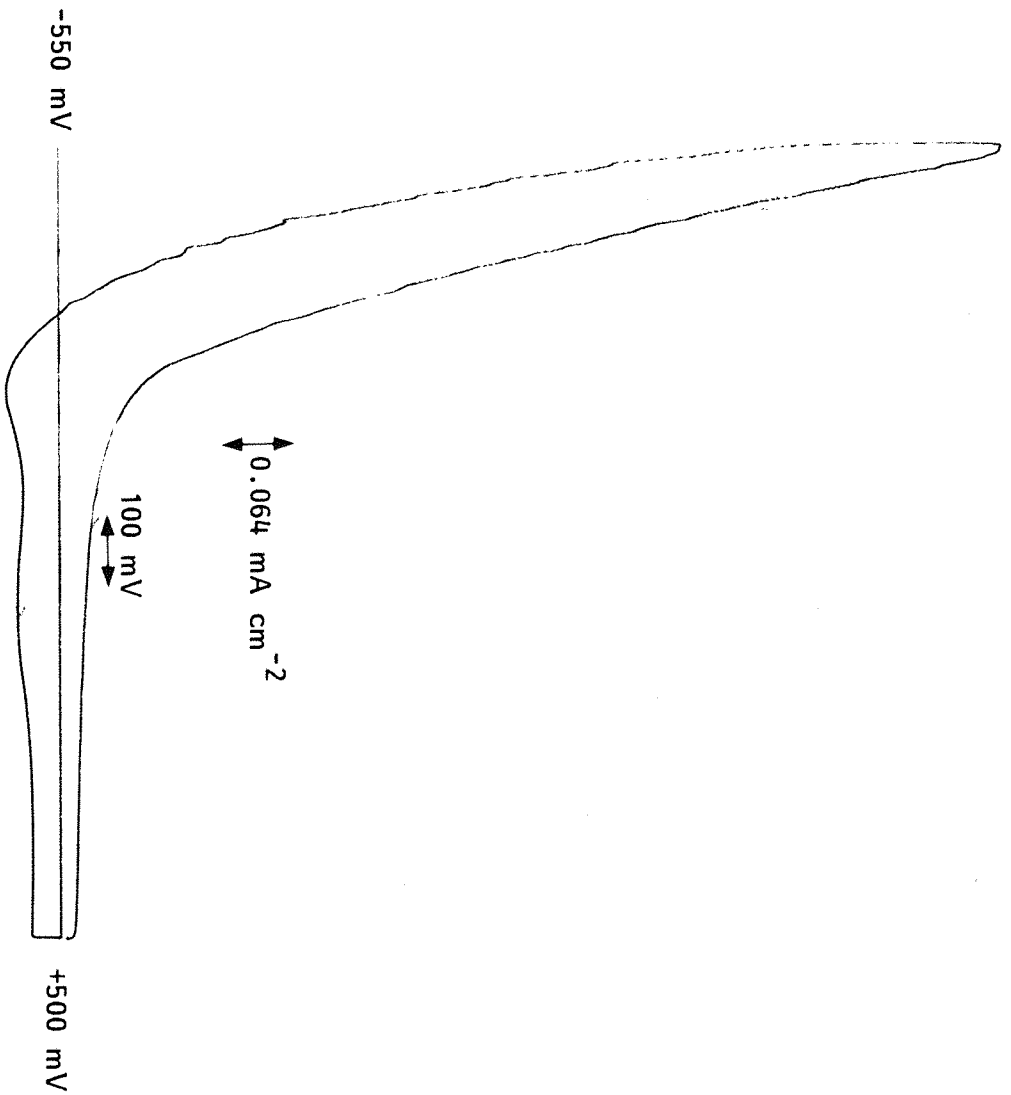

Fig. 4.9 Cyclic voltammogram in 5M sulphuric acid at a sweep rate 200 mV s^{-1} on a cobalt oxide (Co_3O_4) spinel structure electrode.

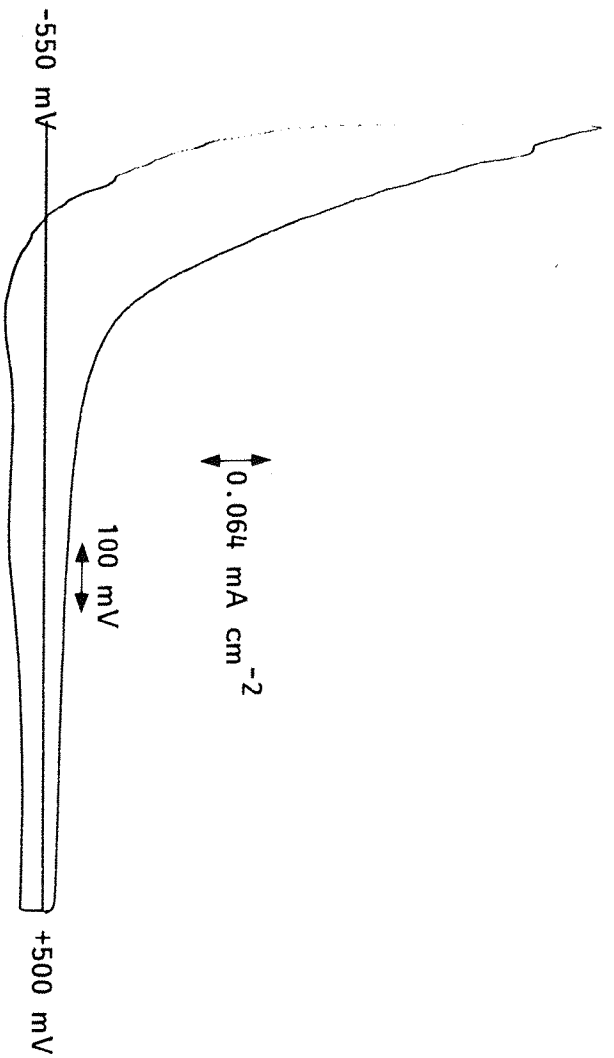

Fig. 4.10 Cyclic voltammogram in 1M sulphuric acid at a sweep rate 200 mV s^{-1} on a cobalt oxide (Co_3O_4) spinel structure electrode.

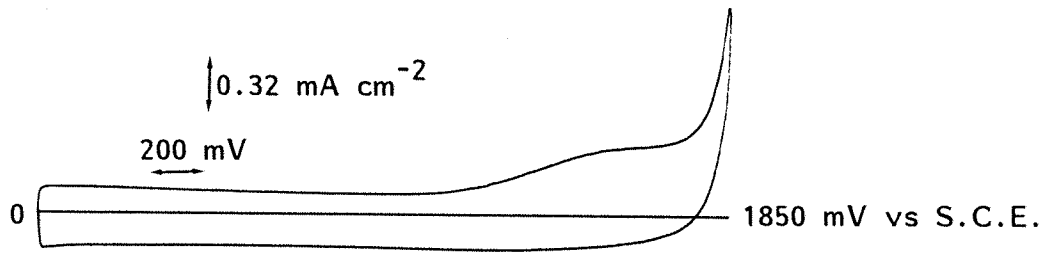

Fig. 4.11 Cyclic voltammogram in 5M sulphuric acid at a sweep rate 350 mV s^{-1} on a cobalt oxide spinel structure $Zn_{0.1}Co_{2.9}O_4$ ($x = 0.1$ in the formula $Zn_xCo_{3-x}O_4$).

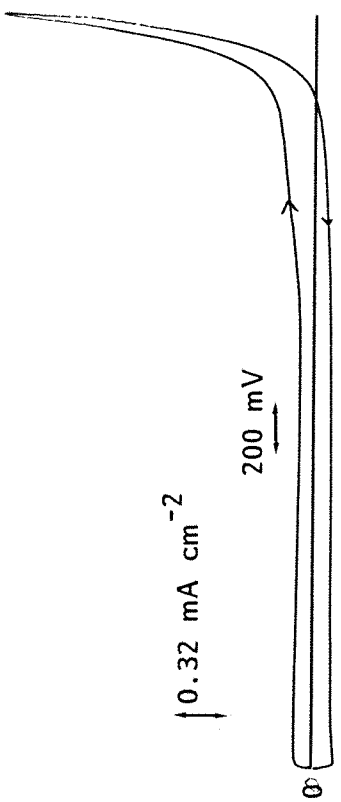

Fig. 4.12 Cyclic voltammogram in 5M sulphuric acid at a sweep rate 200 mV s^{-1} on a cobalt oxide spinel structure $Zn_{0.4}Co_{2.6}O_4$ ($x = 0.4$ in the formula $Zn_xCo_{3-x}O_4$).

References

1. G. Erman, Ann, 1801, 8, 206.
2. C.J. Brockman, Electroorganic Chemistry, Wiley, N.Y. 1926.
3. F. Fichter, Organische Electrochemie, 1942.
4. F.D. Popp and H.P. Schultz, Chem. Rev., 1962, 62, 19.
5. N.L. Weinberg and H.R. Weinberg, Chem. Rev., 1968, 68, 449.
6. M.J. Allen, Organic Electrode Processes, 1958.
7. S. Swann, Jr., J Electrochem. Soc., 1952, 99, 219.
8. K. Natarajan, K.S. Udupa, G.S. Subramani and H.V.K. Udupa, Electro. Chem. Technol., 1966, 2(5-6), 1951.
9. J.A. May and K.A. Kobe, J. Electrochem. Soc., 1950, 97, 183.
10. L.L. Bott, Hydrocarbon Processing, 1965, 44, 115.
11. C.L. Mantell, Electroorganic Chemical Processing, Chemical Process, Rev. No. 14, Noyes Development Corp. New Jersey, 1968.
12. H.J. Wille, D. Knittel, B. Kastening and J. Mergel, J. Appl. Electrochem., 1980, 10, 489.
13. F. Goodridge and O.B. Osifade, Unpublished results.
14. B.E. Conway and A.K. Vijh, Chem. Rev., 1967, 67 623.
15. R.S. Yeo, J. McBreen, A.C.C. Tseung, S. Srinivasan and J. McElroy, J. Appl. Electrochem., 1980, 10, 393.
16. K.L. Hsueh, M.Sc Thesis, Clarkson College, Potsdam, N.Y. 1979.
17. H.D. Law, J. Chem. Soc., 1906, 89, 1437.
18. I.J. Mizuguchi and S. Matsumota, Chem. Abst. 1958, 52, 8794.
19. J.E. Slager and J. Mirza, Chem. Abst. 1966, 64 6561.
20. C.L. Wilson and U.V. Udupa, Trans. Electrochem. Soc., 1952, 99, 289.
21. F.M. Fredriksen, J. Phys. Chem., 1915, 19, 696.
22. X. de Hemptinne and K. Schunck, Trans. Faraday Soc., 1969, 65, 591.

23. K. Sugino and T. Nonaka, Electrochim. Acta, 1968, 13, 613.
24. I.V. Kirilyus, R.P. Silkina and D.V. Sokol'Skii, Chem. Abstr, 77, 108727, 1972.
25. F.C. Walsh and R.J. Marshall, Surface Technol., 1985, 24, 45.
26. M. Fleischmann, J.W. Oldfield and C.L.K. Tennakoon, Symp. on Electrochem. Eng. 1971, Inst. Chem. Engrs. Symp. Series, 1973, 37, 153.
27. M.J. Allen, J. Electrochem. Soc., 1962, 109, 731.
28. R.W. Forman and F. Veetch, U.S. Patent No. 3119760, 1964.
29. C.L. Mantell, Chem. Eng., 1967, 74, 128.
30. J.R. Backhurst, J.M. Coulson, R.E. Plimley and M. Fleischmann, J. Electrochem. Soc., 1969, 116, 1600.
31. M. Fleischmann and J.W. Oldfield, J. Electroanal. Chem., 1971, 29, 211.
32. M. Fleischmann and J.W. Oldfield, J. Electroanal. Chem., 1971, 29, 231.
33. F. Goodridge, D.I. Holden, H.D. Murray and R.E. Plimley, Trans. Inst. Chem. Engrs., 1971, 49, 128.
34. F. Goodridge, D.I. Holden, H.D. Murray and R.E. Plimley, Trans. Inst. Chem. Engrs., 1971, 49, 137.
35. M. Fleischmann and Z. Ibrisagic, J. Appl. Electrochem., 1980, 10, 151.
36. M. Fleischmann and Z.Ibrisagic, J. Appl. Electrochem., 1980, 10, 157.
37. H. Lund, Acta Chim. Scand., 1957, 11, 1323.
38. J. Billion, G. Canquis, J. Combrisson and A. Li, Bull. Soc. Chim., 1960, 2062.
39. A. Zweig, W.G. Hodgson, W.H. Jura and D.L. Maricle, Tetrahedron Lett., 1963, 1821.
40. A. Zweig and W.G. Hodgson, Proc. Chem. Soc., 1964, 417.
41. G. Canquis and G.F. Fanvelot, Bull. Soc. Chim., 1964, 2014.

42. T.M. McKinney and D.H. Geske, J. Am. Chem. Soc., 1965, 87, 3014.
43. C. Walling, Free Radicals, Wiley, N.Y., 1957, p.581.
44. L. Eberson and K. Nyberg, Acta. Chim. Scand., 1964, 18, 1567.
45. K. Shirai and K. Sugino, Denki. Kagaku, 1957, 25, 284.
46. R. Ramaswamy, M.S.V. Pathy and U.V.K. Udupa, J. Electrochem. Soc., 1963, 110, 202.
47. S. Chidambaram, M.S.V. Pathy and U.V.K. Udupa, J. Electrochem. Soc., India, 1968, 17, 95.
48. P.J. Andrulis Jr., M.J.S. Dewar, R. Dietz and R.L. Hunt, J. Amer. Chem.Soc., 1966, 88, 5473.
49. K. Kramer, P.M. Robertson and N. Ibl, J. Appl. Electrochemn., 1980, 10, 29.
50. R. Clarke, A. Kuhn and E. Okoh, Chem. Brit., 1975, 11, 59.
51. P.M. Anatharaman and H.V.K. Udupa, Trans. SAEST, 1974, 9, 108.
52. K. Niki, T. Sekine and K. Sugino, J. Electrochem. Soc., (Japan) 1969, 37, 74.
53. J.A. Shropshire, J. Electrochem. Soc., 1965, 112, 465.
54. J.A. Shropshire, J. Electrochem. Soc., 1967, 114, 773.
55. R. Kalvoda, J. Electroanal. Chem., 1970, 24, 53.
56. J.L. Weininger and M.M. Breiter, J. Electrochem. Soc., 1963, 110, 484.
57. M. Fleischmann, K. Korinek and D. Pletcher, J. Electroanal. Chem., 1971, 31, 39.
58. M. Fleischmann, K. Korinek and D. Pletcher, J. Chem. Soc., Perkin Trans, 2, 1972, 1396.
59. M. Amjad, D. Pletcher and C. Smith, J. Electrochem. Soc., 1977, 124, 203.
60. G.W.D. Briggs and M. Fleischmann, Trans. Faraday Soc., 1966, 62, 3217.
61. M.A. Sattar and B.E. Conway, J. Electrochim. Acta, 1969, 14, 695.

62. M.A. Sattar and B.E. Conway, J. Electroanal. Chem., 1968, 19, 351.
63. D.M. MacArthur, J. Electrochem. Soc., 1970, 117, 422.
64. M. Fleischmann, K. Korinek and D. Pletcher, J. Electroanal. Chem., 1971, 33, 478.
65. J. Kaulen and H.J. Schafer, Tetrahedron, 1982, 38, 3299.
66. J. Kaulen and H.J. Schafer, Synthesis, 1979, 513.
67. P.M. Robertson, P. Berg, H. Reimann, K. Schleich and P. Seiler, J. Electrochem. Soc., 1983, 130, 591.
68. G. Vertes, G. Horanyi and F. Nagy, Croat. Chim. Acta, 1972, 44, 21.
69. R. Konaka, S. Terabe and K. Kuruma, J. Org. Chem., 1969, 34, 1334.
70. K Kakagawa, R. Konaka and T. Nakata, J. Org. Chem., 1962, 27, 1597.
71. M.V. George and K.S. Balachandram, Chem. Rev., 1975, 75, 491.
72. K. Nakagawa and H. Onoue, Tetrahedron Lett., 1965, 1433.
73. K. Nakagawa and T. Tuji, Chem. Pharm. Bull., 1963, 11, 296.
74. K. Nakagawa, H. Onoue and K. Minami, Chem. Comm., 1966, 17.
75. G.W.D. Briggs and W.F.K Wynne-Jones, Electrochim. Acta, 1962, 1, 241.
76. P.M. Robertson, J. Electroanal. Chem., 1980, 111, 97.
77. P.M. Robertson, F. Schwager and N. Ibl, Electrochim. Acta, 1973, 18, 923.
78. G. Vertes, G. Horanyi and F. Nagy, Tetrahedron, 1972, 28, 37.
79. G. Vertes, G. Horanyi and F. Nagy, Acta Chim. Hung., 1971, 67, 145.
80. D.A. Denton, J.A. Harrison and R.I. Knowles, Electrochim. Acta, 1979, 24, 521.

81. R.S. Yeo, J. Orehotsky, W. Visscher and S. Srinivasan, J. Electrochem. Soc., 1981, 128, 1900.

82. D.V. Kokoulina, Yu. I. Krasovitskaya and T.V. Ivanova, Sov. Electrochem., 1978, 14, 470.

83. L.M. Burke and M. McCarthy, Electrochim. Acta, 1984, 29, 211.

84. R.G. Erenburg, L.I. Krishtalik and V.I. Bystrov, Sov. Electrochem., 1972, 8, 1740.

85. E.A. Kalinovskii, R.U. Bondar and N.N. Meshkova, Sov. Electrochem. 1972, 8, 1468.

86. V.I. Bystrov and O.P. Romashin, Sov. Electrochem., 1975, 11 1226.

87. I.E. Veselovskaya, E.K. Spasskaya, V.A. Sokolov, V.I. Tkachenko and L.M. Yakimenko, Sov. Electrochem., 1973, 10, 70.

88. A.T. Kuhn and C.J. Mortimer, J. Electrochem. Soc., 1973, 120, 231.

89. I.R. Burrows, D.A. Denton and J.A. Harrison, Electrochim. Acta, 1978, 23, 493.

90. J.A. Harrison, D.L. Caldwell and R.E. White, Electrochim. Acta, 1983, 28, 1561.

91. J.A. Harrison, D.L. Caldwell and R.E. White, Electrochim. Acta, 1984, 29, 203.

92. D.A. Denton, J.A. Harrison and R.I. Knowles, Electrochim. Acta, 1981, 26, 1197.

93. J.A. Harrison, D.L. Caldwell and R.E. White, Electrochim. Acta, 1984, 29, 1139.

94. D.L. Caldwell and M.J. Hazelrigg, Eur. Pat. Appl. EP 61,717, 1982.

95. P.W.T. Lu and S. Srinivasan, J. Electrochem. Soc., 1978, 125, 1416.

96. P.M. Robertson, J. Electroanal. Chem., 1980, 111, 97.

97. G. Vertes and G. Horanyi, J. Electroanal. Chem., 1974, 52, 47.

98. D.E. Court, Ph.D. Thesis, Southampton University, 1984.

99. D.L. Caldwell and M.J. Hazelrigg, Modern Chloro-technology, ed. M.O. Coulter.

100. L. Iwakura, K. Hirao and H. Tamura, Electrochim. Acta, 1977, 22 335.

101. V.V. Shalaginov, I.D. Belova, Yu. E. Roginskaya and D.M. Shub, Sov. Electrochem., 1978, 14, 1708.